NOTE TO USERS

DISSERTATION

OVERSTORY STRUCTURE AND DETRITAL DYNAMICS OF PONDEROSA PINE FORESTS: INSIGHTS INTO FIRE BEHAVIOR AND ITS CARBON CONSEQUENCES

Submitted by

Sonia A. Hall

Graduate Degree Program in Ecology

In partial fulfillment of the requirements

For the Degree of Doctor of Philosophy

Colorado State University

Fort Collins, CO

Summer, 2005

COLORADO STATE UNIVERSITY

May 27, 2005

WE HEREBY RECOMMEND THAT THE DISSERTATION PREPARED UNDER OUR SUPREVISION BY SONIA A. HALL ENTITLED "OVERSTORY STRUCTURE AND DETRITAL DYNAMICS OF PONDEROSA PINE FORESTS: INSIGHTS INTO FIRE BEHAVIOR AND ITS CARBON CONSEQUENCES" BE ACCEPTED AS FULFILLING IN PART REQUIREMENTS FOR THE DEGREE OF DOCTOR OF PHILOSOPHY.

Committee on Graduate Work

Advisor

Department Head

ABSTRACT OF DISSERTATION

OVERSTORY STRUCTURE AND DETRITAL DYNAMICS OF PONDEROSA PINE FORESTS: INSIGHTS INTO FIRE BEHAVIOR AND ITS CARBON CONSEQUENCES

Large, stand-replacing fires in the ponderosa pine forests of the Colorado Front Range have raised questions about long-term changes in fire severity and the controls on fire behavior. It is widely believed that fire suppression has contributed to fuel accumulation and, consequently, has caused severe fires. My goal was to provide methodological insights into (a) estimating overstory structure, and (b) the relation between fuels and fire behavior, and ecological insights into (c) these forests' detrital dynamics.

I used lidar data to estimate biomass structure. I successfully estimated stand height, total aboveground biomass, basal area and foliage biomass. These technologies showed potential for estimating tree density, canopy base height and canopy bulk density, though more extensive datasets are needed to describe these relationships. These spatially explicit estimates are useful for quantifying carbon stocks and as inputs for fire behavior models.

I analyzed the sensitivity of simulated crown fire hazard to variations in the inputs characterizing surface and canopy fuels. The simple simulation model used predicted that it was harder for a fire to reach the canopy than it was for it to move horizontally through

it, suggesting that active crown fire hazard was particularly sensitive to the description of the surface fuels and to canopy base height.

I described the long-term dynamics of detrital pools (dead wood, litter, duff). Woody detritus accumulated quickly after a fire, as dead material fell. This peak then decomposed before pool size increased again as new material fell. Litter accumulated monotonically, and was most strongly related to canopy cover. Duff was the hardest pool to predict. Topographical and soils characteristics did not appear to constrain these dynamics. The magnitude and timing of changes in detrital pools provide estimates of carbon sequestered in these pools, and inform the debate on whether present fires are outside the historical range of variability.

My studies provide a framework for estimating carbon stocks and inform the debate on the controls over fire behavior. I highlight the importance of surface fuels in controlling crown fire hazard, and quantify the magnitude and timing of changes in detrital mass in these forests.

Sonia A. Hall
Graduate Degree Program in Ecology
Colorado State University
Fort Collins, CO 80523
Summer 2005

ACKNOWLEDGEMENTS

This dissertation, and the learning process it reflects, would not have been possible without the help and support of a large number of people. Many people provided intellectual and educational guidance over the almost five years I have been at Colorado State University. First, I'd like to thank my advisor, Indy Burke, for giving me the opportunity to come to this school, and for her constant and unwavering belief in my capabilities. I have learnt to become an independent, critical thinking scientist, and Indy has contributed substantially to that process. Another person who also contributed enormously to my learning process, and whose belief in my capacity to meet challenges has kept me from faltering, is Tom Hobbs. I am deeply grateful for all he has done for me, and for the respect he has always shown towards me, a feeling that is mutual.

Merrill Kaufmann and Tom Vonder Haar have provided breadth of interests to my committee, and in so doing have opened my eyes to a broader picture. They have always been willing to spend time with me, discuss ideas, and have provided key insights that have contributed to the quality of my dissertation, as well as to my growth as a scientist.

Many other people have, in the course of their work, provided help in a variety of aspects during my time at CSU. These include, though are not limited to, Paula Fornwalt, Laurie Huckaby, Jason Stoker, Bill Lauenroth, Jeri Morgan, Gene Kelly, John Norman, Julie Orwick, Petra Lowe, Dani-ella Betz, Julianne Zimmermann, Evan Stafford, Bill Romme, David Box.

Beyond the call of duty, my fellow students have listened to my ventings, have read my drafts, have discussed ideas and results, have supported me through tough personal times, have celebrated with me, and, most importantly, have become my most valued friends in this country. I thank, for all they have done, Carol Adair, Suzie Bird, John Bradford, Melissa McHale, Sarah Hamman, Peter Adler, Rebecca McCulley, Mo O'Mara, and Floye Wells. My thanks also to the newer members of our lab, Eliana Bontti, Seth Munson and Mark Gathany, for what we have shared in this last year.

I would also like to thank my family, across generations. First, I thank my parents, Anthony and Silvia, for their constant support. They have provided me with two different role models of scientists and human beings, both of which I strive to live up to. Second, I thank Santiago, my son, for helping put my graduate student experience in perspective. And finally, a very, very special thank you for my husband, Moisés Soto, without whom I might never have come here, and without whose support and commitment to my career I would never have made it.

TABLE OF CONTENTS

CHAPTER 1: INTRODUCTION

The area burned annually by wildfires in the western United States has increased during the last decade, despite significantly greater funding invested in fire suppression (Stephens and Ruth 2005). Recent extensive fires, such as the Hayman fire in Colorado (2002), which burned over 55 000 ha, and the Rodeo-Chediski complex in Arizona (2002; 189 000 ha), have contributed considerably to the area burnt, and have increased public and political interest in fire ecology. Both these fires burned large areas of ponderosa pine forests. Fire suppression, which dominated management policy of public lands over much of the 20th century and has likely contributed to the accumulation of surface and ladder fuels in ponderosa pine forests (Covington and Moore 1994). This accumulation, in turn, may have led to a shift in the fire regime, toward greater frequency and extent of crown fires. This view depends on the assumptions that all ponderosa pine forests historically had low severity fire regimes (dominated by surface fires; Schoennagel et al. 2004), and that fuels play a critical role in determining fire behavior. However, there is evidence that Colorado Front Range ponderosa pine forests' fire regime is better represented as mixed severity, rather than low severity (Brown et al. 1999, Veblen et al. 2000). Two questions are therefore actively debated. How important are fuels in determining fire behavior, relative to weather and ignition sources? Were recent fires larger and more severe than those that happened historically?

Another subject of interest to ecologists and policy makers is the quantification of carbon stocks and fluxes in forests. The emergence of the Kyoto Protocol early in 2005 emphasizes the importance of quantifying the carbon budgets of terrestrial ecosystems, particularly forests, given their potential for sequestering carbon. Fire can have important consequences for carbon sequestration, as it releases in hours or days an amount of carbon, previously bound in tree and detrital biomass, that may have taken decades to accumulate. In fire prone systems, such as ponderosa pine forests, potential changes in the fire regime may alter the amounts of carbon fixed in live and dead biomass, and the flux of carbon dioxide released during wildfires. If fire suppression has led to the accumulation of live and dead biomass, it has also caused increased carbon sequestration in these pools. If this accumulation, in turn, has led to the occurrence of larger and more severe wildfires, greater amounts of carbon dioxide will be released, affecting the carbon balances of these forests.

My goal in this dissertation was to provide ecological and methodological insights that can enlighten aspects of the debates on the role played by fuels in controlling fire behavior, and on whether the fire regime in ponderosa pine forests of the Colorado Front Range has changed. I also address issues pertaining to the potential consequences of present fire regimes for carbon sequestration. I studied the use of active remote sensing to provide spatially explicit estimates of overstory structure, the sensitivity of simulated crown fire hazard to variations in inputs describing fuels, and the long-term temporal dynamics of detritus. Below, I briefly provide the context for each of these studies.

Estimating stand structure – Fire is a spatially dynamic process, and occurs at a relatively broad scale. Simulation modeling is often used to direct and inform research on

fire behavior (Perry 1998). Fire behavior models such as BEHAVE (Andrews 1986), FARSITE (Finney 1998) and others (Scott and Reinhardt, 2001) generally span scales of less than one to thousands of hectares or more. To analyze the effect of fuels (relative to the effects of weather or ignitions) on fire behavior, it is necessary to develop spatially explicit inputs that accurately reflect the characteristics of forest structure at these broad scales. Remotely sensed data can be used to estimate forest structure in a timely and cost-effective manner (Franklin 2001). This advantage of remote sensing extends to the quantification of carbon stocks over large areas. My objective in **Chapter 2** was to use data collected by an active, airborne remote sensor to estimate area-based stand structural variables (stand height, canopy bulk density, canopy base height, total aboveground biomass, foliage biomass, basal area and tree density) of ponderosa pine forests in north central Colorado.

Sensitivity of simulated crown fire hazard to variations in fuels – The capacity of simulation models to produce realistic results (in this case, about wildfire behavior) can be limited by the state of knowledge of mechanisms and driving variables controlling the process of interest, or by the quality of the data provided as inputs to the model (Albini 1976). There are a wide variety of studies from different disciplines elucidating mechanisms controlling fire behavior [reviewed by Perry (1998) and Scott and Reinhardt (2001)]. Little work has been done on analyzing the sensitivity of simulation model results to the variability in the input data. These inputs characterize the surface and the canopy fuels, as well as weather and topography. Canopy fuels are quantified using two main metrics: canopy base height (the minimum height at which there is enough biomass to allow a fire to propagate into the canopy), and canopy bulk density (the density of

canopy fuels that would be consumed in an active crown fire) (Finney 1998, Scott and Reinhardt 2001), whose calculations are based on a number of assumptions. My first objective for **Chapter 3** was to evaluate the sensitivity of estimates of canopy base height and canopy bulk density to assumptions used in their calculations. A key aspect of fire behavior, in terms of its potential impact, is the transition from surface fire to active crown fire. My second objective for **Chapter 3** was therefore to determine the sensitivity of model-predicted crown fire hazard to variations in canopy base height, canopy bulk density and the characterization of surface fuels.

Long-term detrital dynamics – Surface fuels (detritus) are composed of dead and fallen organic material, and may represent over 20% of total ecosystem carbon (Pregitzer and Euskirchen 2004). Coarse wood has been studied extensively (see Harmon et al. 1986), but less information is available on finer material. My objectives in **Chapter 4** were (a) to describe the long-term temporal dynamics of different detrital pools (dead wood separated into different size classes, litter, duff), and (b) to determine whether stand structure, topography or soils variables imposed significant constraints on the temporal dynamics of the detrital pools.

In **Chapter 5** I summarize my findings, and address how my results provide useful ecological and methodological insights into the fire ecology debates and the carbon sequestration issue.

REFERENCES

Albini, F.A., 1976. Estimating wildfire behavior and effects. USDA Forest Service General Technical Report INT-30.

Andrews, P.L., 1986. BEHAVE: Fire behavior prediction and fuel modeling system – BURN subsystem, Part 1. USDA Forest Service General Technical Report INT-131.

Brown, P.M., Kaufmann, M.K., Shepperd, W.D., 1999. Long-term, landscape patterns of past fire events in a montane ponderosa pine forest of central Colorado. Landscape Ecology 14, 513-532.

Covington, W.W., Moore, M.M., 1994. Postsettlement changes in natural fire regimes and forest structure: ecological restoration of old-growth ponderosa pine forests. In:Assessing forest ecosystem health in the Inland West. The Haworth Press Journal Co-Editions, New York, New York, USA, pp. 153-181.

Finney, M.A., 1998. FARSITE: Fire Area Simulator - Model development and evaluation. USDA Forest Service Research Paper RMRS-RP-4.

Franklin, S.E., 2001. Remote sensing for sustainable forest management. CRC Press LLC, Boca Raton, Florida, USA.

Harmon, M.E., J.F. Franklin, F.J. Swanson, P. Sollins, S.V. Gregory, J.D. Latiin, N.H. Anderson, S.P. Cline, N.G. Aumen, J.R. Sedell, G.W. Lienkaemper, K.Jr. Cromack, and K.W. Cummins. 1986. Ecology of coarse woody debris in temperate ecosystems. Advances in Ecological Research 15:133-302.

Perry, G.L.W., 1998. Current approaches to modelling the spread of wildland fire: a review. Progress in Physical Geography 22, 222-245.

Pregitzer, K.S., Euskirchen, E.S., 2004. Carbon cycling and storage in world forests: biome patterns related to forest age. Global Change Biology 10, 2052-2077.

Schoennagel, T., Veblen, T.T., Romme, W.H., 2004. The interaction of fire, fuels and climate across Rocky Mountain forests. BioScience 54, 661-676.

Scott, J.H., Reinhardt, E.D., 2001. Assessing crown fire potential by linking models of surface and crown fire behavior. U.S. Forest Service, Rocky Mountain Research Station Research Paper RMRS-RP-29.

Stephens, S.L., Ruth, L.W., 2005. Federal forest-fire policy in the United States. Ecological Applications 15, 532-542.

Veblen, T.T., Kitzberger, T., Donnegan, J., 2000. Climatic and human influences on fire regimes in ponderosa pine forests in the Colorado Front Range. Ecological Applications 10, 1178-1195.

CHAPTER 2: ESTIMATING STAND STRUCTURE USING DISCRETE-RETURN LIDAR: AN EXAMPLE FROM LOW DENSITY, FIRE PRONE PONDEROSA PINE FORESTS

ABSTRACT

The ponderosa pine forests of the Colorado Front Range, USA, have historically been subjected to wildfires. Recent large burns have increased public interest in fire behavior and effects, and scientific interest in the carbon consequences of wildfires. Remote sensing techniques can provide spatially explicit estimates of stand structural characteristics. Some of these characteristics can be used as inputs to fire behavior models, increasing our understanding of the effect of fuels on fire behavior. Others provide estimates of carbon stocks, allowing us to quantify the carbon consequences of fire. My objective was to use discrete-return lidar to estimate such variables, including stand height, total aboveground biomass, foliage biomass, basal area, tree density, canopy base height and canopy bulk density. I developed 39 metrics from the lidar data, and used them in limited combinations in regression models, which I fit to field estimates of the stand structural variables. I used an information-theoretic approach to select the best model for each variable, and to select the subset of lidar metrics with most predictive potential. Observed versus predicted values of stand structure variables were highly correlated, with r^2 ranging from 57% to 87%. The most parsimonious linear models for the biomass structure variables, based on a restricted dataset, explained between 35% and

58% of the observed variability. My results provide useful estimates of stand height, total aboveground biomass, foliage biomass and basal area. There is promise for using this sensor to estimate tree density, canopy base height and canopy bulk density, though more research is needed to generate robust relationships. I selected 14 lidar metrics that showed the most potential as predictors of stand structure. I suggest that the focus of future lidar studies should broaden to include low density forests, particularly systems where the vertical structure of the canopy is important, such as fire prone forests.

INTRODUCTION

Most forests are subject to fire (Attiwill 1994). The importance of fire, and its potential for releasing carbon stored in forest biomass, has become increasingly clear (Houghton et al. 2000). To quantify the role forests play in the global carbon cycle it is necessary to comprehend how fire affects carbon fluxes (e.g. net primary productivity, decomposition), and how these processes interact and feed back on each other. Studies of the effects of fire on the carbon cycle and on forest succession have been carried out in tropical (Hughes et al. 2000, Page et al. 2002), temperate (Keane et al. 1990) and boreal forests (Paré and Bergeron 1995, Wirth et al. 1999), as well as in nonforested vegetation types (Tilman et al. 2000). Climate change is likely to interact with other factors and determine changes in fire regimes and post-fire productivity of many forests in the world (Overpeck et al. 1990, Flannigan and Van Wagner 1991).

The ponderosa pine dominated forests at low elevations in the Rocky Mountains are historically fire prone (Covington and Moore 1994). Over the last century, there have been significant changes in the structure of these forests (Weaver 1959, Cooper 1960,

Kaufmann et al. 2000). Selective logging of large trees, grazing by domestic livestock, tree planting and fire suppression have all been identified as potential contributing factors that have led to an increase in stand densities and an accumulation of biomass and dead fuels in these forests (Covington and Moore 1994). These changes have contributed to the recent occurrence of relatively large, severe wildfires in ponderosa pine forests. There are projects being developed and implemented to restore these forests to their historical condition, and reintroduce fire as a natural process (Moore et al. 1999, Fulé et al. 2001, Brown et al. 2001).

Quantification of the effect of fire on carbon stocks and fluxes require estimates of the amount of biomass in ecosystem components, including actively photosynthesizing tissues. The development and use of spatially explicit maps of forest fuels can enhance our understanding and modeling of fire behavior (Perry 1998). Given that fire is an inherently spatial process, restoration and fuel reduction efforts will be much more effective if the areas to be treated are selected based on data that include the landscape context of the area of interest. Therefore, there is a critical need to estimate structural variables of ponderosa pine forests. Total aboveground biomass, basal area and tree density provide information on carbon stocks. Foliage biomass, as an estimate of active tissues, is useful in estimating primary productivity. Stand height, canopy bulk density and canopy base height are common inputs for fire behavior models (Scott and Reinhardt 2001). Stand height controls wind profiles within the forest; canopy base height is critical in determining whether the fire can reach the crowns of trees, and canopy bulk density quantifies the fuel in the canopy layer, which will feed active crown fires (Scott and Reinhardt 2001).

Extensive, spatially explicit inventories of stand structure are extremely labor intensive and expensive. It is practically impossible to obtain full inventory coverage of large areas on the ground, especially where land ownership is mixed. One of the main advantages of remote sensing is the capacity to obtain spatially explicit data over large areas in a timely and economic fashion. These technologies have been used extensively in different forest types as a means to obtain spatially continuous estimates of stand structural variables (Franklin 2001). Passive optical sensors (such as Landsat TM), as well as the techniques developed to estimate vegetation characteristics from the data they provide, have been around for many years (Wulder 1998). Since these data are both inexpensive and reasonably available, most of the digital remote sensing research on estimating forest biophysical parameters has used these types of sensors. The capacity of these sensors is limited, however, because they provide two-dimensional information from which the three-dimensional structure of forests needs to be estimated. One consequence is that relationships developed to estimate total aboveground biomass or leaf area index are nonlinear, saturating at approximately 100 Mg/ha (Cohen and Spies 1992) and 4 m^2/m^2 (Baret and Guyot 1991, Spanner et al. 1994) respectively. A second consequence is that optical sensors cannot provide information on the vertical structure of biomass. This can be critical in determining fire behavior (van Wagner 1977, 1993) and wildlife habitat potential (e.g. DeGraaf et al. 1998, Hershey et al. 1998).

Recent technological developments have led to a growing availability of active sensors, such as lidar (light detection and ranging) and radar. These sensors are designed to provide three-dimensional data, which makes them prime candidates for overcoming the saturation limitation of passive sensors (Dobson 2000, Lefsky et al. 2001). Single

wavelength radar has been used to estimate forest biomass, but has been shown to have similar limitations to those of passive sensors, saturating at approximately 150 Mg/ha (Waring et al. 1995).

Most topographic lidar sensors emit beams of infrared light, and measure the time it takes for the beamed energy to be reflected back to the sensor (Baltsavias 1999a). The position and height of the reflecting surface is calculated based on the speed of light. There are two broad categories of lidar, large-footprint, continuous-return lidar, and small-footprint, discrete-return lidar (Lefsky et al. 2002b). The first class is characterized by the emission of a wide beam of light (tens of meters in diameter); the returning energy is stored as a height profile of intensity within that beam. These sensors include SLICER, LVIS, the proposed Vegetation Canopy Lidar and ICEsat (Lefsky et al. 2002b). Discrete-return lidar emits a small beam of light (centimeters in diameter), and records the positions from which the returned energy is greater than a certain threshold. Different systems can record from 1 to 5 discrete returns from each laser pulse. These systems are the ones commercially available (Baltsavias 1999b), and are being used routinely to develop digital elevation models (Flood and Gutelius 1997).

Both types of lidar have been used successfully to estimate stand structural variables, such as mean height, total aboveground biomass, basal area, stem volume and stand density, in a variety of forest types (Means et al. 1999, 2000, Lefsky et al. 1999a, b, 2002a, Dubayah and Drake 2000, Drake et al. 2002, Naesset and Bjerknes 2001, Naesset and Økland 2002, Naesset 2002, Drake et al. 2003). The focus of most of the research has been on overcoming the saturation at high biomass levels that limits the use of passive sensors, and no evidence of similar saturation has been found with lidar (Lefsky et al.

2002b). Little work has been done in forests of relatively low density, such as the ponderosa pine forests of the Front Range of Colorado, USA. Stoker (2002) developed models to accurately estimate individual tree height and diameter at breast height in these forests, using discrete, multiple-return lidar. This work needs to be extended to provide area-based estimates of total biomass, as well as other stand structural variables of interest for fire behavior modeling and carbon stock estimation. My objective in this study was to estimate area-based structural variables using discrete, multiple-return lidar, and obtain a set of simple models to accurately estimate stand height, canopy base height, tree density, basal area, crown bulk density, total aboveground and foliage biomass in low density forests. Implicit in this objective is the selection of a subset of lidar-based metrics that were useful predictors of the structural variables of interest.

METHODS

Study area

My study area is in the Front Range of the Rocky Mountains, Colorado, USA. It is located east of the Cheesman Reservoir (39° 11' N, 105° 16' W), and comprises low elevation (2150-2400 m above sea level) montane forests, dominated by ponderosa pine (*Pinus ponderosa* Dougl. ex Laws), with a secondary component of Douglas-fir (*Pseudotsuga menziesii* (Mirb.) Franco). Mean annual rainfall is 413 mm, and mean monthly temperatures range from –2.9 to 18.5 °C (Western Regional Climate Center data, 1948-2004; http://www.wrcc.dri.edu/cgi-bin/cliMAIN.pl?cochee).

Field data

I measured stand structure variables for 14 sites (mean area of 0.32 ha, Table 2.1) within the area of the overflight (see *Lidar data*, below) in the summer of 2001, distributed over a wide range of topographic positions (aspect, slope) and of structural conditions (Table 2.1). At each site I obtained measurements at four to six sampling points, randomly selected along a transect through the site, following the point-centered quarter method (Cottam and Curtis 1956). Following this method I estimated tree density from the point-to-tree distances (Cottam and Curtis 1956). I recorded tree species, diameter at breast height, tree height, height to live crown and crown width for four trees (heights > 3 m) selected at each point. Heights were measured with a Suunto® clinometer, while crown width and distances to trees (for density estimates and clinometer readings) were obtained with measuring tapes. I used allometric equations to estimate foliage and total tree aboveground biomass for each sampled tree (Table 2.2). From these individual tree values I obtained mean tree biomass, which I then multiplied by the estimated densities to obtain stand level (per hectare) values. From the measured values I calculated mean stand height (m), Lorey's height (basal-area-weighed average height [Husch et al. 2003]; m), canopy bulk density (maximum 5-m running mean density of foliage, calculated for 0.3 m high intervals [Scott and Reinhardt 2001]; kg/m^3) canopy base height (minimum height with canopy bulk density greater than 0.037 kg/m^3 [Sando and Wick 1972]; m), basal area (m^2/ha), total aboveground and foliage biomass (Mg/ha). At each site I also measured slope (with the Suunto® clinometer), aspect (compass bearing normal to the plane of the slope), latitude, longitude and elevation (with a Garmin GPS III+ handheld Global Positioning System, Garmin International Inc.,

Olathe, Kansas, USA). Latitude and longitude were used to match sites to the lidar data (see *Lidar data*, below).

I also used data collected in 1997 by M. R. Kaufmann and coworkers (unpublished), from a 15 ha stem-mapped plot within the study area. This dataset contains information on species, diameter at breast height and total height for each tree. The same allometric equations and calculations were applied to these data to obtain all structure variables except tree density, as in this dataset I had complete tree counts. From these data I obtained 27 stand level values for tree density, mean stand height, Lorey's height, basal area, and total and foliage biomass (each from 0.5 ha). Since this dataset did not contain values on height to live crown, I was unable to estimate canopy bulk density or canopy base height. I did not attempt to correct tree heights and diameters for growth occurred since measurements were taken, given the low growth rates of these forests. I assumed that the values of measurements in 2001 would not be greater than the 1997 values plus measurement errors.

Lidar data

The lidar sensor DATISII (3Di/EagleScan Inc.) was deployed over my sites on the 29th September 2001. It was configured to emit laser pulses (wavelength 1064 nm) with a frequency of 36.5 kHz. For each pulse, the system records information of up to five discrete positions where energy is returned to the sensor: easting and northing (datum WGS84; I used these to match these data with my field sites), height above sea level, return intensity and number of returns recorded for that pulse. The system is a scanning lidar, collecting data in only one direction across track. This configuration provided an average of 1.23 returns/m^2 (0.84-1.49 returns/m^2) for my sites. The swath

width was approximately 1000 m (maximum angle was 15° from nadir). The horizontal position of each return has a root mean square error (RMSE) of 0.5 m (equal to the footprint diameter); the vertical RMSE is 0.15 m.

Processing of lidar data

Each return was automatically preclassified by 3Di/EagleScan as "ground" or "vegetation", and subclasses within each (proprietary algorithm). I generated contour lines with an interval of 0.01 m, based on a subset of the "ground" returns. I calculated the height above the ground for each return by subtracting the height of the nearest contour from the height above sea level. The small contour interval was selected to obtain ground height values directly below each return. Pairs of ground points that were within 40 cm horizontal distance of each other, and one of which was greater than 5 cm below the corresponding contour were considered representative of the same position, and their heights were averaged. If any of those points had originally been flagged as vegetation they were included in the "ground" set. The contours were then recalculated. This procedure was iterated until no "ground" return was more than 5 cm above or below its closest contour line. I used this stringent threshold to guarantee that interpolation errors did not surpass the vertical RMSE of the instrument.

For each site I calculated 39 metrics to synthesize the information contained in the cloud of discrete lidar points (Table 2.3, Appendix 2.1). These metrics were developed based on the lidar literature (Lefsky et al. 1999a, b, Means et al. 1999, 2000, Naesset and Bjerknes 2001, Naesset 2002, Naesset and Økland, 2002, Drake et al. 2002) and modifications thereof. I decided to use as complete a set of metrics as possible, in an effort to set the stage for the convergence of studies using continuous- and discrete-return

lidar. The development of lidar metrics for the different types of systems seems to have been relatively independent. Working under the assumption that the technology is likely to develop towards a small-footprint lidar with continuous profiling capacity, I attempted to provide a complete set of metrics that can be applied to all lidar systems, from which I intended to select those metrics most useful for predicting stand structure variables. I then grouped the 39 metrics based on their assumed relationship to different forest biophysical parameters (Table 2.3). The above processing was done in ArcView 3.2 (ESRI, Redlands, California, USA).

Data analysis

I used an information-theoretic approach (Burnham and Anderson 2002) to rank the regression models and select the best model to estimate each stand structural variable from lidar metrics. This methodology uses Akaike's Information Criterion (AIC) to rank a set of models developed *a priori*, based on the support provided by the field data. AIC is an estimate of the information lost when a model is used as an approximation to the truth, so the smaller the AIC value, the closer a particular model is to the (unknown) truth. The distance between models (in AIC units) provides information on whether the models ranked below the best one are close competitors or not. A rough guide is that models within 1 to 2 AIC units of the best model have substantial support; models 3 to 7 units from the best model have less support, and models more than 10 units away from the best model have essentially no support (Burnham and Anderson 2002). In this way, this methodology provides more useful information than other commonly used techniques, such as stepwise regression. I focused my interpretation of results on models within three AIC units of the best model, as having equivalent support in the data.

This is an exploratory analysis, and the incorporation of a large number of predictor variables (39 lidar metrics) might lead me to find spurious relationships. My use of the information-theoretic approach is geared precisely at trying to avoid these spurious relationships. Even for the structural variable for which I developed the largest number of models, this number is lower than the combinations of variables that would be considered if I ran stepwise regression procedures using only six independent variables. The critical advantage of my chosen methodology is that I had control, *a priori*, of the combination of metrics I used within a single model, as well as the number of predictor variables within each model. Though this is not a guarantee against these models portraying spurious relationships, they are at least based on a mechanistic hypothesis of why they should be good predictors of each stand structural variable. Therefore, the only uncertainty left is whether the resulting correlations are due to the hypothesized causations.

This methodology also provides information on model selection uncertainty, using the Akaike weights (w_r). These quantify the uncertainty related to whether the selected best model is the actual best model. They can be interpreted as the probability that the best model would again be selected as the best model, given the same set of candidate models and another sample of similar data (Burnham and Anderson 2002).

For each stand structural variable, I fitted a variety of statistical models to the field data, using lidar metrics as independent variables and each stand structural variable of interest as the dependent variable. These models included linear models with up to three independent variables, and power functions of single metrics. The variables and combinations used for each stand structural variable are described in Appendix 2.2. I log-transformed the stand structure variables to obtain homogeneity of variance and

normality of residuals where necessary. Where variables were log-transformed, the fitted model was modified accordingly, to obtain the proposed relationship between dependent and independent variables (e.g. if he proposed model was $y=b_0+b_1x$, then the model I fit was $z=\log(b_0+b_1x)$, where $z=\log(y)$ and log is the natural log. In the **RESULTS** section, the model would be expressed as $y=b_0+b_1x$). I estimated the bias introduced by the transformation (Sprugel 1983), and used these estimates to correct the predictions.

AIC is calculated based on estimates for model parameters obtained by fitting the data using maximum likelihood techniques. Given the structure of the field data (all variables were either normally or log-normally distributed), I used least squares techniques to fit the models, and estimated the likelihood of each model given the field data as:

$$\log(\ell(\hat{\theta})) = -\frac{n}{2}\log(\hat{\sigma}^2)$$

where $\ell(\hat{\theta})$ is the likelihood of the model given the data, n is the sample size and $\hat{\sigma}^2$ is the residual sum of squares divided by the sample size. Note that the maximum likelihood estimates of the parameters do not change under log transformations, as the density functions differ only by a multiplicative constant that does not depend on the parameter (Lindgren 1993, Section 12.1). This constant additively modifies the absolute value of the $\log(\ell(\hat{\theta}))$. I fitted the regression models using the procedure for nonlinear estimation in SAS (NLIN; SAS Institute Inc., Cary, North Carolina, USA). I calculated the AIC for each model, and corrected these values for bias due to small sample sizes (AIC_c):

$$AIC_c = -2\log(\ell(\hat{\theta})) + 2K + \frac{2K(K+1)}{(n-K-1)}$$

where K is the number of estimated parameters (including an estimate of variance). I ranked the models based on AIC_c, and calculated the Akaike weights for each model as:

$$w_r = \frac{e^{-\frac{1}{2}(AIC_r - AIC_{\min})}}{\sum_{i=1}^{R} e^{-\frac{1}{2}(AIC_i - AIC_{\min})}}$$

where AIC_r is the model's AIC_c, AIC_{min} is the minimum AIC_c of all the models in the candidate set, and R is the number of candidate models. The additive constant in the $\log(\ell(\hat{\theta}))$ for the log-transformed variables affects the absolute value of AIC_c, but not the ranking of the models.

RESULTS

Stand height

The best regression model for mean stand height explained slightly under 60% of the variability of the 41 sites (Table 2.4, Figure 2.1a), based on two independent variables: the mean height of the upper 50% of 1st "vegetation" returns (h_{max50}) and the standard deviation of all 1st returns with height > 3 m (SD_{h3}). This model had only a 9% chance of being the best model, and eleven other models had equivalent support (Table 2.4). The first four competing models had the same structure as the best model, with a different cumulative height or variability metric (Table 2.4). The rest of the top models with significant coefficients (i.e. the 95% confidence limits did not straddle zero) were functions of a single cumulative height metric.

Expressing stand height as the basal-area-weighed average tree height (Lorey's height) increased the fit of the best model (r^2 = 86.8%), and slightly improved the probability that the model was the best one from the candidate set (w_r = 0.16) (Table 2.4, Figure 2.1b). The best model for Lorey's height was a linear function of the mean height of the highest 25% of the 1st "vegetation" returns (h_{max25}; Table 2.4). Another eight models had similar support in the data (Table 2.4). They all had h_{max25} as a predictor. The last six of these had an added predictor, representative of variability in canopy height (Table 2.4). They are equivalent to the best model, though, since the confidence limits of their added coefficients straddled zero.

Biomass structure variables for estimates of carbon stocks

I analyzed four descriptors of stand biomass structure commonly used to quantify carbon stocks and fluxes: total aboveground biomass, basal area, tree density and foliage biomass. All were log-transformed previous to the analysis. The best model for each biomass structure variable explained between 67.2% and 79.4% of the variability of the 41 sites (Table 2.4, Figure 2.2). The best model for these four structural variables was a negative exponential function of the proportion of ground returns that were not intercepted by the canopy ($P_{G/1}$). The model selection uncertainty for tree density, basal area and foliage biomass was negligible ($w_r > 0.99$). The uncertainty was greater for total aboveground biomass (w_r = 0.56). The regressions of predicted vs. observed values of all four variables did not follow the 1:1 line consistently (Figure 2.2). There were four sites with substantially greater biomass and density than the other 37 (Figure 2.2). These were four out of five leverage points identified using objective diagnostics (ROBUSTREG procedure, SAS, SAS Institute Inc., Cary, North Carolina, USA). To analyze the effect of

these values on the regression coefficients and, particularly, on the selection of models, I refit and reranked the models without these five leverage points (i.e. based on what I will call the restricted dataset). For all four biomass structure variables, the new regression coefficients of the original best model were outside the approximate 95% confidence limits of the original values. The coefficient of determination of the best models decreased in all cases (Table 2.5).

The models selected for total aboveground biomass and basal area with the restricted dataset were almost all linear. The top seven models for total aboveground biomass were functions of a height metric and a metric related to canopy cover, and all explained approximately 60% of the variability. The top 15 models for basal area had r^2 ranging from 48.1% to 57.8%. The equivalent to the original best model for basal area was ranked tenth. A linear function of the same independent variable was ranked 7^{th}. The rest of the top models linearly combined a height metric with a canopy cover or biomass density metric (some with interaction terms), similar to the models for total aboveground biomass (Table 2.6).

The best model for tree density was again a nonlinear function of a canopy cover related metric. The linear function of the same variable was a close competing model, though the fit of both models was low (Table 2.6). A linear function of a height metric, a cover metric and a crown height metric was the best model for foliage biomass. The linear version of the original best model for foliage biomass was within one AIC_c unit of the best model.

Fire behavior modeling variables

The values for the two main fire behavior model inputs, canopy base height and canopy bulk density, were log-transformed. One of the 14 sites for which I had measurements of height to live crown (required to estimate both canopy base height and canopy bulk density) did not have densities greater than 0.037 kg/m^3 at any height (threshold value used to define canopy base height, Sando and Wick 1972), so I was unable to calculate its canopy base height. Therefore, the regressions for this variable were fitted to 13 points.

The best model describing canopy base height was linear, with two independent variables: the mean height of 1st "vegetation" returns from multiple-return pulses (h_{1m}) and the standard deviation of the heights of all 1st returns more than 3 m from the ground (SD_{h3}; Table 2.4). This model had a 39% chance of being selected as the best model using another dataset. Only one other model had equivalent support in the data (Table 2.4): a function of the mean height of 1st "vegetation" returns from 3-return pulses (h_{13}) and the range in height of all 1st returns more than 3 m from the ground ($range_{h3}$), with an interaction term.

The coefficient of determination of the best model for canopy base height seemed to be dominated by two sites, with CBH values of 11.25 m and 0.45 m (Figure 2.3). I was unable to objectively determine if these were leverage points, as I did for the C stock variables above, since the log-transformation of this linear model is nonlinear, and the software used does not provide diagnostics for nonlinear models. The reanalysis described below must therefore be considered tentative. The results of refitting and reranking the models without the high value supported the same best model (Table 2.6),

and the regression coefficients were within one standard error of the original values. The models that resulted from rerunning the analysis without both the large and the small value had very low goodness of fit; the best model explained 12.4% of the variability. The range of predicted values was substantially smaller than that of the observed (1.1 m vs. 3.3 m).

I had estimates of canopy bulk density for all 14 sites measured in the summer of 2001. The best model was a negative exponential function of the proportion of ground returns that were not intercepted by the canopy ($P_{G/I}$; Table 2.4), which was the same as the best models for the biomass structure variables. This model explained 82.8% of the variability (Table 2.4), and there were no identifiable leverage points in the data. The Akaike weight for the best model was 0.56. The linear function of this same predictor variable ($P_{G/I}$) was not a close competitor, though it was within 10 AIC_c units of best model. A linear function of a biomass density variable (δ_{12}; Table 2.3) was within 6 AIC_c units of the best model.

DISCUSSION

The cumulative height metrics in the top models for mean tree height were the lower fractions of returns ($\leq 50\%$), and are therefore dominated by reflection from the upper canopy (i.e. the height of large trees). Stands with greater variability in canopy surface height are likely composed of large trees, mixed in with gaps filled by smaller trees. The mean height of these stands is likely lower than the cumulative height metric would suggest, as the height of those smaller trees needs to be incorporated. This explains

the selection of a model where mean height is positively related to a cumulative height metric and negatively related to variability in height.

The discrete lidar points provide information on the integrated stand, and are therefore dominated by the large trees that form the surface of the canopy. The values of Lorey's height are dominated by the height of large trees, and therefore are more consistent with the height information provided by the lidar data than the mean height values. The goodness of fit of my models for Lorey's height was similar to those found by Stoker (2002) for lidar-identified individual tree heights (these probably represent clumps of trees indistinguishable from each other with lidar data). Lidar-derived heights explained 91% of the variability in height of known individual trees (Stoker 2002).

I used the mean height of cumulative fractions of 1st returns (h_{maxi}, Table 2.3) as predictor variables in an effort to select those returns that characterize the surface of the canopy. My results for Lorey's height indicate that the tallest 25% of 1st returns (h_{max25}) are a good approximation to this surface. I suggest that these cumulative height metrics should be more robust than percentile heights, such as those used in other studies (Naesset 2002, Naesset and Økland 2002). The fraction of returns that represent the canopy surface should be a function of only canopy cover of the dominant trees, while the percentile heights are a function of the complete, three dimensional leaf area index profile (Magnussen and Boudewyn 1998).

Nonlinear functions of h_{max25} and models with two predictor variables were close competitors to the best model for Lorey's height. However, there are reasons to support the use of the simple, linear model, even given its model selection uncertainty. First, the high model selection uncertainty is likely due to the large number of candidate models I

included in this analysis. Second, lidar measures height directly (Lefsky et al. 2002b), and other studies have found strong linear relationships ($r^2 > 90\%$) between lidar height metrics and stand height (Means et al. 1999, 2000, Holmgren et al. 2003).

My capacity to predict canopy base height (CBH) from lidar metrics was limited. The fit of the original best model was very good, but this seemed to be dominated by two sites with extreme values. Given the consistency of results with and without the large value, and the lack of fit without both extremes, I conclude that lidar has the potential to predict CBH in areas where there is a wide range of observed values. Naesset and Økland (2002) explained 71% of the variability in mean crown height in a boreal forest, where values had a range of 6.3 m. More work is needed to generate useful models to predict this variable using lidar, as it is unclear why the best model selected in this study should describe CBH as proportional to the variability in stand height and inversely proportional to that height.

Some lidar studies have found nonlinear relationships between lidar metrics and aboveground biomass (Lefsky et al. 1999b, 2002a, Naesset 2002) and basal area (Naesset 2002). These were generally masked by the use of log-transformed equations, the use of squared or cubic values of the lidar metrics as predictor variables, and the presentation of plots of observed vs. predicted, rather than field values vs. lidar metric values. My initial results seemed to support this: a nonlinear regression was the best model for all four biomass structure variables and canopy bulk density (Table 2.4). The predictor variable ($P_{G/1}$) is inversely related to canopy closure (Table 2.3). It is possible that in these forests with relatively low biomass density (Peet 2000), the correlation between cover and biomass characteristics is stronger than in high biomass systems, where most lidar studies

have been developed (Lefsky et al. 1999b, Means et al. 1999, Drake et al. 2002). This might explain the selection of this predictor variable.

However, there are factors that suggest that the selection of a nonlinear model to describe biomass structure could simply be an artifact of my sample. First, my field data were clumped at the lower end of the range of biomass structure and density values. Second, other studies have found increasing variability in the predictions of biomass from lidar metrics as biomass levels increase (Lefsky et al. 1999a, b, Drake et al. 2002). Third, the sites with greatest biomass values were the four sites with highest tree density. I estimated biomass from a sample of trees at these sites (see **Methods**). At high density sites, this sample was a small proportion of the total tree population (three sites had less than 5% sample). Deviations between sample mean tree biomass and the true mean tree biomass were also inflated in these high density sites by the way I calculated per hectare biomass values. These factors, combined with outlier and leverage diagnostics, led me to refit and rerank the models without the four largest values plus one other leverage point, to test the sensitivity of the relationships to these sites (Table 2.6). The possibility that the error in four of these values is large led me to consider this a necessary step in arriving at my conclusions. This restriction of the domain tends to increase the fit of linear models. I have presented the most parsimonious models, based on the information provided by the information-theoretic approach (Table 2.6).

All the top models for total aboveground biomass are linear functions. Theoretically, the combination of a height metric with a cover metric provides the three-dimensional information needed to estimate biomass without saturation of the relationship at high biomass values. This supports the use of lidar to obtain nonsaturating

relationships to estimate total biomass, though the values represented in this restricted dataset are within the range that can be estimated using optical sensors (<150 Mg/ha; Waring et al. 1995).

My capacity to estimate basal area with lidar data is due to the correlation between basal area and total amount of reflecting surfaces in the stand (i.e. total biomass), rather than a direct measurement. Eight of the top models for basal area included an interaction term. The difficulty in clearly interpreting these models, combined with the similarity of some of the close competitors to the models selected for total aboveground biomass, led me to conclude that the most practical model to predict basal area in this system is a linear function of a height metric and a cover-related metric (Table 2.6). The selection of this model simplified the subset of potentially useful lidar metrics. The variability left unexplained by these models is likely also due to sampling error, given the methodology I used to estimate basal area.

The best model for tree density, selected with the restricted dataset, was still a nonlinear function of a metric inversely related to canopy cover (Table 2.6). These estimates were the least robust (Table 2.5). This could be due to errors in its estimation on the ground, particularly if trees are not randomly distributed, as assumed by the point-centered quarter method. It is possible to combine tree density and individual tree sizes in a variety of ways resulting in similar amounts of reflecting surfaces, which would also make it difficult to consistently predict density from lidar metrics. Naesset and Bjerkes (2001) found similar low fit for their regression model for density of young Norway spruce and Scots pine plantations. A close competitor to the best model (based on the restricted dataset) that had similar support and goodness of fit (r^2 and standard errors) was

a linear function of the same lidar metric. I therefore consider that there is potential for obtaining linear relationships to estimate tree density using discrete-return lidar. More work needs to be done in this area, since the indirectness of the relationship between the information gathered by the sensor and tree density might determine that relationships are consistent only over a very limited range of conditions.

Two of the top four models for foliage biomass were linear functions of the canopy cover metric in the original best model, combined with a height metric and the height to the base of the canopy metric. In both cases the confidence limits of the coefficient for the height metric straddled zero. *A posteriori*, I fit a linear regression based solely on the metrics related to cover and canopy base height (r^2 = 58.7%, SE = 0.13). Its capacity to explain the variability in foliage biomass is a strong indicator of its potential for prediction, and should be considered in further studies of this kind. The linear function of the canopy cover metric in the original best model has a similar goodness of fit (Table 2.6), proving the most parsimonious *a priori* model. These results support the use of linear models to estimate foliage biomass from discrete-return lidar.

Canopy bulk density, critical for fire behavior modeling (Scott and Reinhardt 2001), is related to foliage biomass and canopy volume. My dataset is likely too small to provide parsimonious model selection (Burnham and Anderson 2002). Though the best model was nonlinear, linear functions of the cover related metric ($P_{G/1}$) and a biomass density metric (δ_{12}) had slight support. I suggest that further studies aimed at estimating canopy bulk density will prove discrete-return lidar's capacity to estimate this variable with models that do not saturate at high values.

This exploratory analysis has allowed me to present regression models that explain a substantial portion of the variability in the stand structural variables I was interested in. I have also selected a subset of the 39 lidar metrics analyzed. Based on the best selected models, the position of confidence intervals of parameters relative to zero, the need to avoid overfitting the data and the capacity of metrics to predict a variety of structural variables, I have selected a subset of 14 lidar metrics (Table 2.7). I recommend that further studies concentrate on these metrics as useful predictors of stand structural variables in ponderosa pine forests.

CONCLUSIONS

This study confirmed discrete-return lidar's capacity to measure stand height, and identified the fraction of the tallest 1st returns that directly relate to Lorey's height in these ponderosa pine forests. The selected linear models offer useful estimates of total aboveground biomass, basal area and foliage biomass. The models selected for tree density provide an initial estimate, though the lack of a direct relationship between characteristics measured by lidar sensors and this variable makes more research in this area necessary. Using lidar to predict canopy base height and canopy bulk density is still an unresolved issue. My results suggest that there is potential, and studies with a greater number of samples, evenly stratified across the complete range of values found in these forests, will hopefully identify the necessary predictor variables and functional relationships.

I identified a subset of lidar metrics that should be considered in future studies. The use of an information-theoretic approach to model selection provided me with a

wealth of information on model and variable ranking. I consider this approach particularly useful, and its application to this study gives me confidence that the selected lidar metrics have potential as predictors of stand structure.

In a broader context, my results are consistent with other studies using lidar. I agree that lidar can provide estimates of forest biomass based on nonsaturating relationships, though I highlight the need to carefully interpret the results presented to support this. My results also provide some insight into the importance of carrying out lidar studies in a variety of ecosystems, and of broadening the focus of future studies to include low biomass forests, where the best lidar metrics may not be the same as in high density forests. Low biomass systems have been mostly neglected, as lidar studies have focused on accurately estimating high levels of biomass (Lefsky et al. 1999a, Drake et al. 2002), or on commercial forestry inventories (Naesset 2002). I have addressed this issue, and my results support the need for more studies in low density systems.

The number of extreme fires in forests in the western United States highlights the need to increase our understanding of the effect of stand structure and its spatial arrangement on fire behavior. Spatially explicit estimates of tree density, canopy base height and canopy bulk density are required to focus efforts of forest restoration and fuels mitigation treatments. I hope that this will provide the necessary motivation for these studies to be carried out.

REFERENCES

Attiwill, P.M., 1994. The disturbance of forest ecosystems: the ecological basis for conservative management. For. Ecol. Manage. 63, 247-300.

Baltsavias, E.P., 1999a. Airborne laser scanning: basic relations and formulas. ISPRS J. Photogramm. Rem. Sens. 54, 199-214.

Baltsavias, E.P., 1999b. Airborne laser scanning: existing systems and firms and other resources. ISPRS J. Photogramm. Rem. Sens. 54, 164-198.

Baret, F., Guyot, G., 1991. Potentials and limits of vegetation indexes for LAI and APAR assessment. Rem. Sens. Environ. 35, 161-173.

Brown, P.M., D'Amico, D.R., Carpenter, A.T., Andrews, D., 2001. Restoration of montane ponderosa pine forests in the Colorado Front Range. Ecol. Restoration 19, 19-26.

Burnham, K.P., Anderson, D.R., 2002. Model selection and multimodel inference - A practical information-theoretic approach. Springer-Verlag, New York, USA.

Cohen, W.B., Spies, T.A., 1992. Estimating structural attributes of Douglas-fir/western hemlock forest stands from Landsat and SPOT imagery. Rem. Sens. Environ. 41, 1-17.

Cooper, C.F., 1960. Changes in vegetation, structure, and growth of southwestern pine forests since white settlement. Ecol. Monog. 30, 129-164.

Cottam, G., Curtis, J.T., 1956. The use of distance measures in phytosociological sampling. Ecology 37, 451-460.

Covington, W.W., Moore, M.M., 1994. Postsettlement changes in natural fire regimes and forest structure: ecological restoration of old-growth ponderosa pine forests. In: Sampson, R. N., Adams, D. L. (Eds.), Assessing forest ecosystem health in the Inland West. The Haworth Press Journal Co-Editions, New York, New York, USA, pp. 153-181.

DeGraaf, R.M., Hestbeck, J.B., Yamasaki, M., 1998. Associations between breeding bird abundance and stand structure in the White Mountains, New Hampshire and Maine, USA. For. Ecol. Manage. 103, 217-233.

Dobson, M.C., 2000. Forest information from synthetic aperture radar. J. For. 98, 41-43.

Drake, J.B., Dubayah, R.O., Clark, D.B., Knox, R.G., Blair, J.B., Hofton, M.A., Chazdon, R.L., Weishampel, J.F., Prince, S.D., 2002. Estimation of tropical forest characteristics using large-footprint lidar. Rem. Sens. Environ. 79, 305-319.

Drake, J.B., Knox, R.G., Dubayah, R.O., Clark, D.B., Condit, R., Blair, J.B., Hofton, M., 2003. Above-ground biomass estimation in closed canopy Neotropical forests using lidar remote sensing: factors affecting the generality of relationships. Global Ecol. Biogeog. 12, 147-159.

Dubayah, R.O., Drake, J.B., 2000. Lidar remote sensing for forestry. J. For. 98, 44-46.

Edminster, C.B., Beeson, R.T., Metcalf, G.E., 1980. Volume tables and point sampling factors for ponderosa pine in the Front Range of Colorado. USDA Forest Service Research Paper RM-218.

Flannigan, M.D., Van Wagner, C.E., 1991. Climate change and wildfire in Canada. Can. J. For. Res. 21, 66-72.

Flood, M., Gutelius, B., 1997. Commercial implications of topographic terrain mapping using scanning airborne laser radar. Photogramm. Eng. Rem. Sens. 63, 327-366.

Franklin, S.E., 2001. Remote sensing for sustainable forest management. CRC Press LLC, Boca Raton, Florida, USA.

Fulé, P.Z., Waltz, A.E.M., Covington, W.W., Heinlein, T.A., 2001. Measuring forest restoration effectiveness in reducing hazardous fuels. J. For. 99, 24-29.

Gholz, H.L., Grier, C.C., Campbell, A.G., Brown, A.T., 1979. Equations for estimating biomass and leaf area of plants in the Pacific Northwest. Forest Research Lab, School of Forestry, Oregon State University. Research Paper 41.

Hershey, K.T., Meslow, E.C., Ramsey, F.L., 1998. Characteristics of forests at spotted owl nest sites in the Pacific Northwest. J. Wildl. Manage. 62, 1398-1410.

Holmgren, J., Nilsson, M., Olsson, H., 2003. Estimation of tree height and stem volume on plots using airborne laser scanning. For. Sci. 49, 419-428.

Houghton, R.A., Hackler, J.L., Lawrence, K.T., 2000. Changes in terrestrial carbon storage in the United States. 2. The role of fire and fire management. Global Ecol. Biogeog. 9, 145-170.

Hughes, R.F., Kauffman, J.B., Cummungs, D.L., 2000. Fire in the Brazilian Amazon. 3. Dynamics of biomass, C, and nutrient pools in regenerating forests. Oecologia 124, 574-588.

Husch, B., Beers, T.W., Kershaw, J.A.Jr., 2003. Forest Mensuration. John Wiley and Sons, Inc. Hoboken, New Jersey, USA.

Kaufmann, M.R., Regan, C.M., Brown, P.M., 2000. Heterogeneity in ponderosa pine/Douglas fir forests: age and size structurre in unlogged and logged landscapes of central Colorado. Canadian Journal of Forest Research 30, 698-711.

Keane, R.E., Arno, S.F., Brown, J.K., 1990. Simulating cumulative fire effects in ponderosa pine/Douglas-fir forests. Ecology 71, 189-203.

Lefsky, M.A., Cohen, W.B., Acker, S.A., Parker, G.G., Spies, T.A., Harding, D., 1999a. Lidar remote sensing of the canopy structure and biophysical properties of Douglas-fir western hemlock forests. Rem. Sens. Environ. 70, 339-361.

Lefsky, M.A., Cohen, W.B., Harding, D.J., Parker, G.P., Acker, S.A., Gower, S.T., 2002a. Lidar remote sensing of above-ground biomass in three biomes. Global Ecol. Biogeog. 11, 393-399.

Lefsky, M.A., Cohen, W.B., Parker, G.G., Harding, D.J., 2002b. Lidar remote sensing for ecosystem studies. BioSci. 52, 19-30.

Lefsky, M.A., Cohen, W.B., Spies, T.A., 2001. An evaluation of alternate remote sensing

products for forest inventory, monitoring, and mapping of Douglas fir forests in western Oregon. Can. J. For. Res. 31, 78-87.

Lefsky, M.A., Harding, D., Cohen, W.B., Parker, G., Shugart, H.H., 1999b. Surface lidar remote sensing of basal area and biomass in deciduous forests of eastern Maryland, USA. Rem. Sens. Environ. 67, 83-98.

Lindgren, B.W., 1993. Statistical Theory. Chapman and Hall, New York, USA.

Magnussen, S., Boudewyn, P., 1998. Derivations of stand heights from airborne laser scanner data with canopy-based quantile estimators. Can. J. For. Res. 28, 1016-1031.

Means, J.E., Acker, S.A., Fitt, B.J., Renslow, M., Emerson, L., Hendrix, C.J., 2000. Predicting forest stand characteristics with airborne scanning lidar. Photogramm. Eng. Rem. Sens. 66, 1367-1371.

Means, J.E., Acker, S.A., Harding, D.J., Blair, J.B., Lefsky, M.A., Cohen, W.B., Harmon, M.E., McKee, W. A., 1999. Use of large footprint scanning airborne lidar to estimate forest stand characteristics in the Western Cascades of Oregon. Rem. Sens. Environ. 67, 298-308.

Moore, M.M., Covington, W.W., Fulé, P.Z., 1999. Reference conditions and ecological restoration: a southwestern ponderosa pine perspective. Ecol. Appl. 9, 1266-1277.

Naesset, E., 2002. Predicting forest stand characteristics with airborne scanning laser using a practical two-stage procedureand field data. Rem. Sens. Environ. 80, 88-99.

Naesset, E., Bjerknes, K.-O., 2001. Estimating tree heights and number of stems in young forest stands using airborne laser scanner data. Rem. Sens. Environ. 78, 328-340.

Naesset. E., Økland, T., 2002. Estimating tree height and tree crown properties using airborne scanning laser in a boreal nature reserve. Rem. Sens. Environ. 79, 105-115.

Overpeck, J.T., Rind, D., Goldberg, R., 1990. Climate-induced changes in forest disturbance and vegetation. Nature 343, 51-53.

Page, S.E., Slegert, F., Rieley, J.O., Boehm, H.-D.V., Jaya, A., Limin, S., 2002. The amount of carbon released from peat and forest fires in Indonesia during 1997. Nature 420, 61-65.

Paré, D., Bergeron, Y., 1995. Above-ground biomass accumulation along a 230-year chronosequence in the southern portion of the Canadian boreal forest. J. Ecol. 83, 1001-1007.

Peet, R.K., 2000. Forests and meadows of the Rocky Mountains. In: Barbour, M.G., Billings, W.D.e. (Eds.), North American terrestrial vegetation. Cambridge University Press, Cambridge, U.K..

Perry, G.L.W., 1998. Current approaches to modelling the spread of wildland fire: a review. Prog. Phys. Geog. 22, 222-245.

Sando, R.W., Wick, C.H., 1972. A method of evaluating crown fuels in forest stands. U. S. Forest Service Research Paper, p. 10.

Scott, J.H., Reinhardt, E.D., 2001. Assessing crown fire potential by linking models of surface and crown fire behavior. U.S. Forest Service, Rocky Mountain Research Station Research Paper.

Spanner, M., Johnson, L., Miller, J., McCreight, R., Fremantle, J., Runyon, J., Gong, P., 1994. Remote sensing of seasonal leaf area index across the Oregon transect. Ecol. Appl. 4, 258-271.

Sprugel, D.G., 1983. Correcting for bias in log-transformed allometric equations. Ecology 64, 209-210.

Stoker, J.M., 2002. Evaluating small-footprint multiple-return lidar to indentify individual tree characteristics. Thesis. Colorado State University, Fort Collins, Colorado, USA.

Ter-Mikaelian, M.T., Korzukhin, M.D., 1997. Biomass equations for sixty-five North American tree species. For. Ecol. Manage. 97, 1-24.

Tilman, D., Reich, P., Phillips, H., Menton, M., Patel, A., Vos, E., Peterson, D., Knops, J., 2000. Fire suppression and ecosystem carbon storage. Ecology 81, 2680-2685.

van Wagner, C.E., 1977. Conditions for the start and spread of crown fire. Can. J. For. Res. 7, 23-34.

van Wagner, C.E., 1993. Prediction of crown fire in two stands of jack pine. Can. J. For. Res. 23, 442-449.

Waring, R.H., Way, J.B., Hunt, E.R.Jr., Morrissey, L., Ranson, K.J., Weishampel, J.F., Oren, R., Franklin, S.E., 1995. Imaging radar for ecosystem studies. BioSci. 45, 715-723.

Weaver, H., 1959. Ecological changes in the ponderosa pine forest of the Warm Springs Indian Reservation on Oregon. J. For. 57, 15-20.

Wirth, C., Schulze, E.-D., Schulze, W., von Stunzner-Karbe, D., Ziegler, W., Miljukova, I.M., Sogatchev, A., Varlagin, A.B., Panvyorov, M., Grigoriev, S., Kusnetzova, W., Siry, M., Hardes, G., Zimmermann, R., Vygodskaya, N.N., 1999. Above-ground biomass and structure of pristine Siberian Scots pine forests as controlled by competition and fire. Oecologia 121, 66-80.

Wulder, M., 1998. Optical remote-sensing techniques for the assessment of forest inventory and biophysical parameters. Prog. Phys. Geog. 22, 449-476.

Table 2.1. Range of topographic, stand and biomass structure conditions covered by the field data.

Variables	Average	Minimum	Maximum
Slope (%)[1]	32	17	57
Aspect (° from N) [1]	157	37	311
Elevation (m a.s.l.) [1]	2236	2157	2417
Area of site (ha)	0.32	0.16	0.75
Mean height (m)	12.6	8.1	17.2
Lorey's height (m)	15.7	12.7	21.2
Tree density (trees/ha)	329.7	90.0	1932.1
Basal area (m^2/ha)	19.4	9.8	73.1
Foliage biomass (Mg/ha)	7.4	3.3	31.1
Tree aboveground biomass (Mg/ha)	105.4	51.1	396.4
Canopy bulk density (kg/m^3) [1]	0.102	0.028	0.306
Canopy base height (m) [1]	3.3	0.45	11.25

[1] Only measured in the dataset collected in the summer of 2001 (14 sites). The rest of the variables were estimated for all 41 sites.

Table 2.2. Allometric equations used to calculate foliage and total aboveground biomass for individual trees; mean tree values were multiplied by estimated tree density to provide stand level values.

Biomass component	Allometric equations[1]	Reference
Pinus ponderosa		
Bole biomass (without bark)	$BB=BV x \delta_w$ $BV=3.25x10^{-5}DBH^2H$ $\delta_w=537.58$ kg/m^3	Edminster et al. 1980 this study
Bark biomass on bole	lnBkB=-4.2063+2.2312lnDBH	Gholz et al. 1979
Foliage biomass	$FB^2=(0.1167DBH^{1.5774})x1.112$	Ter-Mikaelian and Korzukhin 1997
Branch biomass	$BrB^2=(0.0469DBH^{2.1315})x1.172$	Ter-Mikaelian and Korzukhin 1997
Total aboveground biomass	TAB=BB+BkB+FB+BrB	
Pseudotsuga menziesii		
Bole biomass (without bark)	lnBB=-3.0396+2.5951lnDBH	Gholz et al. 1979
Bark biomass on bole	lnBkB=-4.3103+2.43lnDBH	Gholz et al. 1979
Foliage biomass	$FB^2=(0.3021DBH^{1.3076})x1.158$	Ter-Mikaelian and Korzukhin 1997
Branch biomass	$BrB^2=(0.2624DBH^{1.5464})x1.244$	Ter-Mikaelian and Korzukhin 1997
Total aboveground biomass	TAB=BB+BkB+FB+BrB	

[1] BB: bole biomass (kg), BkB: bark biomass (kg), FB: foliage biomass (kg), BrB: branch biomass (kg), TAB: total aboveground biomass (kg), DBH: diameter at breast height (cm), H: height (m), BV: bole volume (m^3), δ_w: wood density, ln: natural log.
[2] The constant by which the equation is multiplied is a bias correction factor published with these equations, as the models were fit as log transformed variables.

Table 2.3. Composite metrics derived from discrete cloud of lidar points to represent forest biophysical parameters. These metrics were used in models to predict stand structural variables.

Biophysical parameter represented		LiDAR-based metrics
Height	Mean tree height	h_{25}: mean height of all 1st "vegetation" returns from multiple-return pulses, with height > 3 m [1]. h_{35}: mean height of all 1st "vegetation" returns from pulses with 3 or more returns, with height > 3 m [1].
	Mean canopy height	h_1: mean height of all 1st returns classified as vegetation. h_3: mean height of all 1st returns with height > 3 m [1]. h_{12}: mean height of all 1st "vegetation" returns from 2-return pulses. h_{13}: mean height of all 1st "vegetation" returns from 3-return pulses. h_{1m}: mean height of all 1st "vegetation" returns from multiple-return pulses. QMCH: quadratic mean canopy height: mean standardized intensities [2] per height bin (0.5 m), weighed by the square of the height of the bin. [3] CH: mean height of the highest "vegetation" return in each m^2.
	Maximum tree height	h_{max}: height of the highest return in the site.
	Cumulative canopy height	h_{maxi}: mean height of the highest *i* % of 1st "vegetation" returns (*i* = 5, 10, 25, 50, 75, 90, 95).
	Median canopy height	medCH: height of the midpoint of the 0.5 m tall height bin with 50% of cumulative standardized intensity of returns (defined in Appendix 2.1) above it and 50% below it.
Crown height		HC: height of the midpoint of the 0.5 m tall bin with the minimum number of "vegetation" returns.
Variability in canopy height		SD_{h3} [4]: standard deviation in height of returns used to calculate h_3. CV_{h3}: SD_{h3}/h_3. $range_{h3}$ [4]: range of heights of returns used to calculate h_3. rel-$range_{h3}$: $range_{h3}/h_3$.

Table 2.3. *continued*

Biophysical parameter represented	LiDAR-based metrics
Biomass density	CRS: canopy reflection sum: sum of intensity of all returns reflected by the canopy. [3] CRS_3: canopy reflection sum, considering only returns higher that 3 m [1]. rel-CRS_1: canopy reflection sum relative to total reflection intensity (i.e. reflected by both the canopy and the ground). [3] rel-CRS_2: rel-CRS_1, corrected for ground surface reflectance (*sensu* Lefsky et al. 1999b). [3] wCRS: weighted canopy reflection sum: similar to CRS, but the intensity of each return is weighed by the inverse of its height above the ground. [3] RperP: number of "vegetation" returns, relative to the number of pulses. δ_{veg}: number of "vegetation" returns per unit area. δ_{12}, δ_{13}, δ_{1m}: number of 1st "vegetation" returns from pulses with 2, 3, or multiple returns, respectively, per unit area. δ_3: number of returns with height > 3 m [1] per unit area (initially considered metric for tree density).
Canopy cover	CR_1: proportion of total energy returned reflected by the canopy. [3] CR_2: CR_1, corrected for ground surface reflectance (assumed to be half the reflectance of the canopy; *sensu* Lefsky et al. 1999b). [3] δ_{11}: density of returns from 1-return pulses. $P_{G/1}$: proportion of ground returns that are also 1st returns. $P_{1/G}$: proportion of 1st returns that are also ground returns.

[1] Height threshold follows sampling decisions in the field: only trees greater than 3 m in height were sampled.
[2] Standardized intensities: intensity of a single return, expressed as the proportion of the total intensity returned for that particular pulse.
[3] Rationale and calculations developed in Appendix 2.1.
[4] Absolute measures of variability.

Table 2.4. Top models describing each stand structure variable.

Stand structure (dependent) variable	Best regression model [1]	Coefficients (standard error) b_0	b_1	b_2	c	w_r [2]	r^2 [3]	SE [4]	Number of competing models [5]	Predictor variables in competing models [6]
Mean stand height (m)	$b_0+b_1h_{max50}+b_2SD_{h3}$ (5)	4.52 (1.40)	0.82 (0.12)	-0.78 (0.36)		0.09	57.1	1.18	11	h_{max75} (2), $_{95, 90, 25, 10}$, CV_{h3}, $range_{h3}$ (1)
Lorey's height (m)	$b_0+b_1h_{max25}$ (9)	1.90 (0.87)	0.86 (0.05)			0.16	86.8	0.69	8	SD_{h3}, $range_{h3}$ (2), CV_{h3}, $rel\text{-}range_{h3}$ (1)
Total aboveground biomass (Mg/ha)	$b_1P_{G/l}{}^c$ (2)		35.79 (3.61)		-2.67 (0.25)	0.56	74.2	0.20	1	-
Foliage biomass (Mg/ha)	$b_1P_{G/l}{}^c$		2.06 (0.20)		-3.06 (0.25)	>0.99	79.4	0.20	0	-
Basal area (m^2/ha)	$b_1P_{G/l}{}^c$		6.17 (0.57)		-2.76 (0.23)	>0.99	78.5	0.19	0	-
Tree density (trees/ha)	$b_1P_{G/l}{}^c$		56.39 (9.94)		-3.94 (0.44)	>0.99	67.2	0.36	0	-
Canopy base height (m)	$b_0+b_1h_{1m}+b_2SD_{h3}$ (1)	0.27 (1.83)	-0.57 (0.08)	2.20 (0.51)		0.39	79.8	0.36	1	h_{13}, $range_{h3}$ (1)
Canopy bulk density (kg/m^3)	$b_1P_{G/l}{}^c$		0.018 (0.004)		-3.45 (0.45)	0.56	82.8	0.32	0	-

[1] Independent variables follow names in Table 2.3. In parentheses is the number of competing models these variables formed part of.
[2] Akaike weights (probability that the model would be selected as the best model from the same candidate set, given another dataset).
[3] Coefficient of determination of the regression. Values are in natural log space for all variables except mean stand height and Lorey's height.
[4] Standard error of estimates. Values are in natural log space for all variables except mean stand height and Lorey's height (m).
[5] Competing models are defined as those within 3 AIC_c units of the best model (number does not include the best model).
[6] Variables are ordered by the number of competing models they form part of, which is shown in parentheses.

Table 2.5. Goodness of fit of original best models when fitted to the restricted datasets. I restricted the data by eliminating five leverage points (the same five for all response variables), to determine their effect on model parameters and ranking.

Dependent variable	N	r^2 [1]	SE [2]
Total aboveground biomass (Mg/ha)	36	37.9	0.18
Foliage biomass (Mg/ha)	36	53.8	0.14
Basal area (m^2/ha)	36	48.1	0.14
Tree density (trees/ha)	36	33.8	0.26

[1] Coefficient of determination of the regression (in natural log space).
[2] Standard error of estimates (in natural log space).

Table 2.6. Most parsimonious model describing each stand structure variable, fitted to the restricted datasets [N=36 for all variables except canopy base height (N=12)]. I restricted the data to determine their effect on model parameters and ranking. I eliminated five leverage points for all four C stock variables (the same five for all response variables). For canopy base height, I eliminated one high value, subjectively considered a potential outlier.

Stand structure (dependent) variable	Best regression model [1]	Coefficients (standard error)			w_r [2]	r^2 [3]	SE [4]	Distance from best model [5]	Number of competing models [6]	Predictor variables in competing models [7]
		b_0	b_1	b_2						
Total aboveground biomass (Mg/ha)	$b_0+b_1CH+b_2P_{I/G}$ (2) (4)	90.62 (14.96)	9.33 (1.63)	-185.0 (31.06)	0.11	58.1	0.14	0	6	CR_2 (3), h_{max95}, $_{90}$ (2), h_I (1)
Foliage biomass (Mg/ha)	$b_0+b_1P_{G/I}$ (4)	17.63 (1.83)	-16.64 (2.53)		0.04	54.5	0.14	0.6	3	HC (2), h_{max}, h_{25} (1)
Basal area (m^2/ha)	$b_0+b_1CH+b_2P_{I/G}$ (2) (6)	19.43 (2.51)	1.12 (0.27)	-30.3 (5.27)	0.03	49.8	0.14	1.3	14	medCH, h_{max90} (4), RperP (3), rel-CRS_2, h_{max95}, $P_{G/I}$ (2), h_I, rel-CRS_I (1)
Tree density (trees/ha)	$b_0+b_1P_{I/G}$ (2)	418.5 (50.41)	-482.7 (110.1)		0.25	34.9	0.26	1.1	3	$P_{G/I}$ (2)
Canopy base height (m)	$b_0+b_1h_{1m}+b_2SD_{h3}$ (2)	1.75 (2.06)	-0.54 (0.07)	1.70 (0.56)	0.37	76.2	0.33	0	3	h_{13} (1)

[1] Independent variables follow names in Table 2.3. In parentheses is the number of competing models these variables formed part of.
[2] Akaike weights (probability that the model would be selected as the best model from the same candidate set, given another dataset).
[3] Coefficient of determination of the regression (in natural log space).
[4] Standard error of estimates (in natural log space).
[5] Distance, in AIC_c units, that the most parsimonious model is from the model ranked as best.
[6] Competing models are defined as those within 3 AIC_c units of the best model (number does not include the selected model).
[7] Variables are ordered by the number of competing models they form part of, which is shown in parentheses.

Table 2.7. Lidar metrics that were useful predictors of stand structure variables.

Stand structure variable represented	Useful predictors (lidar-based metrics [1])
Mean height	h_{max50}, h_{max95}, h_{max90}, h_{max25}, h_{max10}, SD_{h3}, $range_{h3}$
Lorey's height	h_{max25}, SD_{h3}, $range_{h3}$
Total aboveground biomass	h_{max95}, h_{max90}, CH, h_1, $P_{G/1}$, $P_{1/G}$
Foliage biomass	$P_{G/1}$, HC
Basal area	h_{max90}, h_{max95}, CH, h_1, $P_{G/1}$, $P_{1/G}$
Tree density	$P_{G/1}$, $P_{1/G}$
Canopy bulk density	$P_{G/1}$
Canopy base height	h_{1m}, h_{13}, SD_{h3}, $range_{h3}$

[1] Names of lidar metrics described in Table 2.3.

Figure 2.1. Observed values of stand height versus values predicted by the best regression model. **(a)** Mean height of sampled trees. **(b)** Basal-area-weighed average height (Lorey's height) of sampled trees. Full and empty squares represent the two sets of data used (14 and 27 points, respectively). The solid gray line represents the 1:1 line, where observed = predicted. The dotted black lines are the limits of the 95% prediction intervals for the plotted model. Models are presented in Table 2.4.

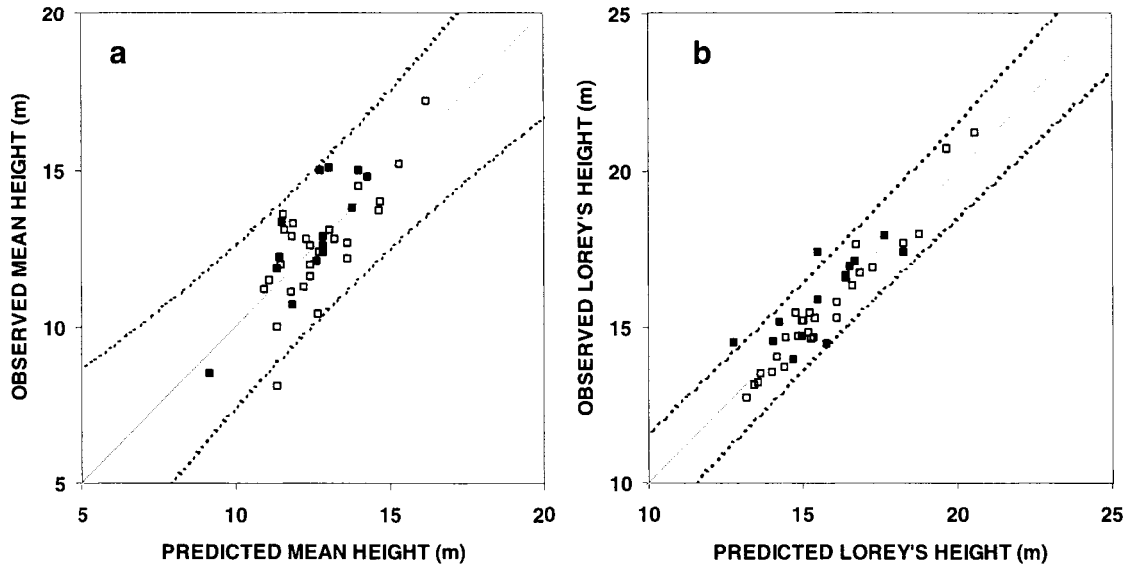

Figure 2.2. Observed values of biomass structure variables versus values predicted by the best regression model. The biomass structure variables analyzed were: **(a)** total tree aboveground biomass (Mg/ha); **(b)** foliage biomass (Mg/ha); **(c)** basal area (m^2/ha); **(d)** tree density (trees/ha). Full and empty squares represent the two sets of data used (14 and 27 points, respectively). The solid gray line represents the 1:1 line, where observed = predicted. The dotted black lines are the limits of the 95% prediction intervals for the plotted model. Model coefficients are presented in Table 2.4.

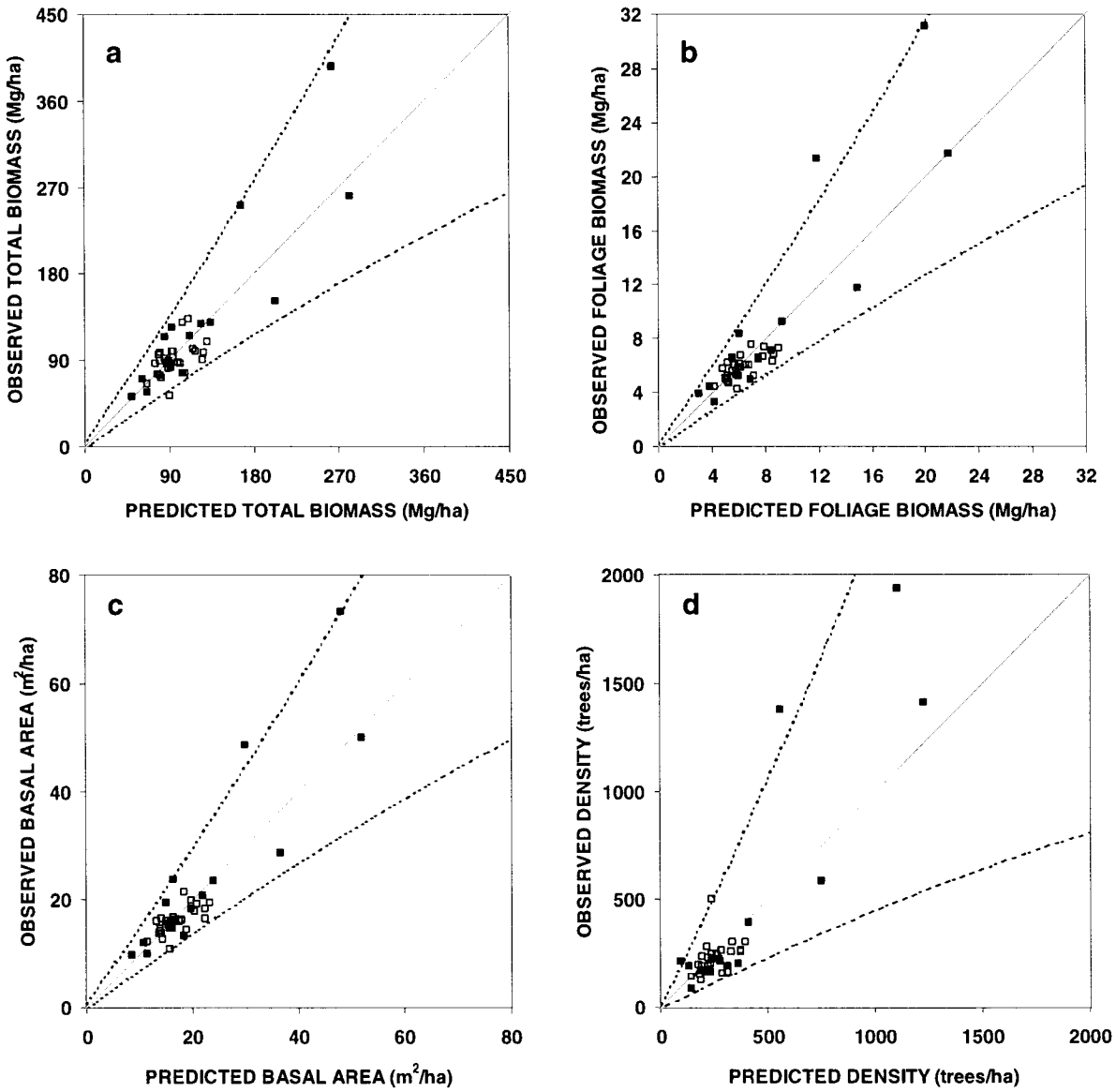

Figure 2.3. Observed values of canopy base height (CBH) versus values predicted by the best regression model, in natural log space. The arrows identify the two points I suspected might have undue influence on the regression fit and model ranking. The solid gray line represents the 1:1 line, where log (observed) = log (predicted). The dotted black lines are the limits of the 95% prediction intervals for the original best model (N=13). The model is presented in Table 2.4.

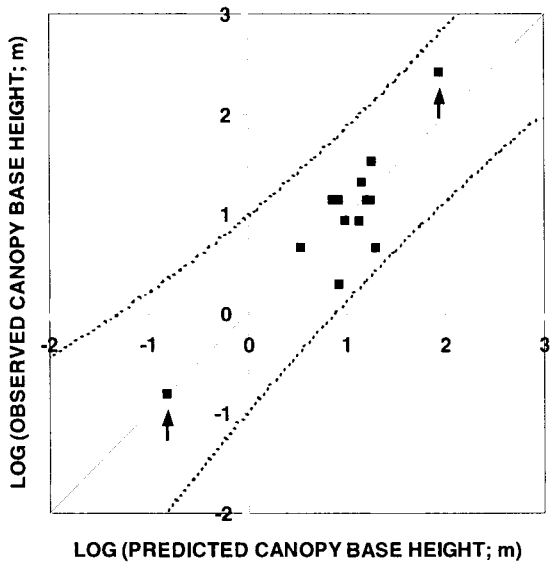

APPENDIX 2.1 – DESCRIPTION AND CALCULATION OF COMPLEX LIDAR METRICS (see Table 2.3)

CRS: canopy reflection sum. *Rationale:* this metric is analogous to variable by the same name defined by Means et al. 1999.

$$CRS = \frac{\sum_{i=1}^{N} I_i}{A}$$

(For all symbol descriptions, see Table A.2.1).
rel-CRS$_1$: relative canopy reflection sum. *Rationale:* Expressing CRS relative to the intensity of returns from the canopy and the ground should incorporate the effect of variations in canopy cover.

$$relCRS_1 = \frac{\sum_{i=1}^{N} I_i}{\sum_{i=1}^{T} I_i} \times \frac{1}{A}$$

rel-CRS$_2$: corrected relative canopy sum. *Rationale:* assuming the ground is covered in litter, the reflectance at 1064 nm of the ground is approximately half the reflectance of the green canopy (*sensu* Lefsky et al. 1999b).

$$relCRS_2 = \frac{\sum_{i=1}^{N} I_i}{\sum_{i=1}^{T} (I_i \times \rho)} \times \frac{1}{A}$$

wCRS: the weighted canopy reflection sum. *Rationale:* number and size of trees taper off high in the canopy (i.e. less biomass). In the center of a crown one return may be representative of the area around it, this is less likely at higher points in the canopy. This metric weighs the intensity of each return by the inverse of the height of that return. This will weigh returns closer to the ground more heavily, potentially correcting for the attenuation of incoming radiation close to the ground. I limited the vegetation returns to those above 3 m, to avoid over-weighing returns from understory vegetation. It is necessary to divide the weighted sum by the area of the sample site to make this metric comparable across sites of variable area.

$$wCRS = \left[\sum_{i=1}^{M} \left(I_i \times \frac{1}{z_i} \right) \right] \times \frac{1}{A}$$

QMCH: quadratic mean canopy height. *Rationale:* This metric is analogous to the variable by the same name defined by Lefsky et al. (1999b), modified to apply to discrete

return lidar data. This metric is based on the standardized intensity of returns with heights > 3 m. It is necessary to divide the weighted sum by the area of the sample site to make this metric comparable across sites of variable area.

$$QMCH = \left(\sqrt{\sum_{i=1}^{\max h} B_i \times h_i^{\,2}} \right) \times \frac{1}{A}$$

CR_1: proportion of energy returned by the canopy. *Rationale:* analogous to the inverse of the ground return ratio defined by Drake et al. (2002), modified for discrete return lidar.

$$\text{For pulse } i,\ CR_{1i} = \frac{\sum_{j=1}^{v} I_{ij}}{\sum_{k=1}^{t} I_{ik}} \qquad \text{For the site, } CR_1 = \frac{\sum_{i=1}^{P} CR_{1i}}{P}$$

CR_2: proportion of energy returned by the canopy, corrected for variations in reflectance (*sensu* Lefsky et al. 1999b).

$$\text{For pulse } i,\ CR_{2i} = \frac{\sum_{j=1}^{v} I_{ij}}{\sum_{k=1}^{t} I_{ik} \times \rho} \qquad \text{For the site, } CR_2 = \frac{\sum_{i=1}^{P} CR_{1i}}{P}$$

Table A.2.1. Symbols used in equations for lidar metrics, described in Appendix 2.1.

Symbol	Definition
A	Area of the sampled site.
M	Number of vegetation returns in a site with height > 3 m.
N	Total number of vegetation returns in a site.
v	Number of vegetation returns within pulse i.
T	Total number of returns (vegetation + ground) in a site.
t	Total number of returns (vegetation or ground) within pulse i.
I_i	Intensity (in raw counts) of return i.
I_{ij}	Intensity of vegetation return j of pulse i.
I_{ik}	Intensity of return k (vegetation or ground) of pulse i.
z	Height above the ground of return i (ground returns have z = 0).
B_i	Sum of the standardized intensities of all returns classified as vegetation within height bin i. I standardized the intensities of all returns from one pulse, expressing the intensity of each return as the proportion of the total intensity returned for that particular pulse.
h_i	Height above the ground of the midpoint of height bin i. I used 0.5 m height bins.
$maxh$	Total number of height bins, 0.5 m tall, in the site.
CR_{1i}	Proportion of energy from pulse i returned by the canopy (i.e. in all vegetation returns).
CR_{2i}	Proportion of energy from pulse i returned by the canopy, corrected for variations in reflectance.
P	Total number of pulses within a site.
ρ	Reflectance factor: ρ = 1 for vegetation returns, ρ = 2 for ground returns.

APPENDIX 2.2 – CANDIDATE REGRESSION MODELS FOR EACH STAND STRUCTURAL VARIABLE

Mean height and lorey's height (h)

(For symbols used in equations see Table A.2.2).

$h = \beta_0 + \beta_1 h_x$ (18)

$h = \beta_0 + \beta_1 h_x + \beta_2 var_x$ (18 x 4)

$h = \beta_0 + \beta_1 h_x + \beta_2 var_x + \beta_3 h_x var_x$ (only absolute variability metrics) (18 x 2)

Variability in tree heights could determine that measures of canopy surface height are not representative of the stand height. The compensating effect due to variability can be additive or multiplicative.

$h = \beta_0 + \beta_1 h_{avg} + \beta_2 h_{med}$ (9)

$h = \beta_0 + \beta_1 h_{avg} + \beta_2 h_{med} + \beta_3 h_{med} h_{avg}$ (9)

When tree height distributions are not normal, the difference between mean and median heights could describe stand height better than only the mean. This effect can be additive or multiplicative.

$h = \beta_1 h_x^c$ (18)

$h = \beta_0 + \beta_1 h_x^c$ (18)

Canopy base height (CBH)

$CBH = \beta_0 + \beta_1 HC_x$ (1)

$CBH = \beta_0 + \beta_1 HC_x^c$ (1)

$CBH = \beta_1 HC_x^c$ (1)

$CBH = \beta_0 + \beta_1 HC_x + \beta_2 var_x$ (4)

$CBH = \beta_0 + \beta_1 HC_x + \beta_2 var_x + \beta_1 HC_x var_x$ (4)

Variability in tree heights may be related to variability in crown heights. Therefore, combining a measure of variability in height with the metric representing crown base height could better predict canopy base height. This effect can be additive or multiplicative.

$CBH = \beta_0 + \beta_1 h_x + \beta_2 HC_x$ (18)

$CBH = \beta_0 + \beta_1 h_x + \beta_2 HC_x + \beta_3 h_x HC_x$ (18)

Since the lidar does not distinguish foliage from other biomass components, the representativeness of the lidar metric for crown base height might be dependent on stand height or age, described by a canopy height metric. This effect can be additive or multiplicative.

$CBH = \beta_0 + \beta_1 h_x$ (18)

$CBH = \beta_0 + \beta_1 h_x^c \quad (0 \leq c \leq 1; c > 1)$ (18 x 2)

$CBH = \beta_1 h_x^c \quad (0 \leq c \leq 1; c > 1)$ (18 x 2)

As tree heights increase, so should height to crown, due to shading and dying of lower branches. The increase in these two measures might be proportional or not.

$CBH = \beta_0 + \beta_1 h_x + \beta_2 var_x$ (18 x 4)

$CBH = \beta_0 + \beta_1 h_x + \beta_2 var_x + \beta_3 h_x var_x$ (only absolute variability metrics) (18 x 2)

The proportionality in the relationship between tree heights and crown heights might vary at the stand level if the individual tree heights are more or less variable.

Total aboveground biomass (TAB)

$TAB = \beta_0 + \beta_1 B_x$ (11)

$TAB = \beta_0 + \beta_1 B_x^c$ (11)

$TAB = \beta_1 B_x^c$ (11)

$TAB = \beta_0 + \beta_1 cover_x$ (5)

$TAB = \beta_0 + \beta_1 cover_x^c$ (5)

$TAB = \beta_1 cover_x^c$ (5)

Tree biomass in low density forests could be well represented by canopy cover, linearly or nonlinearly.

$TAB = \beta_0 + \beta_1 h_x^c \quad (0 \leq c \leq 1; c > 1)$ (18 x 2)

$TAB = \beta_1 h_x^c \quad (0 \leq c \leq 1; c > 1)$ (18 x 2)

Tree allometries indicate that tree biomass is related to tree height. As height is one-dimensional and biomass is three-dimensional, this relationship is likely to be nonlinear.

$TAB = \beta_0 + \beta_1 h_x + \beta_2 HC_x$ (18 x 1)

$TAB = \beta_0 + \beta_1 h_x + \beta_2 HC_x + \beta_3 h_x HC_x$ (18 x 1)

The crown makes up an important part of the tree biomass. So the relationship between height and biomass might be more precise if I include information on how much of that height is part of the crown. This effect can be additive or multiplicative.

$TAB = \beta_0 + \beta_1 h_x + \beta_2 cover_x + \beta_3 cover_x h_x$ (18 x 5)

$TAB = \beta_0 + \beta_1 h_x + \beta_2 cover_x$ (18 x 5)

Stand height and stand cover represent the three dimensions over which the biomass is distributed, so representing these two measures in a model could be used to describe stand biomass.

$TAB = \beta_0 + \beta_1 h_x + \beta_2 var_x$ (18 x 4)

$TAB = \beta_0 + \beta_1 h_x + \beta_2 var_x + \beta_3 h_x var_x$ (only absolute variability metrics) (18 x 2)

The greater the variability in heights in a stand, the more likely there are to be gaps in the canopy. These gaps may loosen the correlation between height and biomass, and this difference can be accounted for by a measure of variability. This effect can be additive or multiplicative.

Foliage biomass (FB) and canopy bulk density (CBD)

All the same regression models as for TAB, plus:

$FB/CBD = \beta_0 + \beta_1 h_x + \beta_2 cover_x + \beta_3 HC_x$ (18 x 5)

The amount of foliage biomass should relate to crown height rather than tree height. Including a measure of height to crown will account for the difference.

Basal area (BA)

$BA = \beta_0 + \beta_1 B_x$ (without δ_3) (10)

$BA = \beta_0 + \beta_1 B_x^c$ (without δ_3) (10)

$BA = \beta_1 B_x^c$ (without δ_3) (10)

$BA = \beta_0 + \beta_1 cover_x$ (5)

$BA = \beta_0 + \beta_1 cover_x^c$ (5)

$BA = \beta_1 cover_x^c$ (5)

$BA = \beta_0 + \beta_1 h_x$ (18)

$BA = \beta_0 + \beta_1 h_x^c$ (18)

$BA = \beta_1 h_x^c$ (18)

Stand basal area relates to tree size (diameter and height) and tree density. These measures are also determinants of tree biomass and canopy cover. Therefore, biomass density, cover and height metrics should correlate with basal area.

$BA = \beta_0 + \beta_1 h_x + \beta_2 B_x$ (without δ_3) (18 x 10)

$BA = \beta_0 + \beta_1 h_x + \beta_2 B_x + \beta_3 h_x B_x$ (18 x 10)

If biomass is distributed over a large stand height, basal area may be smaller than expected based on stand biomass. Combining a height and a biomass density metric could therefore predict basal area more accurately than either on its own. This effect can be additive or multiplicative.

$BA = \beta_0 + \beta_1 h_x + \beta_2 cover_x + \beta_3 h_x cover_x$ (18 x 5)

$BA = \beta_0 + \beta_1 h_x + \beta_2 cover_x$ (18 x 5)

Canopy cover has an absolute maximum. Once this is reached, increases in height should correlate with increases in basal area that cannot be explained by canopy cover.

Tree density (δ)

$\delta = \beta_0 + \beta_1 cover_x$ ($\beta_1 > 0$ and $\beta_1 \leq 0$ for δ_{11}) (5 + 1)

$\delta = \beta_0 + \beta_1 cover_x^c$ ($\beta_1 > 0$ and $\beta_1 \leq 0$ for δ_{11}) (5 + 1)

$\delta = \beta_1 cover_x^c$ ($\beta_1 > 0$ and $\beta_1 \leq 0$ for δ_{11}) (5 + 1)

The greater the number of trees, the greater the canopy cover. This relationship could be linear or nonlinear.

$\delta = \beta_0 + \beta_1 var_x$ ($\beta_1 > 0$ and $\beta_1 \leq 0$) (4 x 2)

$\delta = \beta_0 + \beta_1 var_x^c$ (4)

$\delta = \beta_1 var_x^c$ (4)

Greater tree densities will favor competition. This could generate variability in individual tree growth, and therefore variability in stand height.

$\delta = \beta_0 + \beta_1 h_x^c$ (18)

$\delta = \beta_1 h_x^c$ (18)

The older a stand, the greater the tree heights. Stand age should also correlate with variations in stand density. The correlation of both with stand age explains why stand height might be used to predict stand density.

Table A.2.2. Symbols used in equations of candidate models for each stand structure variable, described in Appendix 2.2.

Symbol	Metric representative of:
h_x	Tree or canopy heights
h_{avg}	Mean tree or canopy heights
h_{med}	Median canopy heights
var_x	Variability in canopy height
$cover_x$	Canopy cover
B_x	Biomass density
HC_x	Crown height
$\beta_0, \beta_1, \beta_2, \beta_3, c$	Regression coefficients

CHAPTER 3: CONSIDERATIONS FOR DEVELOPING FUEL INPUT LAYERS FOR FIRE BEHAVIOR MODELS

ABSTRACT

Fire behavior models help researchers understand the transition from surface to crown fires. These models require data inputs on both surface and canopy fuels. Surface fuels are commonly classified using standard "fuel models", such as the 13 "fuel models" established by the Fire Behavior Prediction System (FBPS). Canopy fuels are characterized by calculating canopy base height (CBH) and canopy bulk density (CBD). My objectives were: (1) to analyze the sensitivity of CBH and CBD to assumptions made in their calculations, and (2) to determine the consequences for crown fire hazard of variability in CBH, CBD and between selected "fuel models". I calculated CBH and CBD for 14 ponderosa pine stands in the Colorado Front Range, USA, using a range of assumptions. Seven of these sites burned during the Hayman fire (June 2002), four sites with low severity, and three with high severity. I used NEXUS, a spreadsheet model, to predict the open wind speed under which a fire will reach the crown of trees and, independently, the wind speed needed for a fire to actively spread through the tree crowns. I used a range of CBH and CBD values, and four different FBPS "fuel models". I found that CBH and CBD were sensitive to crown shape, so if shapes were observed in the field, these metrics would better represent canopy structure when used as inputs to fire behavior models. NEXUS predictions provided evidence that stronger winds are

generally needed for wildfires to reach the crowns of trees than for the fires to actively spread once they have crowned. The selection of the "fuel model" was the main variable that affected crown fire hazard. Correspondence between observed burn severity and NEXUS predictions of fire behavior was generally high. Where this correspondence was weak, the differences could be assigned to variation in weather conditions or to possible errors in selecting the "fuel model". These results highlight the inputs to fire behavior models that researchers and managers need to estimate carefully to enhance the models' predictive capacity. They also suggest that prescribed fires are necessary, and likely effective, fuel reduction treatments.

INTRODUCTION

Forest fires and their consequences have emerged as a fundamental issue for land managers and policy makers throughout the world. In the western United States extensive, high severity fires have occurred during the last decade. Efforts to understand what controls fires like these have included the development and use of simulation models (Perry 1998). At present there are a variety of fire behavior models in use (see examples in Scott and Reinhardt 2001 and Cruz et al. 2003). Given the severity and impact of active crown fires, one of the most important processes that need to be understood is the transition from a surface to an active crown fire (Fig. 3.1; Scott and Reinhardt 2001). Although models vary in the mathematical description of processes and variables controlling the behavior of wildland fires, many of the extant models are based on similar principles. A surface fire will transition to a passive crown fire (i.e. torching) when the intensity of the surface fire surpasses a certain threshold, which Van Wagner

(1977) defined as a function of the height from the ground to the base of the canopy and the moisture content of the overstory foliage (Fig. 3.1). Surface intensities will reach this threshold depending on the weather conditions the site is under, the fuel load on the ground, and its moisture (Byram 1959, Rothermel 1972). Once a fire has extended into the tree crowns, it must maintain a minimum rate of spread to become an active crown fire (Van Wagner 1977). The actual spread rate of the fire is largely determined by weather conditions and topography (as well as foliar moisture content; Scott and Reinhardt 2001), and the minimum rate of spread required depends on the density of fuels in the canopy, known as the canopy bulk density (Fig. 3.1; Van Wagner 1977).

There is theoretical and empirical evidence suggesting that, in many forest types, fuel characteristics may significantly affect fire behavior, at least under so-called moderate weather conditions (Turner and Romme 1994, Bessie and Johnson 1995). Schoennagel et al. (2004) concluded that in systems with mixed severity fire regimes heterogeneous fuels and climate interact in influencing fire frequency, severity and size. These mixed severity regimes are mostly found in mixed conifer forests, but include pure ponderosa pine stands such as those found in some areas of the Colorado Front Range (USA) (Schoennagel et al. 2004). Fuel reduction treatments in these ponderosa pine forests may reduce fire severity under moderate weather conditions, though extreme temperatures and wind speeds can override the influence of fuels (Schoennagel et al. 2004). The size and position of the treatment areas will affect their relative success (Martinson et al. 2003). Given that managers can modify fuels, but not the weather, there is substantial interest in understanding how they affect fire behavior. This is particularly true in areas on the urban-wildland interface, where there is strong social pressure to

actively reduce fire hazard. Therefore, without overlooking the importance of weather as a driver of fire behavior, I will focus on the effects of fuels, through which management can potentially affect wildfires.

The two-step transition from surface to active crown fires is governed by the surface fuel load, canopy base height and canopy bulk density (as well as weather and fuel moisture) (Fig. 3.1). Given that this transition is a key process for fire behavior, these three fuel-related inputs to fire behavior models become critical to our understanding of crown fire hazard (I am considering foliar moisture content to be climatically driven (*sensu* Rothermel 1972) and significantly less spatially variable than the structural variables; therefore, it is outside the scope of this paper). Measuring fuel loads (kg ha^{-1} of dead woody material in different size classes) in the field is extremely expensive, and therefore practically impossible across large areas with the necessary spatial and temporal detail for real-time fire behavior modeling. The fuels in different stands can be characterized using standard "fuel models" (Rothermel 1972, Albini 1976). Throughout, I will place "fuel models" between quotation marks, to avoid confusion between the characterization of understory fuels, and simulation or mathematical models. Each "fuel model" is assigned standard loads of fuels of different diameters, and these values are used to calculate intensity of surface fire and related variables (Rothermel 1972), under specified weather and fuel moisture conditions. Canopy base height is the lowest height above the ground at which there is sufficient canopy fuel to propagate fire vertically through the canopy (Scott and Reinhardt 2001). It is a complex stand-level variable, and not easy to estimate or measure (Van Wagner 1993). Canopy bulk density is the density of the canopy fuels that would be consumed in the flaming front of a fully active crown

fire (Scott and Reinhardt 2001). In practice, this variable has never been measured directly (Scott and Reinhardt 2001), and is estimated based on tree crown dimensions and foliage and fine branch biomass.

Calculations of canopy base height and canopy bulk density include certain assumptions, such as the shapes of tree crowns, the inclusion or not of seedlings, the vertical distribution of foliage and fine branches within tree crowns, and the threshold biomass density used to define the base of the canopy. These assumptions can lead to errors in the calculation of these variables (Sando and Wick 1972). The use of standard "fuel models" can also lead to inaccurate predictions of fire behavior (Albini 1976). Considering the importance of these three variables in defining fire behavior, my objectives were: 1) to evaluate the sensitivity of canopy base height and canopy bulk density to assumptions about crown shapes, vertical biomass distribution, and the inclusion of small trees in the sample; and 2) to determine the consequences for crown fire hazard of variability in canopy base height, canopy bulk density and the selection of "fuel models" to describe the understory fuel loads. I focused my efforts on ponderosa pine forests of the Colorado Front Range, USA, across a wide elevational gradient, such that a large portion of the study area historically had a mixed severity fire regime (Veblen et al. 2000).

METHODS

Study area and data

I collected data on fuel loads and stand structure for 14 sites in the Colorado Front Range, in the summer of 2001 (Fig. 3.2). All sites were dominated by ponderosa pine

(*Pinus ponderosa* Dougl. ex Laws), with secondary components of Douglas-fir (*Pseudotsuga menziesii* (Mirb.) Franco) and Rocky Mountain juniper (*Juniperus scopulorum* L.). Sites presented a range of topographic and structure conditions (Table 3.1). At each site, I sampled ten points, selecting four trees greater than 3 m in height, following the point-centered quarter method (Cottam and Curtis 1956). I classified crown shape (cylinder, cone, ellipsoid, hemi-ellipsoid or double cone; Appendix 3.1), and measured diameter at breast height, tree height, crown base height and crown width of selected overstory trees, using a Suunto® clinometer (for heights) and metric tapes. I estimated ponderosa pine and Douglas-fir foliage biomass, branch biomass and the proportion of the crown in fine branches (less than 6 mm in diameter) using species-specific equations developed by Brown (1978) and Ter-Mikaelian and Korzukhin (1997). I am not aware of the existence of published allometries for foliage and twig biomass of Rocky Mountain juniper, of sizes similar to my sample. I calculated total bole and branch volume using allometric equations based on diameter at the root collar (Chojnacky 1985), assuming boles are conical. To estimate foliage and twig biomass I assumed junipers had the same ratio of these tissues to bole and branch biomass as Douglas-fir trees with the same dimensions, and wood density of 559 kg/m^3 (Reinhardt and Crookston 2005). I estimated tree densities based on the distance of sampled trees to the sample point (Cottam and Curtis 1956). At each point I also collected data on dead woody debris in four size classes along a planar transect (*sensu* Brown et al. 1982), established in a random direction starting at the sample point. I measured heights of trees lower than 3 m in a 15 m^2 circular plot, centered at the opposite end of the above-mentioned transect. For each quarter of the transect length I randomly selected a point on which I centered a 0.25

m^2 circular plot. From these four plots I collected, air-dried and weighed litter and herbaceous biomass.

Objective 1: Sensitivity of calculated canopy base height and canopy bulk density to assumptions

For each sampled tree, I defined its crown as a solid of revolution (see definition in www.mathwords.com/s/solid_of_revolution.htm), and calculated the crown volume within each 0.3 m height increment along the length of the crown (Appendix 3.1). The vertical distribution of estimated biomass within each tree crown was assumed to be proportional to the fraction of the volume of the crown in each height interval. I calculated the amount of biomass in each height increment, added it across trees, and then corrected for the site's tree density to obtain biomass along a height profile, in kg ha^{-1}, as defined by Sando and Wick (1972). I converted the biomass profile (kg ha^{-1}) to a biomass density profile (kg m^{-3}) using the height of each bin (0.3 m). From this profile I obtained two values of canopy base height (CBH), defined as the minimum height (midpoint of a 0.3 m height increment) with biomass density greater than 0.037 kg m^{-3} (Sando and Wick 1972; CBH_1) or 0.011 kg m^{-3} (Scott and Reinhardt 2001; CBH_2), respectively. To calculate the canopy bulk density (CBD) for each site I smoothed the biomass density profile by computing a 4.5 m deep running mean. The maximum value of biomass density from this smoothed profile was selected as CBD (Scott and Reinhardt 2001). I implemented these calculations with a routine coded in Visual Basic for Applications behind Excel (Microsoft Corp., Redmond, WA, USA).

I then modified this routine to calculate canopy base heights and canopy bulk densities using different assumptions:

A. Crown shape:
   - All trees are cylinders (simplest volume equation).
   - All trees are cones (shape most commonly assigned to conifers).
   - All trees are hemi-ellipsoids (expected shape of mature ponderosa pine trees).
   - All ponderosa pine trees are hemi-ellipsoids, Douglas-fir and juniper trees are cones.

B. Foliage distribution: I characterized the vertical distribution of foliage and twigs within individual crowns by the ratio of the density of biomass in the upper third versus the lower two thirds of the crown (*sensu* Brown 1978). The ratios I used were 0.75, 1, 1.25, 1.5, 1.75 and 2. I also used a ratio of 1.64, based on data from Brown (1978).

C. Seedlings: I determined the effect of including trees less than 3 m in height (sampled separately) on CBH and CBD.

D. Running mean depth: I analyzed the effect of modifying the depth of the running mean, from 0.9 m to 6.3 m, in 0.6 m increments, on canopy bulk density.

Objective 2: Effect of variations in input layers on crown fire hazard

(a) Model, inputs and runs

NEXUS is a spreadsheet model in which existing models of surface and crown fire dynamics are linked to assess crown fire potential (NEXUS User Guide, http://fire.org/nexus/nexus.html). This model requires inputs on weather conditions,

topography and fuel characteristics (CBH, CBD and "fuel model"). NEXUS outputs include two indices of crown fire hazard: the Torching Index and the Crowning Index. The Torching Index is defined as the open wind speed (at 6.1 m above the ground) at which crown fire activity can initiate, and is affected by the selected "fuel model", CBH and foliar moisture content, as described by Van Wagner (1977). The Crowning Index is the open wind speed at which an active crown fire is possible, given the stand's CBD and the environmental conditions of interest (Scott and Reinhardt 2001). I chose to use NEXUS, rather than other models commonly used (such as Fuels Management Analyst Plus), for three reasons. First, I was able to modify canopy inputs independently, thereby incorporating my results from *Objective 1* into the analysis of crown fire hazard. Second, through the Torching and Crowning Indices it is possible to directly compare the two steps in the surface to active crown fire transition (Fig. 3.1). And third, NEXUS is based on the same studies as FMAPlus (Rothermel 1972, 1991, Van Wagner 1997), while being freely available to users.

I ran NEXUS for my 14 sites under different scenarios, characterized by particular combinations of moisture conditions, CBH, CBD and "fuel model". I classified moisture conditions as mean or extreme by selecting values of mean and very dry live and dead understory fuel moisture, respectively, based on the literature (Table 3.2). For each site I used the defined canopy base height or the minimum canopy base height, obtained by modifying the underlying calculation assumptions in the sensitivity analysis. I used one of five canopy bulk density values, based on the observed range obtained from the sensitivity analysis. Guided mainly by the estimates of dead woody debris in different size classes I had obtained in the field, as well as overall characteristics of forest

structure, I selected one of the 13 standard "fuel models" established by the Fire Behavior Prediction System (FBPS). I limited my selection to the "fuel models" commonly used in montane forests ("fuel models" 2, 8, 9 and 10; see complete descriptions in Anderson 1982). Data used as inputs are detailed in Appendix 3.2. All the NEXUS runs mentioned above (14 sites x 2 moisture conditions x 2 CBH values x 5 CBD values) used the selected "fuel model" as a fixed input for each site.

Given that I had selected the "fuel model" based on field data, without qualitative measures of fuel arrangement and type, I considered it critical to study the sensitivity of my analysis to the selected "fuel model". To determine how sensitive crown fire hazard is to the selection of a "fuel model", I ran NEXUS under the most hazardous moisture and overstory structure conditions (extreme moisture (Table 3.2), minimum CBH and maximum CBD) four times for each site, using different "fuel models" ("fuel models" 2, 8, 9 and 10; Appendix 3.2), independently of the "fuel model" I had selected for the runs described above.

(b) Qualitative validation of model predictions

Seven of the sites used in this study were within the perimeter of the Hayman fire, which burned over 55000 ha in June 2002 (Graham 2003), one year after I had sampled their fuel characteristics. I classified the severity of the fire at each site, as proposed by Omi and Martinson (2002). Severity of damage to the trees was coded from 0 (no damage) to 4 (extreme damage; almost all crowns consumed by the fire). Severity of the ground char was coded from 0 (unburned) to 3 (deep char; alterations to mineral soil's color or texture). When NEXUS is provided with an open wind speed, it compares that value to the Torching and Crowning Indices, and determines the type of fire (surface,

passive crown, active crown, independent or conditional fire; Scott and Reinhardt 2001) that would burn at that site under the given conditions. I used a daily mean wind speed of 19.2 km/hr to characterize conditions when the Hayman fire burned (Bradshaw et al. 2003). I compared actual type of fire, based on the severity classes observed in the field, to the type of fire that NEXUS predicted would occur at each of the 7 burned sites, with minimum CBH, maximum CBD (+40% of calculated value), and each of the four "fuel models" I compared before.

The serendipitous burning of these sites in the Hayman fire allowed me to qualitatively validate the crown fire hazard predictions obtained from NEXUS, and thereby provide support for my conclusions on how sensitive crown fire hazard is to the different fuel input layers: canopy base height, canopy bulk density and selected "fuel model".

RESULTS

Objective 1: Sensitivity of canopy base height and canopy bulk density to assumptions

Values of canopy base height, using a threshold density of 0.037 kg m^{-3} (CBH_1) varied between 0.15 m (lowest possible value: midpoint of the lowest 0.3 m height increment) and 2.85 m (Fig. 3.3A). The maximum of the range decreased to 1.95 m when I used a threshold of 0.011 kg m^{-3} (CBH_2) (Fig. 3.3A). I used CBH_1 in the sensitivity analysis and the crown fire hazard predictions because the variability in CBH_1 was substantially greater than in CBH_2, and the values of my sites were more evenly distributed across this range.

Modifying crown shapes had very large effects on sites with small CBH values (e.g. Cheesman West and Cheesman South), but also increased these values by up to 84.2% at sites with relatively high original values (Fig. 3.3B). On average, the increases caused by assuming all trees were cylinders were greater than the decreases generated when all trees were considered cones. The trends observed when modifying crown shape were repeated with the modifications of the vertical distribution of biomass, though the changes in CBH were not as pronounced (Fig. 3.3B). Including small trees did not modify the values of CBH at any of the sites.

Calculated values of canopy bulk density (CBD) varied between 0.011 kg m^{-3} and 0.322 kg m^{-3} for the 14 sites (Fig. 3.4A). When I modified crown shape, CBD varied from –36.4% to +32.4% of the original value. Consistently, assuming all trees were cones generated the greatest increase in CBD, while assuming they were all cylinders generated the greatest decrease in CBD (Fig. 3.4B). The vertical distribution of biomass within tree crowns had relatively small effects on the values of CBD (less than 15% in either direction; Fig. 3.4B). The distributions of biomass that caused this metric to increase or decrease were not consistent across sites. The value of CBD changed by up to 27.3% when I modified the depth of the running mean (Fig. 3.4B). Including small trees (< 3 m tall) in the estimate of CBD had no effect.

Objective 2: Effect of variations in input layers on crown fire hazard

(a) Torching: transition of the fire from the surface to individual tree crowns

The Torching Index represents the wind speed under which a fire can reach the canopy, and depends only on CBH and the "fuel model" (as well as fuel moisture conditions, which I maintained constant) (Fig. 3.1). The Torching Index varied greatly

between sites (7 to 1005 km hr^{-1}; Fig. 3.5A), when I modeled it under mean moisture conditions (Table 3.2) and with the original estimation of CBH and the selected "fuel model" (Appendix 3.2). At five sites (Cheesman North and West, Eldorado East and West, and Tyler), fires were very likely to reach the tree crowns, even under moderate winds (low Torching Index). At other sites it was very unlikely that the canopy would burn, no matter how extreme the conditions (very high Torching Index; Fig. 3.5A). At a given site, the effect of decreasing CBH to its minimum value (Fig. 3.3A) was similar or smaller than the effect of modifying the moisture conditions (Fig. 3.5A).

Almost all the sites would require high winds (>100 km/hr or more) for fires to reach the canopy when the dead woody debris load was characterized as "fuel model" 8 (closed timber litter; Fig. 3.5B). At the opposite extreme, if the debris was characterized by "fuel model" 2 (timber, grass and understory), the canopy in practically all the sites would be reached by fire (Fig. 3.5B). "Fuel models" 9 and 10 (long-needle pine litter and timber, litter and understory, respectively) were intermediate, though closer to the results with "fuel model" 2 than with "fuel model" 8 (Fig. 3.5B). Running NEXUS based on my field estimates of fuel loads I obtained Torching Indices that were substantially higher, except at Creekside, where it was similar to the value obtained using "fuel model" 8 (results not shown). The Torching Index was more sensitive to modifications in the "fuel model" used (particularly between using "fuel model" 8 or field estimated loads and using any of the other three "fuel models") than to either moisture conditions or CBH (Figs. 5A and B).

(b) Crowning: transition from passive to active crown fire

The Crowning Index is sensitive to CBD, as it quantifies the wind speed that would be necessary for a fire to actively move through the canopy, assuming it can reach the tree crowns (whether it does is quantified by the Torching Index) (Fig. 3.1). I defined five CBD values per site, based on the sensitivity analysis results: -40%, -20%, equal, +20% and +40% of the original CBD value for each site. Crowning Index values for many sites were lower than the corresponding Torching Index values, under extreme moisture conditions and the original "fuel model" (Fig. 3.6), and lower than corresponding Torching Index values obtained using field estimated fuel loads at all sites (results not shown). The variability in Crowning Index values between sites was also substantially less than for the Torching Index values (4-fold versus 144-fold, under mean conditions; Figs. 5A and 7). The Crowning Index responded more to changes in CBD (from –40% to +40%) than to changes in the moisture conditions (Fig. 3.7). Modifying surface fuel moisture and CBD together had slightly less effect on the Crowning Index than the cumulative effects of modifying these two inputs independently (Fig. 3.7).

(c) Qualitative validation of crown fire hazard predictions

My goal was to determine whether NEXUS could reproduce the actual type of fire under conditions studied in the previous analyses. I did not attempt to reproduce observed values exactly; rather, I intended to determine under which fuel conditions (CBH, CBD and "fuel model") predictions corresponded to observed burn patterns. I only analyzed NEXUS predictions based on standard "fuel models", as these are usually the only available inputs when modeling burn patterns post-fire.

NEXUS's predictions of surface fire occurrence corresponded well to observed type of fire (determined from the fire severity classes) at sites burned by the Hayman fire (Table 3.3). The occurrence of active crown fire during Hayman was not predicted as well. Two of the sites with highest canopy fire severity (Powerline and Cheesman West) had the potential for crown fire occurrence, at least under one of the scenarios analyzed ("fuel model" 2 for Powerline, "fuel model" 10 and maximum CBD for Cheesman West). At Poweline, the occurrence of an active crown fire was predicted to be conditional on the fire having crowned before it reached the site. If surface fuels were better characterized with "fuel model" 2, NEXUS would predict an active crown fire. At Cheesman West NEXUS predicted that the fire would reach the tree crowns, but would not actively spread through the canopy, underestimating crown fire hazard. At Cheesman East NEXUS results did not indicate high crown fire hazard (Table 3.3). Modifying the "fuel model" used to obtain predicted type of fire did not affect NEXUS's output.

DISCUSSION

Objective 1: Sensitivity of canopy base height and canopy bulk density to underlying calculation assumptions

My results highlight where efforts should focus for estimates of key canopy inputs to fire behavior models to better reflect fuel structure. Greater accuracy in the input data would reduce the observer error component of model prediction uncertainty, allowing scientists to focus on the remaining process error: how well do simulation models represent the processes that determine fire behavior. Crown shape had a substantial effect on both canopy base height and canopy bulk density estimates; vertical foliage

distribution mainly affected CBH. Different assumptions of shapes tended to increase the values of CBH rather than decrease them, so the presently used definitions and distribution ratios are unlikely to underestimate crown fire hazard. Changes in shape effectively modify the vertical distribution of biomass at the stand level. It is relatively simple to observe crown shape of sampled trees in the field, but estimating the vertical distribution of foliage within individual crowns would require substantial effort (e.g. see Brown 1978). Therefore, I recommend observing crown shape, and keep using a distribution ratio of 1 (i.e. assume that foliage biomass is evenly distributed, vertically, throughout each crown). This will modify the broad scale (stand) distribution of biomass, without the need to estimate fine scale (individual tree crowns) variations, thereby allowing users to better estimate CBH and CBD relatively simply. The effort required to sample small trees seems unjustified, at least in these ponderosa pine forests and other forest types with similar tree size distributions. I have not found any theoretical justification in the literature for the selection of 4.5 m as the running mean depth (i.e. averaging across 4.5 m in height to smooth the biomass density profile) when calculating CBD, yet it provides reasonable results, and does not have a particularly large effect on the values obtained. It would be interesting to develop a theoretical rationale for the selection of the running mean depth, such as relating it to the minimum flame length required to sustain a fire moving horizontally through the tree crowns. Until such a development exists, I do not suggest modifying this value.

Objective 2: Effect of variations in input layers on crown fire hazard

The Torching Index quantifies how extreme the weather needs to be for a wildfire to reach the tree crowns in a stand. The Crowning Index, on the other hand, describes the

conditions under which the fire will actively move through the canopy (as opposed to individual trees torching), independently of whether the fire can reach the canopy or not. Both indices are expressed as wind speeds, so their comparison for a given site is an indication of which of the two steps necessary for a fire's transition from the surface to the canopy (torching, or actively moving horizontally) is limiting (Fig. 3.1).

My results indicate that at many of the study sites the critical factor determining whether active crown fires are possible is the fire's capacity to reach the tree crowns (i.e. the Torching Index was greater than the Crowning Index under the same conditions; Fig. 3.6), which is dependent on the understory fuel conditions (quantified by the "fuel model") and canopy base height (as well as fuel moisture; Byram 1959, Van Wagner 1977). A landscape level modeling study in mixed conifer forests (Sierra Nevada, California, USA) found that only fuel treatments that reduced surface fuel loads had an impact on fire hazard (Stephens 1998). In my study, the four sites that had a Crowning Index that was greater than the Torching Index (i.e. where it was possible to have a passive crown fire without it becoming active) had the four lowest Torching Indices (Fig. 3.5A), and also had the main wind direction coming from close to uphill, which may explain why at these sites the crown fire hazard was limited by canopy density. A consequence of the Torching Index being greater than the Crowning Index, in the forests that I studied, is that if the fire reaches the crowns, driven by a few strong gusts of wind or patches of particularly flammable forest, it will most likely become an active crown fire. Conditions would need to get much better (i.e. less hazardous) for the fire to fall once more to the surface, and to again be under the influence of surface fuels and CBH. Scott and Reinhardt (2001) call this "hysteresis in crown fire". Hazard predictions,

therefore, need to be interpreted in a landscape-level context (Stephens 1998), or we run the risk of underestimating a forest's crown fire hazard.

Canopy base height and the selected "fuel model" interacted in determining where a fire was likely to reach the tree crowns and where it was not. The three sites with very high Torching Indices (Creekside, Shadow Canyon and Payne West; Fig. 3.5A) were originally characterized by "fuel model" 8 (Appendix 3.2). All three were likely to have torching of trees under moderate wind speeds if they were actually better characterized by "fuel models" 2, 9 or 10 (Fig. 3.5B). The five sites that had the lowest Torching Indices (Fig. 3.5A) were all either characterized by the "fuel models" that determine greater surface fire intensities ("fuel models" 2 and 10; Appendix 3.2), and/or had a very low canopy base height (< 1 m). These results highlight the need to correctly quantify the understory fuels, either through a correct selection of a "fuel model", or through measurement of the critical quantities that affect surface fire intensity (Rothermel 1972).

NEXUS, similar to other fire behavior models, particularly those of greater complexity, are very difficult to validate, as the required inputs are rarely measured or observed independently. Many inputs are estimated or inferred based on situations after a fire has burned (Scott and Reinhardt 2001). NEXUS also has other limitations. It is based on linking models that were independently developed to model surface fires (Rothermel 1972), crown fires (Rothermel 1991), and the transition between them (Van Wagner 1977). Not only are these different models not validated, but the combination of the three has not been comprehensively tested (Scott and Reinhardt 2001). Therefore, the conclusions I have reached must be considered tentative.

My comparison of model predictions to actual fire behavior was qualitative, as I lacked the detailed inputs needed for a rigorous validation. However, this analysis provided interesting insights. NEXUS correctly predicted the occurrence of surface fires at Creekside, Turkey Creek, Cheesman North and South (Table 3.3). There was a tendency to underestimate crown fire hazard: NEXUS did not predict the occurrence of active crown fires at the other three sites, though at Powerline and Cheesman West the potential was identified (conditional and passive crown fire, respectively). It is worth keeping in mind that during the day, there are periods or gusts of wind with substantially greater speeds than the mean daily wind speed I used as input to NEXUS. At Powerline, the Torching Index was 28.2 km/hr. Therefore, gusts of 30 km/hr would transform the predicted conditional fire into an active crown fire. Similarly, at Cheesman West, the Crowning Index was 21.1 km/hr, so wind speeds of more than 20 km/hr would transform it into an active crown fire. The underestimate of crown fire hazard was clearest at Cheesman East, where NEXUS predicted a surface fire rather than an active crown fire. This held even when I modified the "fuel model" used (results not shown). A possible explanation has to do with the stand's structure. There was a doghair thicket of ponderosa pine saplings at the foot of the slope, from where the wind was predominant, which may not be represented in the integrated CBH value due to its small area, but may have allowed the fire to reach the crowns. Van Wagner (1993) identified the lack of representativeness of estimates of CBH in a two-layer canopy. The moderate Crowning Index at Cheesman East (54 km/hr under extremely dry conditions) would indicate that the fire could become active if it reached the tree crowns.

Five of the seven sites were within the perimeter of the June 9 high severity run. However, my sites were on the leeward side of Cheesman Reservoir, which likely protected them and explains the low to moderate burn severity (see Graham 2003). The other two sites (Cheesman North and Turkey Creek) burned in subsequent days. Therefore, my sites may not be representative of what occurred during what Graham (2003) called "the extreme weather episodes", but should present a reasonable picture for fire behavior during more moderate conditions.

Being able to compare these model results to actual wildfire behavior provided strong support for the critical role played by the understory fuels in controlling crown fire hazard in these forests.

Management and modeling implications

My results have led me to consider crown shape a necessary parameter to be observed in the field, when collecting data to create input layers for fire behavior models. In these ponderosa pine forests, the extra effort required to measure small trees seems unjustified. I would like to highlight, however, that this may not hold for all forest types, and should be tested elsewhere.

NEXUS is a simple, easy to understand model that allows calculation of two comparable crown fire hazard indices, expressing the wind conditions under which a fire is likely to reach or actively spread through the canopy (Fig. 3.1; Scott and Reinhardt 2001). Results from my study highlight the importance of correctly identifying the "fuel model" that best describes the understory fuels, as this input into NEXUS has significant impacts on model results. This effect is more critical than the precision of the estimates of

canopy base height or canopy bulk density, at least in the ponderosa pine forests I studied.

These results have direct management implications. There are a variety of restoration efforts taking place in the ponderosa pine forests of the Front Range (e.g. Brown et al. 2001). In these forests, the ecological restoration objectives are well aligned with hazardous fuel reduction treatments, and include silvicultural treatments and prescribed fire (Brown et al. 2001). If crown fire hazard is most sensitive to surface fuel conditions than to overstory characteristics, as my results suggest, then prescribed fire, or other treatments that could reduce the surface fuel loads, are both necessary and likely to be effective in reducing the risk of active crown fires. However, I did not examine potential interactions between effects of fuels under a variety of weather conditions, so this conclusion is limited to so-called moderate moisture and wind conditions. The dominance by surface fuels does not mean, however, that canopy bulk density or, particularly, canopy base height, can be ignored. The fact that I was unable to predict the active crown fire at Cheesman East using NEXUS, possibly due to the existence of a doghair thicket, highlights the need to find a way to effectively incorporate seedlings and other "ladder fuels" into fire behavior models. The lack of sensitivity of canopy base height calculations to the inclusion of seedlings, combined with their capacity to explain the lack of correspondence between observed and predicted fire behavior, suggests that they may be better characterized as part of the surface fuels, or may even need to be incorporated independently, as a third category of fuels (surface, ladder and overstory fuels).

Fire behavior modeling is a very useful tool for understanding conditions and controls over the transition from surface to active crown fires. This understanding will help managers strategically select stands for fuel reduction treatments, and predict treatment effects (Fulé et al. 2001). Modeling is also a key component of understanding the effects of fire on the structure and processes in forest stands, as well as the feedbacks of stand structure on fire behavior.

REFERENCES

Albini, F.A., 1976. Estimating wildfire behavior and effects. USDA Forest Service GTR-INT-30.

Anderson, H.E., 1982. Aids to determining fuel models for estimating fire behavior. USDA Forest Service GTR-INT-22.

Bessie, W.C., Johnson, E.A., 1995. The relative importance of fuels and weather on fire behavior in subalpine forests. Ecology 76, 747-762.

Bradshaw, L., Bartlette, R., McGinely, J., Zeller, K., 2003. Fire, weather, meteorology and climate. In: Graham, R.T. (Ed.)., Hayman fire case study. USDA Forest Service RMRS-GTR-114.

Brown, J.K., 1978. Weight and density of crowns of Rocky Mountain conifers. USDA Forest Service RP-INT-197.

Brown, J.K., Oberheu, R.D., Johnston, C.M., 1982. Handbook for inventorying surface fuels and biomass in the Interior West. USDA Forest Service GTR-INT-129.

Brown, P.M., D'Amico, D.R., Carpenter, A.T., Andrews, D., 2001. Restoration of montane ponderosa pine forests in the Colorado Front Range. Ecol. Restoration 19, 19-26.

Byram, G.M., 1959. Combustion of forest fires. In: Davis, K.P. (Ed.), Forest fire - control and use. McGraw Hill, New York, New York, USA, pp. 61-89.

Chojnacky, D.C., 1985. Pinyon-juniper volume equations for the Central Rocky Mountain States. USDA Forest Service RP-INT-339.

Cottam, G., Curtis, J.T., 1956. The use of distance measures in phytosociological sampling. Ecology 37, 451-460.

Cruz, M.G., Alexander, M.E., Wakimoto, R.H., 2003. Assessing canopy fuel stratum characteristics in crown fire prone fuel types of western North America. Int. J. Wildland Fire 12, 39-50.

Fulé, P.Z., Waltz, A.E.M., Covington, W.W., Heinlein, T.A., 2001. Measuring forest restoration effectiveness in reducing hazardous fuels. J. For. 99, 24-29.

Graham, R.T., 2003. Hayman fire case study. USDA Forest Service RMRS-GTR-114.

Martinson, E., Omi, P.N., Shepperd, W., 2003. Effects of fuel treatments on fire severity. In: Graham, R.T. (Ed.)., Hayman fire case study. USDA Forest Service RMRS-GTR-114.

Omi, P. N., Martinson, E. J. 2002. Effects of fuel treatments on wildfire severity. Final Report submitted to the Joint Fire Science Program Governing Board. Western Forest Fire Research Center, Colorado State University.

Perry, G.L.W., 1998. Current approaches to modelling the spread of wildland fire: a review. Prog. Phys. Geog. 22, 222-245.

Reinhardt, E.D., Crookston, N.L., 2005. The Fire and Fuels Extension to the Forest Vegetation Simulator – Addendum. USDA Forest Service RMRS-GTR-116 (2003). http://www.fs.fed.us/fmsc/ftp/fvs/docs/gtr/FFEaddendum.pdf

Rothermel, R.C., 1972. A mathematical model for predicting fire spread in wildland fuels. USDA Forest Service RP-INT-115.

Rothermel, R.C., 1991. Predicting behavior and size of crown fires in the Northern Rocky Mountains. USDA Forest Service RP-INT-438.

Sando, R.W., Wick, C.H., 1972. A method of evaluating crown fuels in forest stands. USDA Forest Service RP-NC-84, p. 10.

Schoennagel, T., Veblen, T.T., Romme, W.H., 2004. The interaction of fire, fuels and climate across Rocky Mountain forests. BioSci. 54, 661-676.

Scott, J.H., Reinhardt, E.D., 2001. Assessing crown fire potential by linking models of surface and crown fire behavior. USDA Forest Service RMRS-RP-29.

Stephens, S.L., 1998. Evaluation of the effects of silvicultural and fuels treatments on potential fire behaviour in Sierra Nevada mixed-conifer forests. For. Ecol. Manage. 105, 21-35.

Ter-Mikaelian, M.T., Korzukhin, M.D., 1997. Biomass equations for sixty-five North American tree species. For. Ecol. Manage. 97, 1-24.

Turner, M.G., Romme, W.H., 1994. Landscape dynamics in crown fire ecosystems. Landscape Ecol. 9, 59-77.

Van Wagner, C.E., 1977. Conditions for the start and spread of crown fire. Can. J. For. Res. 7, 23-34.

Van Wagner, C.E., 1993. Prediction of crown fire in two stands of jack pine. Can. J. For. Res. 23, 442-449.

Veblen, T.T., Kitzberger, T., Donnegan, J., 2000. Climatic and human influences on fire regimes in ponderosa pine forests in the Colorado Front Range. Ecol. Appl. 10, 1178-1195.

Table 3.1. Range of topographic and stand structure conditions covered by the field data.

Site	Slope (%)	Aspect (degrees)	Elevation (m)	Tree density (trees/ha)	Basal area (m^2/ha)
Mountain Park	47.6	292	2225	629	32.78
Powerline	31.4	151	2227	1617	59.25
Creekside	56.4	37	2167	128	14.87
Cheesman E	25.9	110	2295	214	16.27
Turkey Creek	21.6	183	2415	181	15.44
Cheesman N	26.3	81	2200	277	23.45
Cheesman W	21.3	302	2220	793	34.66
Eldorado E	43.8	69	1929	257	11.12
Eldorado W	40.0	256	1899	1286	39.09
Tyler	25.4	151	2673	120	16.56
Shadow Canyon	26	150	1948	120	10.55
Payne E	15.9	30	2530	361	33.31
Payne W	29.0	172	2521	198	20.17
Cheesman S	27.3	260	2191	207	11.35

Table 3.2. Values of climatic variables for mean and extreme moisture scenarios used for NEXUS runs.

Fuel type		Mean moisture conditions (%) [1]	Extreme moisture conditions (%) [1]
	Diameter range		
Dead fuels	0 – 0.6 cm	6	3
	0.6 – 2.5 cm	8	4
	2.5 – 7.6 cm	10	6
Live fuels		117	70

[1] Fuel moisture contents obtained from Rothermel (1991) for a normal summer (mean moisture conditions) and late summer severe drought (extreme moisture conditions).

Table 3.3. Predicted and actual type of fire at the 7 sites that burned in the Hayman fire (2002). Possible fire types are: conditional, used when conditions will allow active spread of fire once it is in the crown, but are not conducive to torching (type of fire is conditional on what kind of fire reaches the stand; Scott and Reinhardt 2001); active crown fire; surface fire; passive crown fire (Scott and Reinhardt 2001). Fire severity classes are described in Omi and Martinson (2002).

Site	Selected "fuel model"	Model predicted	Fire Severity		Actual (Hayman)
			ground	canopy	
Powerline	10	conditional	2	4	active crown
Creekside	8	surface	2	2	surface
Cheesman E	9	surface	2	4	active crown
Turkey Creek	9	surface	3	3	surface
Cheesman N	10	surface	2	2	surface
Cheesman W	10	passive crown	2	4	active crown
Cheesman S	8	surface	1	1	surface

Figure 3.1. Schematic description of the two-step process from a surface fire to an active crown fire, and the factors that control each step (variables I studied in *italics*). NEXUS output characterizes the first step (from a surface to a passive crown fire) with the Torching Index, and the second step (from a passive to an active crown fire) with the Crowning Index.

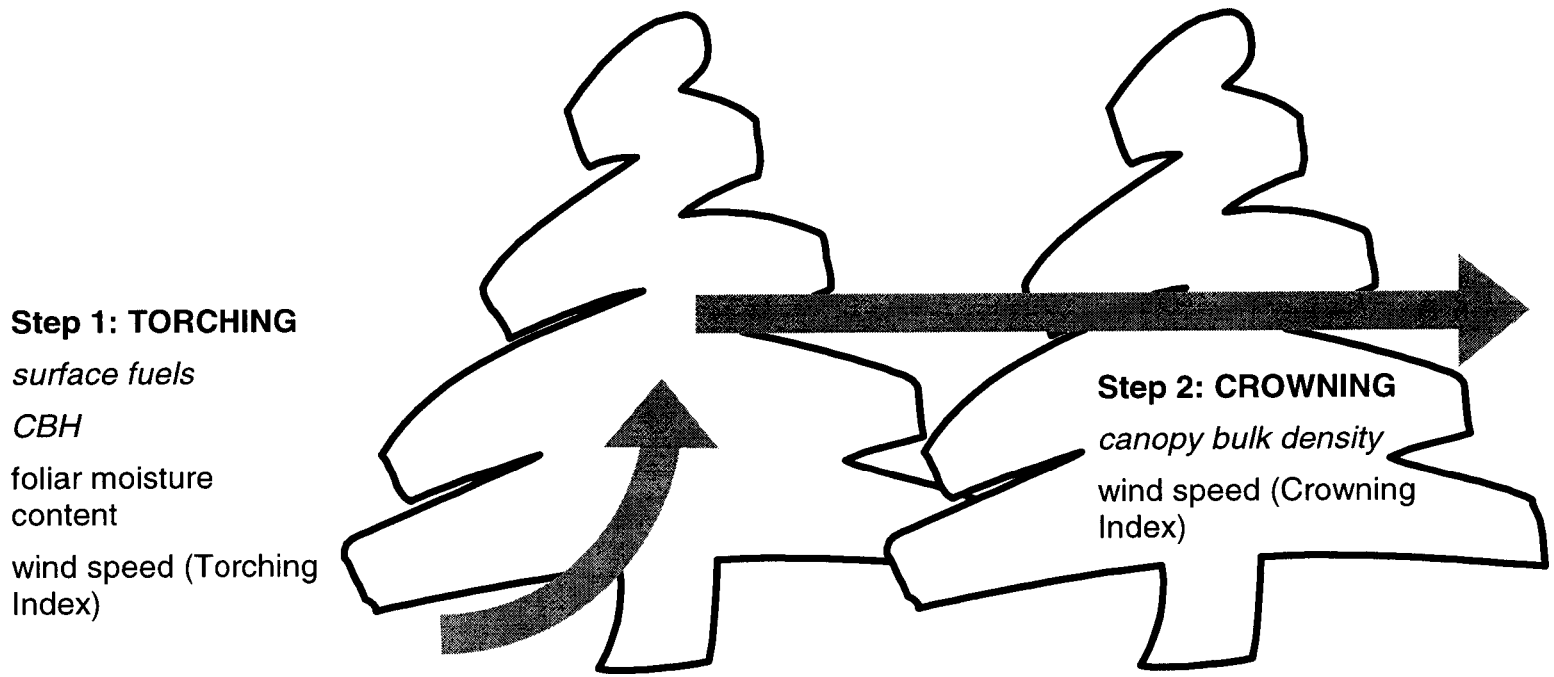

Figure 3.2. Sites where I collected fuel and stand structure data in the Colorado Front Range. The inset map shows the location of the study area within the western states of the conterminous USA.

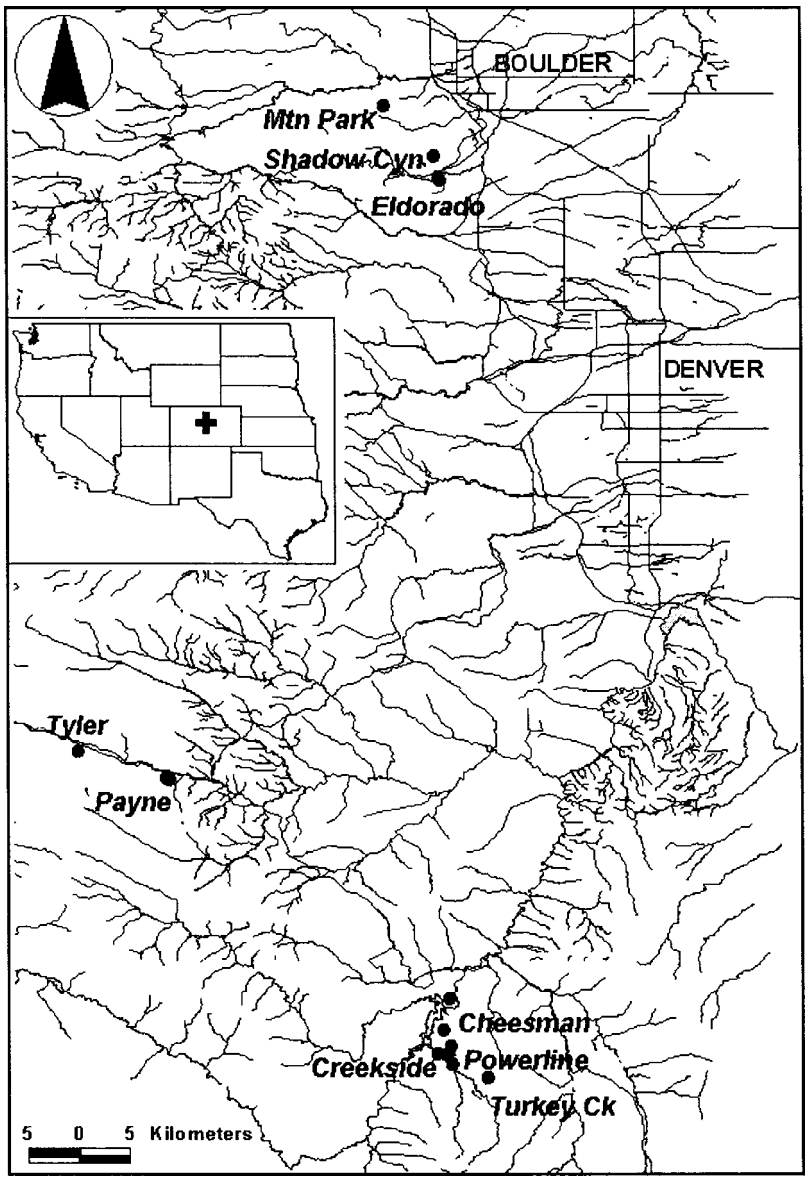

Figure 3.3. Canopy base height (CBH). (**A**) Values of canopy base height for each site, and minimum value obtained in the sensitivity analysis. CBH was calculated using a threshold biomass density of 0.037 kg/m^3 (CBH1) and 0.011 kg/m^3 (CBH2). (**B**) Sensitivity of CBH1 to underlying assumptions. Sensitivity is expressed as percent of the canopy base height calculated using the definition described in Methods, using observed crown shape, and distribution of biomass proportional to crown volume. Trees less than 3 m in height were not included.

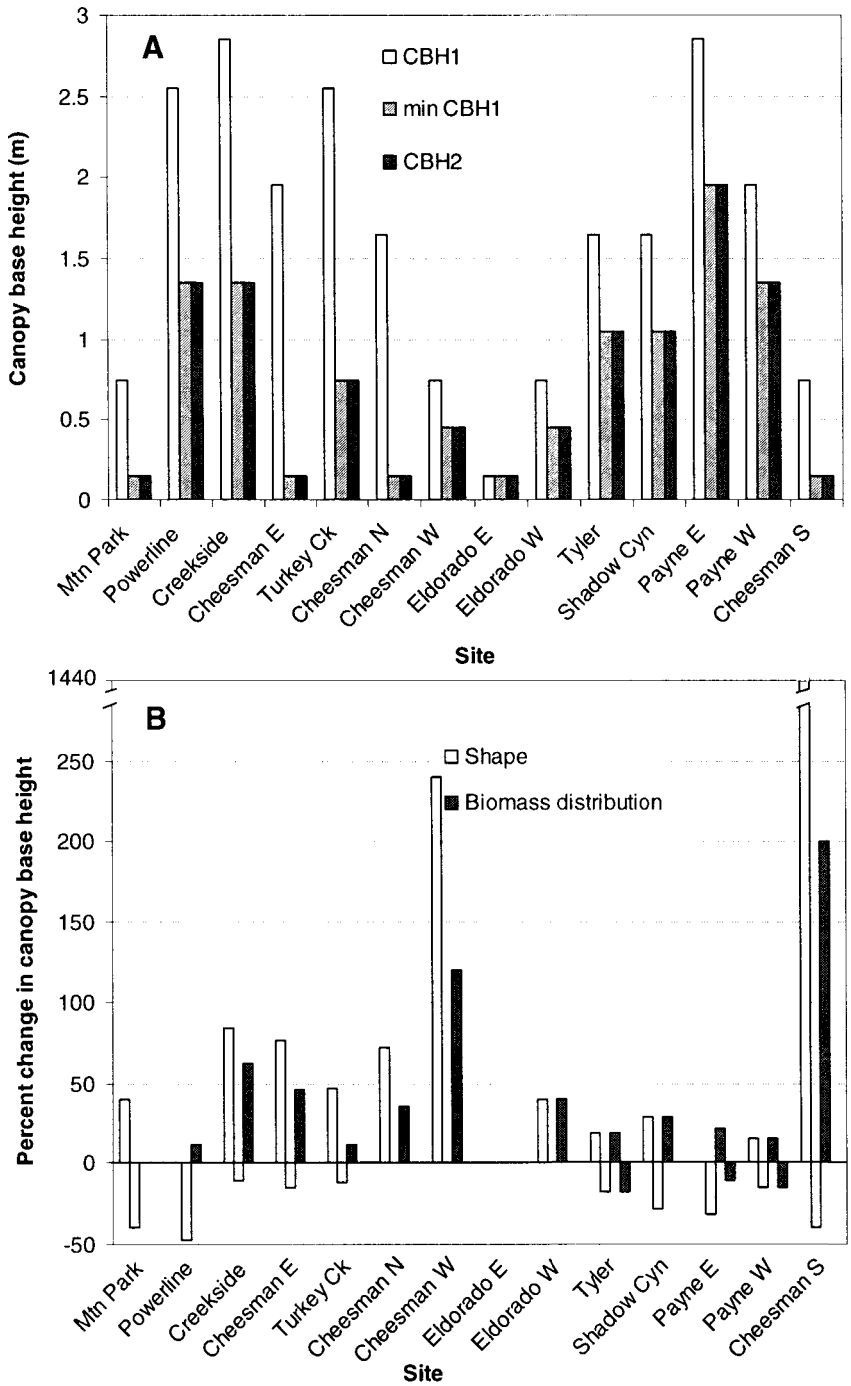

Figure 3.4. Canopy bulk density (CBD). (**A**) Values of canopy bulk density for each site. (**B**) Sensitivity of CBD to underlying assumptions. Sensitivity is expressed as percent of the original value of canopy bulk density (CBD), calculated using the definition described in Methods, using observed crown shape, and distribution of biomass within each tree crown proportional to crown volume. Trees less than 3 m in height were not included.

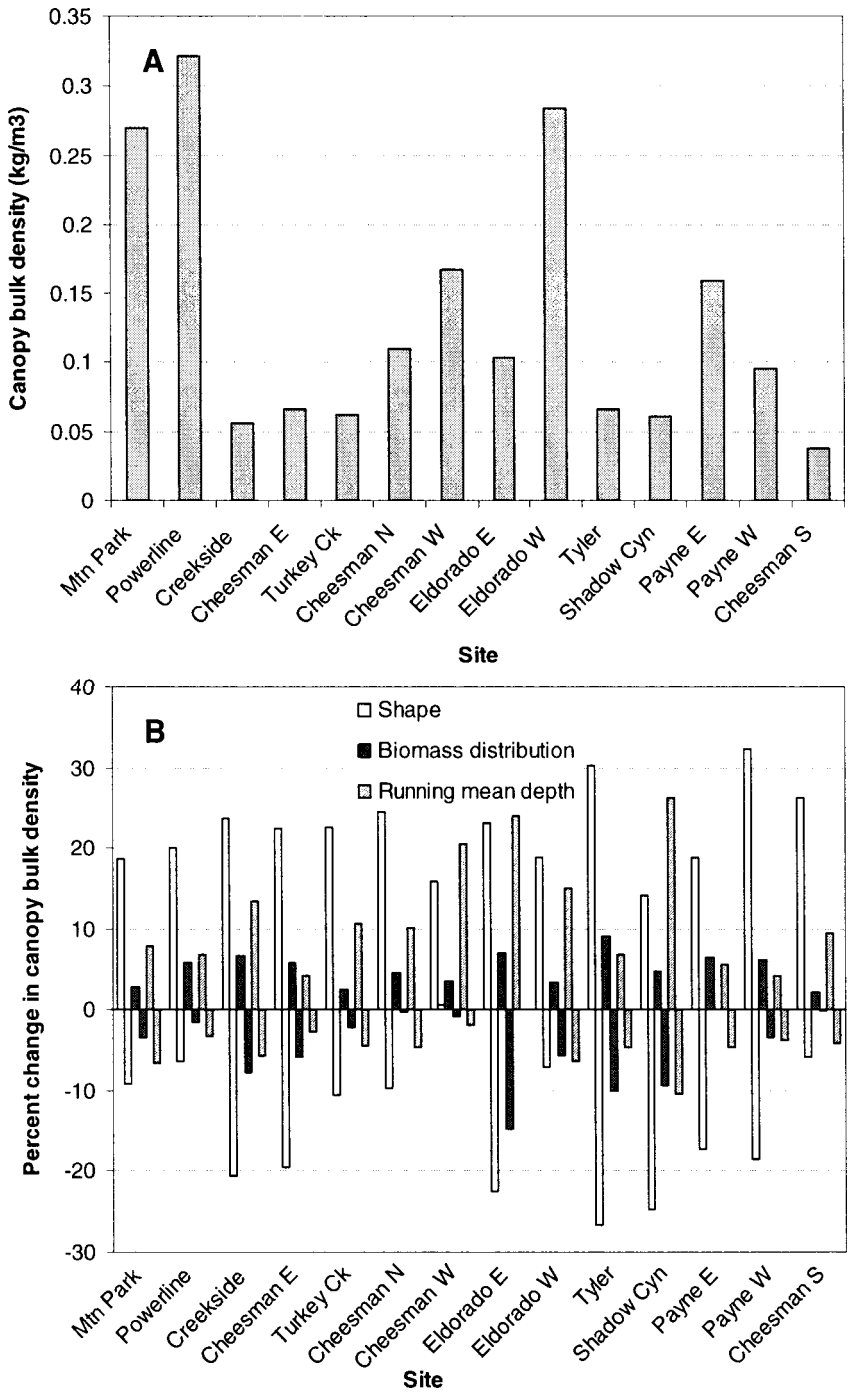

Figure 3.5. Torching Index values predicted for each site by NEXUS. (**A**) Different moisture and canopy base height (CBH) scenarios, using the selected "fuel models". (**B**) Different "fuel model" scenarios, using minimum CBH and extreme moisture conditions.

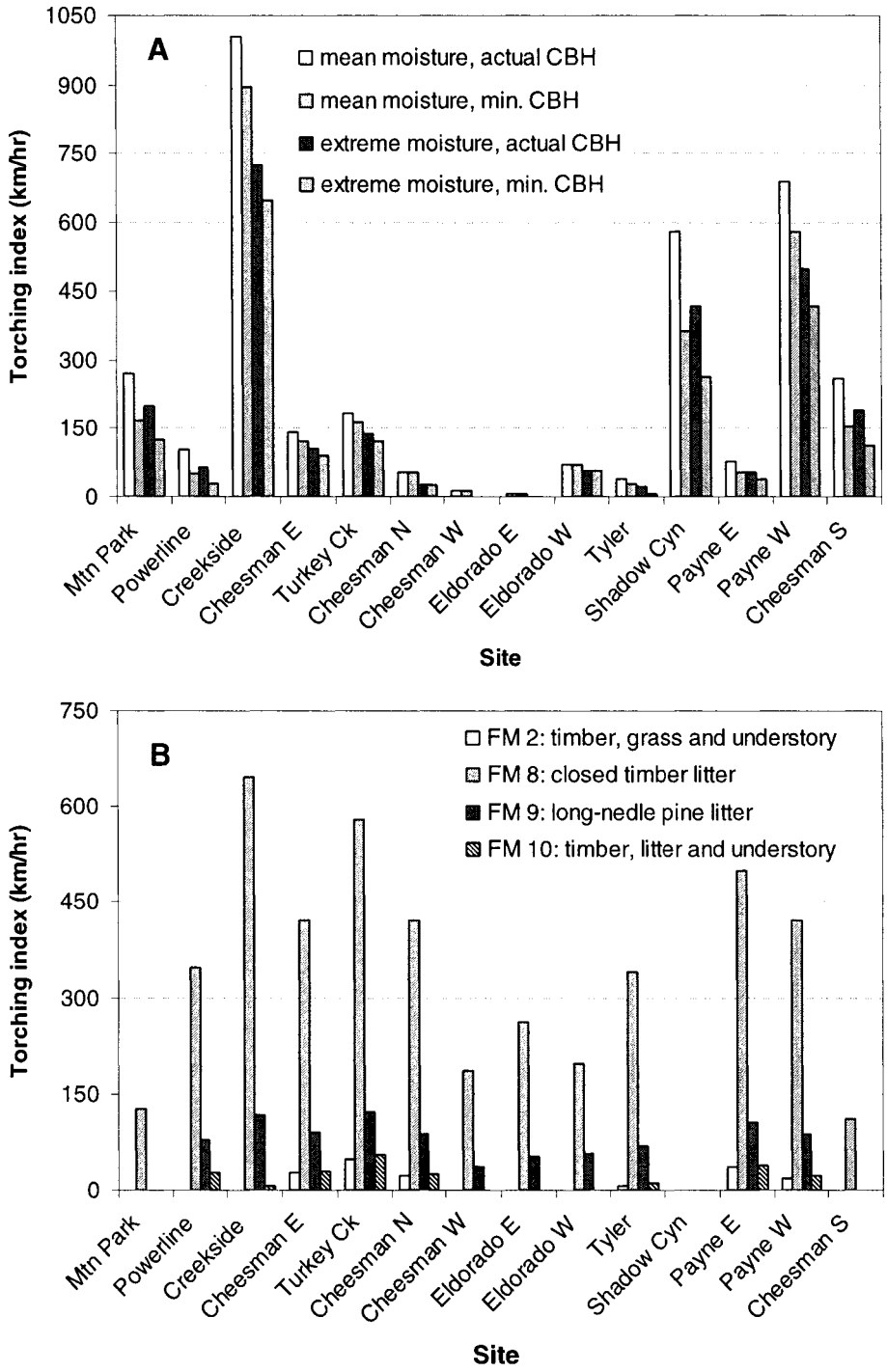

Figure 3.6. Difference between the Torching Index and the Crowning Index at each site. At sites with positive values crown fire hazard is limited by the fire's capacity to reach the tree crowns. Where the difference is negative, hazard is limited by the fire's capacity to spread through the canopy.

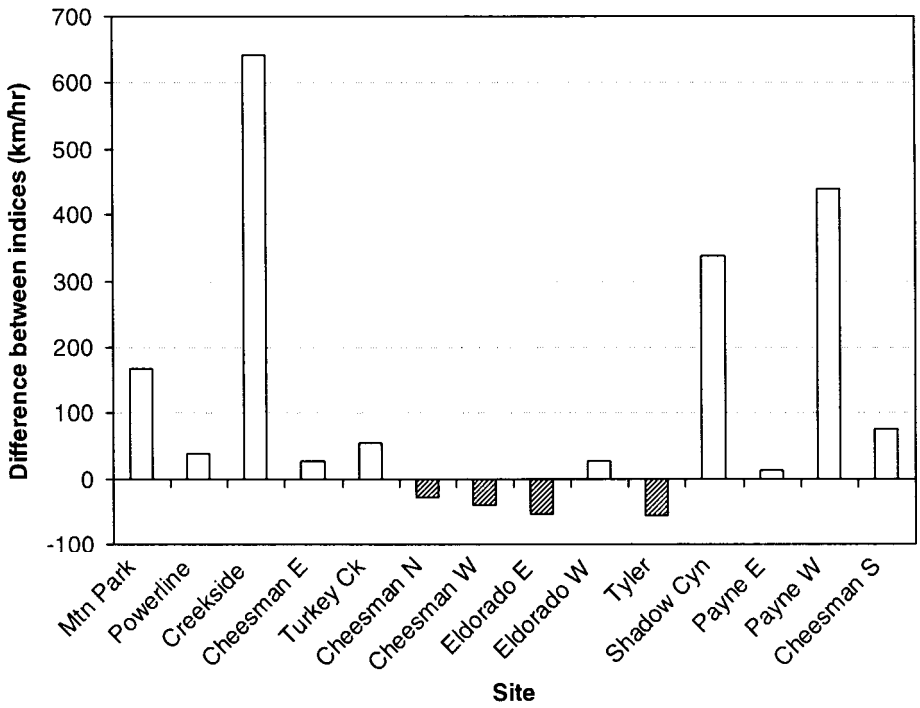

Figure 3.7. Crowning Index values predicted for each site by NEXUS, under different moisture conditions and extremes of canopy bulk density (CBD).

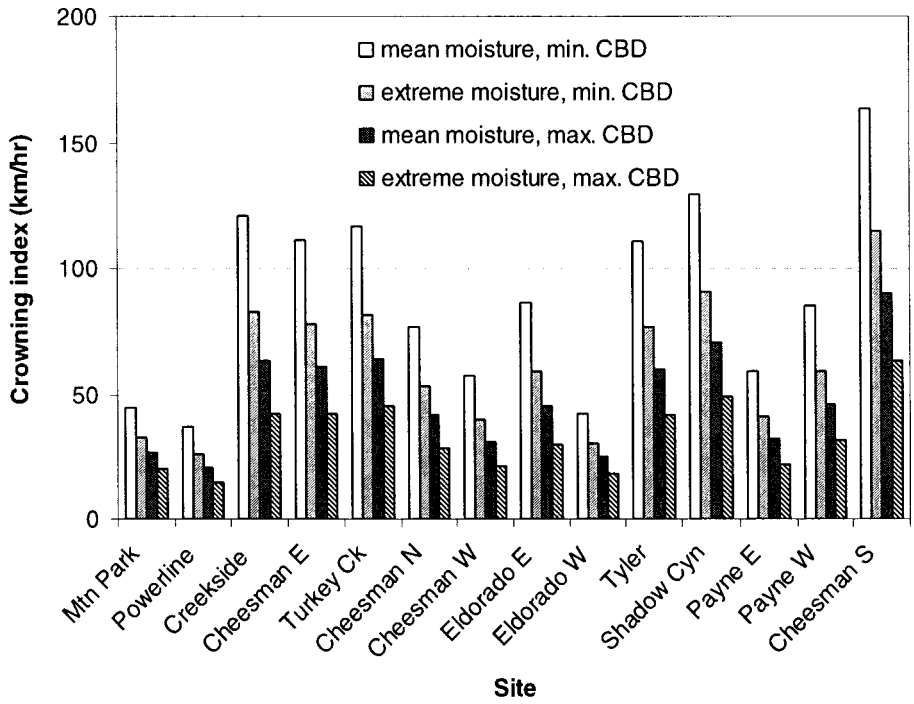

Appendix 3.1 – CALCULATIONS OF CROWN VOLUME.

Idealized crown shapes used in this study. Each shape is presented as two-dimentional cross-section, with the crown edge (y) described as a function of height (x) and crown dimensions: CR - crown radius; HLC - height to live crown; TH - tree height; CH - crown height (TH – HLC).

CYLINDER

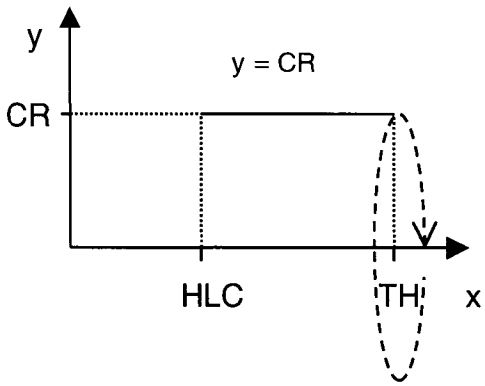

CONE

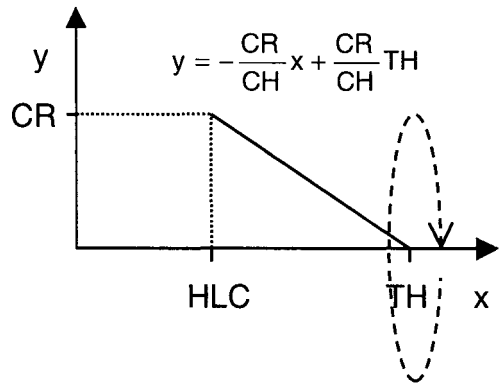

ELLIPSOID

$$y^2 = -4\frac{CR^2}{CH^2}x^2 + \left(8\frac{CR^2}{CH^2}HLC + 4\frac{CR^2}{CH}\right)x - \left(4\frac{CR^2}{CH^2}HLC^2 + 4\frac{CR^2}{CH}HLC\right)$$

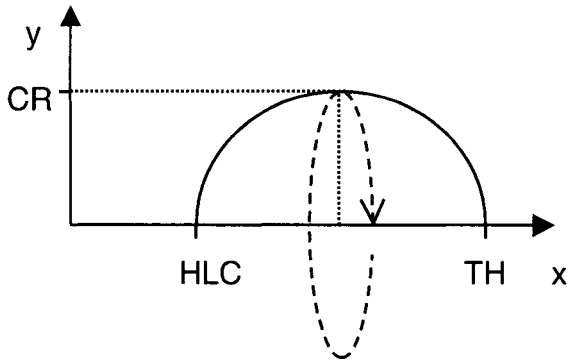

HEMI-ELLIPSOID

$$y^2 = -\frac{CR^2}{CH^2}x^2 + 2\frac{CR^2}{CH^2}HLCx - \frac{CR^2}{CH^2}HLC^2 + CR^2$$

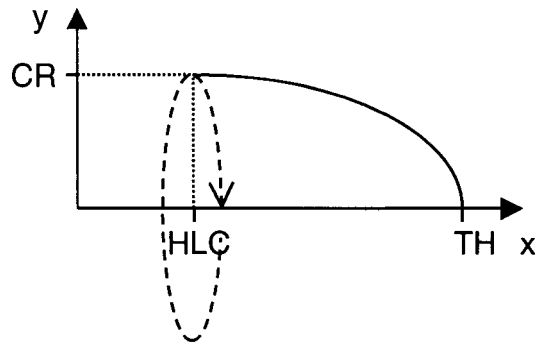

DOUBLE CONE

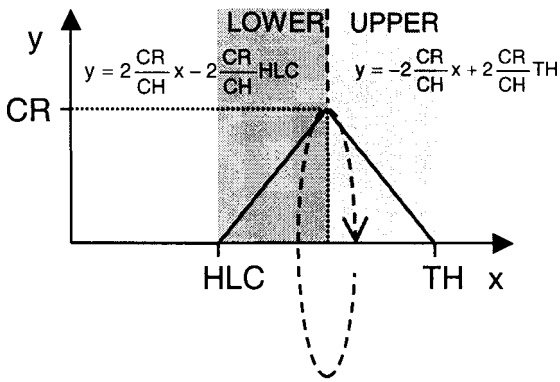

Table A.3.1. Equations used to calculate crown volume for 0.3 m height intervals, considering each crown to be a solid of revolution. Definitions of all the variables are given in the above Figure.

Crown shape	Crown volume	Section volume
Cylinder	$V = \pi CR^2 CH$	$V = \pi \int_l^u y^2 dx = \pi CR^2 (u - l)$
Cone	$V = \frac{1}{3}\pi CR^2 CH$	$V = \pi \int_l^u y^2 dx = \pi \frac{CR^2}{CH^2}\left(\frac{1}{3}(u^3 - l^3) - TH(u^2 - l^2) + TH^2(u - l)\right)$
Double cone	$V = \frac{1}{3}\pi CR^2 CH$	$LV = \pi \int_l^u y^2 dx = 4\pi \frac{CR^2}{CH^2}\left(\frac{1}{3}(u^3 - l^3) - HLC(u^2 - l^2) + HLC^2(u - l)\right)$ $UV = \pi \int_l^u y^2 dx = 4\pi \frac{CR^2}{CH^2}\left(\frac{1}{3}(u^3 - l^3) - TH(u^2 - l^2) + TH^2(u - l)\right)$
Ellipsoid	$V = \frac{2}{3}\pi CR^2 CH$	$V = \pi \int_l^u y^2 dx =$ $= \pi\left(-\frac{4}{3}\frac{CR^2}{CH^2}(u^3 - l^3) + \left(4\frac{CR^2}{CH^2}HLC + 2\frac{CR^2}{CH}\right)(u^2 - l^2) - \left(4\frac{CR^2}{CH^2}HLC^2 + 4\frac{CR^2}{CH}HLC\right)(u - l)\right)$
Hemiellipsoid	$V = \frac{2}{3}\pi CR^2 CH$	$V = \pi \int_l^u y^2 dx =$ $= \pi CR^2\left(-\frac{1}{3CH^2}(u^3 - l^3) + \frac{HLC}{CH^2}(u^2 - l^2) + \left(1 - \frac{HLC^2}{CH^2}\right)(u - l)\right)$

Appendix 3.2 – VALUES OF INPUTS TO NEXUS, FOR THE 14 SITES I USED TO STUDY ACTIVE CROWN FIRE HAZARD

Surface fuels classes: see Table A.3.2 (for complete description see Anderson 1982).

2: Timber (grass and understory).
8: Closed timber litter.
9: Hardwood (long-needle pine) litter.
10: Timber (litter and understory).

Dead and live fuel moisture: see Table 3.2 for values under mean and extreme weather conditions.

Canopy fuels:

Canopy bulk density (CBD): see Figure 3.4A for mean values.
Foliar moisture content (FMC): Scott and Reinhardt (2001) recommend values between 80% and 120%. During the days the Hayman fire burnt (extreme weather), foliar moisture content of ponderosa pine averaged 110.4%, and Douglas-fir foliage averaged 107.8%. I therefore chose a fixed value of FMC of 110%, under both mean and extreme weather conditions.
Canopy base height (CBH): see Figure 3.3A for estimated and minimum values.
Canopy fuel load (CFL): see Table A.3.2.

Site characteristics:

Slope: see Table 3.1.
Open wind speed: 19.2 km/hr.
Wind direction: Daily wind direction data was obtained from three RAWS Meteorological Stations [Cheesman (1987-2003), Boulder (2001-2003) and Bailey (1995-2003)]. I selected the mean of the monthly modal direction (° from north) from all available data from May to August, classified into 20° intervals (Cheesman: 200°; Boulder: 270°; Bailey: 290°). The wind direction value for the station closest to each site was combined with the site's aspect to express wind direction as ° from the uphill direction (see Table A.3.2).
Wind reduction factor: I used the NEXUS default of 0.1.

Multipliers: I used the NEXUS default of 1.0 for all multipliers.

Table A.3.2. Fuel and topographic characteristics for each site.

Site	Selected surface fuels class	CFL (kg/m^2)	Wind direction (° from uphill)
Mountain Park	8	1.42	158.4
Powerline	10	2.56	229.2
Creekside	8	0.50	342.6
Cheesman E	9	0.59	269.7
Turkey Creek	9	0.56	197.3
Cheesman N	10	0.86	299.0
Cheesman W	10	1.45	77.8
Eldorado E	8	0.47	20.6
Eldorado W	9	1.74	194.4
Tyler	2	0.55	319.0
Shadow Canyon	8	0.38	300.2
Payne E	2	1.21	80.1
Payne W	8	0.73	297.7
Cheesman S	8	0.43	37.6

CHAPTER 4: LITTER AND DEAD WOOD DYNAMICS IN PONDEROSA PINE FOREST ALONG A 160-YEAR CHRONOSEQUENCE

ABSTRACT

Understanding the role of disturbance in controlling ecosystem structure offers a fundamental challenge to contemporary ecologists. Organic detritus in fire prone forests comprises a large pool of carbon and can control the frequency and intensity of fire. The ponderosa pine forests of the Colorado Front Range, USA, where fire has been suppressed for a century, provide an ideal system for studying the long-term dynamics of detrital pools. My objectives were (a) to quantify the long-term temporal dynamics of detrital pools; and (b) to determine to what extent present stand structure, topography and soils constrain these dynamics. I collected data on downed dead wood, litter, duff (partially decomposed litter on the forest floor), stand structure, topographic position, and soils for 31 sites along a 160-year chronosequence. I hypothesized five patterns for pool sizes through time. I developed three additional sets of models, quantifying the hypothesized relationship between pool size and (1) stand structure, (2) topographic, and (3) soils variables, and interactions. I contrasted how much support each hypothesis had in the data using Akaike's Information Criterion (AIC).

Time since fire explained 30-72% of the variability in dead wood of different size classes. Pool size increased to a peak as material killed by the fire fell, then decomposed rapidly to a minimum (26-92 years after fire). It then increased, as new detritus was

produced by the regenerating stand. Litter was most strongly related to canopy cover (r^2=77%), suggesting litter fall, rather than decomposition, controls its dynamics. The temporal dynamics of duff were the hardest to predict. Environmental variables did not substantially constrain these dynamics, adding little to the explanatory power of the temporal models. Woody debris peak-to-minimum time was 19-73 years, overlapping the range of historical fire return intervals (1 to >100 yrs). Fires may therefore have burned under a wide range of fuel conditions, supporting the hypothesis that this region's fire regime was mixed severity.

INTRODUCTION

Understanding the role of disturbance in controlling ecosystem structure offers a fundamental challenge to contemporary ecologists. Organic detritus in forested ecosystems can be a significant pool of carbon (C). Coarse dead wood alone accounts for 18% of total ecosystem C in temperate forests (Pregitzer and Euskirchen 2004). Projected shifts in climate may substantially modify forest detrital pools, by affecting inputs (net primary productivity) and outputs (decomposition rates), and will likely increase the magnitude or frequency of disturbances, such as fire (Overpeck et al. 1990, Dale et al. 2001). Detritus plays a dual role in fire prone forests: it is a source of CO_2 during decomposition and combustion, and it comprises the forest fuel bed (Van Wagner 1977), acting as a control over fire behavior (Nalder and Wein 1999). The role of fuels in controlling fire behavior (e.g. Schoennagel et al. 2004) in forests of the western United States makes understanding the temporal dynamics of detritus in these forests critical.

Historical and present disturbance regimes, as well as climate and resource availability, control ecosystem level C accumulation (Chapin et al. 2002). Fire suppression in forests in the western United States has likely contributed to an accumulation of fuels on the ground (Covington and Moore 1994). This has become an issue of concern in forests that historically had relatively short fire intervals, such as the ponderosa pine forests of the Colorado Front Range, because fire has been suppressed, on average, for longer than one fire cycle (mean fire intervals ranged from 9 to 43 years; Brown et al. 1999, Veblen et al. 2000). These unusually long fire free intervals make them ideal for studying the long-term trends in accumulation of detrital material (Robertson and Bowser 1999), as well as the relative strength of other constraints on their temporal dynamics. Understanding these detrital dynamics and their constraints would provide a baseline against which to compare detritus in other dry, fire prone forests, as well as potential changes in these dynamics through time. Temporal changes may be particularly important in semi-arid areas, such as these ponderosa pine forests, where water availability limits productivity, because climate change projections envision increases in water deficits (Lauenroth et al. 2004). Care must be taken, though, in using these studies to define the historical range of variability in pool sizes, because the disturbance regime has been altered (Bond-Lamberty et al. 2003).

The detrital pool comprises a set of sub-pools, each with different accumulation and decomposition dynamics (Perruchoud and Fischlin 1995), and with differential effects on fire behavior (Rothermel 1972). I refer to the sum of downed dead wood in different size classes (twigs, branches, medium branches, logs), litter (fallen leaves and needles, cones and bark scales), and duff (partially decomposed but recognizable plant

material on the surface of the mineral soil) generically as "detritus". There is a wealth of research on the long-term dynamics of coarse dead wood in coniferous forests of western North America, highlighting its importance for habitat and its effect on many ecological processes. This literature includes both theoretical and empirical studies (Harmon et al. 1986, Spies et al. 1988, Sturtevant et al. 1997, Clark et al. 1998, Hély et al. 2000, Janisch and Harmon 2002). Less information is available on the dynamics of fine dead wood, litter and duff (Agee and Huff 1987, Nalder and Wein 1999, Wang et al. 2003, MacKenzie et al. 2004).

Aboveground biomass theoretically accumulates in predictable patterns after a disturbance (Bormann and Likens 1979). Variations in forest biomass (either dependent or independent of post-disturbance successional changes) could determine inputs and, consequently, detrital dynamics. Though other factors may be affecting the magnitude of output fluxes from the detrital pool, the effect of stand structure on detrital dynamics may predominate. Moisture and temperature can affect both the inputs and outputs from detrital pools, through their effect on net primary production and decomposition (Chapin et al. 2002). At broad scales, these controls have been quantified using mean annual precipitation, temperature, and actual evapotranspiration (Whittaker 1970, Meentemeyer 1978). In the Rocky Mountains, altitude and orientation of a particular site affect its radiative load, precipitation and temperature, thereby determining its water balance (Peet 2000). Soil characteristics, such as depth and texture, may also play a role (Peet 2000). Topographic or soil conditions could therefore control detrital pool size, through their influence on net primary production and decomposition. My objectives in this study were (a) to quantify the long-term temporal dynamics of detrital pools (downed dead wood in

different size classes, litter, duff); and (b) to determine to what extent present stand structure and environmental characteristics (topography, soils) constrain these temporal dynamics.

METHODS

Study area and data

I selected 31 sites in the Colorado Front Range of the Rocky Mountains, USA, between the 39° 7' and 40° 2' N, obtaining a chronosequence of time since fire from 1 to 159 years (Fig. 4.1, Appendix 4.1). Fire history information was obtained from published work (Brown et al. 1999, Veblen et al. 2000, Huckaby et al. 2001), and from USDA Forest Service staff. All sites were dominated by *Pinus ponderosa* Dougl. ex Laws, with secondary components of *Pseudotsuga menziesii* (Mirb.) Franco and *Juniperus scopulorum* L. Within each burn, I randomly selected one or two sites (depending on fire extent) with different aspects. These sites covered a range of soils, topographic positions and stand structure conditions (Appendix 4.1). Fire severity was high at all the sites that burned since 1963 (sites 15 to 31), except one (site 15), where many large trees survived. Burn severity at the older sites is unknown. Some of these older sites may have also burned more recently than the date I considered for this study. There was no clear evidence of such burnings in the field or in the fire history information, which gives me confidence that these potential burns did not significantly affect my results.

Each site was a relatively homogeneous stand (approximately 100 m x 50 m). I used the point-centered quarter method (Cottam and Curtis 1956), randomly selecting 10 points along the stand's main axis. At each point I counted downed wood pieces in four

diameter classes (twigs: <0.6 cm; branches: 0.6-2.5 cm; medium branches: 2.5-7.6 cm; and logs: >7.6 cm; Brown 1974) that intersected a planar transect (maximum length 15 m, *sensu* Brown et al. 1982). I collected litter (obtaining air-dried weights) and measured duff depth in four 0.25 m^2 circular plots along the transect. I measured height (with a Suunto® clinometer) and diameter at breast height (DBH) of four trees. I estimated canopy cover with 12 densitometer readings taken every 5 m in a 15 x 10 m grid. I measured aspect (compass bearing from north), slope (clinometer reading), geographical coordinates and elevation (Garmin III+ handheld Global Positioning System, Garmin International Inc., Olathe, Kansas, USA).

I estimated dead wood and duff weights using published algorithms (Brown 1974, Brown et al. 1982). I used point-to-tree distances to estimate tree density, and combined it with the trees' DBH to estimate basal area (Cottam and Curtis 1956). I used published allometric equations (Brown 1978, Gholz et al. 1979, Edminster et al. 1980, Ter-Mikaelian and Korzukhin 1997) to estimate mean tree total, branch and foliage biomass, and multiplied these by tree density to obtain per hectare values. I cosine-transformed the aspect readings into a relative sun exposure range (0: north-facing, 1: south-facing slopes; McCune and Keon 2002). In addition, I calculated two composite exposure indices from slope, aspect and latitude. The topographic index (TI) is the cosine of the incidence angle of solar radiation at solar noon of the summer solstice (Bonan 2002); the heat load index (HLI) is based on an empirical function (McCune and Keon 2002). Finally, I obtained coarse scale soils data for each site on the A horizon's permeability (cm/hr), organic matter (g/100g) and clay content (%), soil profile mean available water content (%) and rock depth (cm) (STATSGO Data Base; USDA 1994).

Hypothesized temporal dynamics of detrital pools

To quantify the temporal dynamics of detritus, I developed *a priori* candidate models describing each detrital pool (total dead wood, and dead wood in each of the four size classes, litter, duff) as a function of time since fire. I hypothesized five different patterns for changes in pool size with time since fire (Fig. 4.2, *left panel*): (a) detritus accumulates linearly through time; (b) residual material is consumed by the fire, and new detrital accumulation is approximately linear, leveling off at a maximum pool size as detrital fall and decomposition equalize; (c) initially, detritus accumulates slowly, accelerating as the new stand regenerates; pool size then stabilizes as decomposition compensates detrital fall; (d) residual detritus (produced in the preceding fire) decomposes rapidly and reaches a minimum, and then new detritus from the regenerating forest accumulates to a maximum stable value (Harmon et al. 1986); and finally, (e) the standing aboveground biomass killed by the fire falls gradually, generating a peak in residual detritus; this then decomposes, and new detritus accrues nonlinearly (Harmon et al. 1986).

Hypotheses (a) through (d) were easily quantified by single mathematical equations. The dynamics described by hypothesis (e) were too complex to be captured by one equation. I fit a statistical distribution (Gamma, Cauchy, Laplace or logistic) to model the residual pool, combined with either a linear or a power function to describe the increase of new detritus (Fig. 4.2, *left panel*). This limited the number of estimated parameters to six, reducing the risk of overfitting the data. Although the purely statistical models described above allowed me to quantitatively represent the shape of the curve for hypothesis (e), the parameters of those models do not provide insight into the magnitude

of fluxes associated with the detrital pools. To gain this insight I developed a model of detrital turnover using linked differential equations that portrayed the dynamics of live aboveground biomass (*AB*, Mg/ha), standing dead biomass (*SD*, Mg/ha) and detritus (*Det*, Mg/ha). I modeled net primary productivity (NPP) as a Gompertz function (Winsor 1932), in which the relative growth rate decreases exponentially through time. Mortality, fall and decomposition were modeled as first order functions of the source pool (Appendix 4.2). I refer to this as the compartment model:

$$\frac{dAB}{dt} = NPP - mortality = r_{\max} AB\left[1 - \frac{c}{r_{\max}} \ln \frac{AB}{AB_0}\right] - mAB$$

$$\frac{dSD}{dt} = mortality - fall = mAB - fSD$$

$$\frac{dDet}{dt} = fall - decomposition = fSD - kDet$$

AB_0 is the initial size of the *AB* pool, t is time (yr), r_{max} is the maximum relative growth rate of the live biomass pool (yr^{-1}) and c is the exponential decay rate of the relative growth rate (yr^{-1}); m, f and k are the rate constants of the corresponding fluxes (yr^{-1}).

Hypothesized stand structure and environmental constraints

I represented hypotheses on the non-temporal constraints on detrital pool sizes using three sets of candidate models. I hypothesized that detrital pool size could be linearly or nonlinearly dependent on basal area, live tree density, canopy cover, and aboveground biomass (first set; Fig. 4.2, *right panel*). I further hypothesized that topographic position and soils characteristics could constrain detrital dynamics, through their effect on a site's water balance. I developed topographic (second set) and soils (third

set) models to quantify these hypotheses. I limited these relationships to linear functions of one to three topographic or soils variables.

To determine to what extent non-temporal constraints added to the explanatory power of the temporal models, I compared the best temporal models to the models selected from each non-temporal set (see selection criteria in the *Model fitting, ranking and selection* section, below), and additional models that included interactions with the selected topographic or soils variables. These interaction models used topographic or soils variables as multipliers affecting the parameters of the temporal or structure models. I did not add interactions to the compartment or statistical models for hypothesis (e) because of my small sample size. I also did not combine variables with obvious multicollinearity problems (variance inflation factor (VIF) > 2 or tolerance < 0.6), such as rock depth and clay content (VIF = 2.8, tolerance = 0.35, r = 0.80).

Model fitting, ranking and selection

I determined how well the mathematical expressions for hypotheses (a) through (d) represented the data by fitting the single equation models using PROC NLIN (SAS 9.1; SAS Institute Inc., Cary, North Carolina, USA), log-transforming dependent variables where necessary to fulfill normality and constant variance assumptions. NLIN cannot handle dynamic models, so I used a non-linear steepest gradient search (using Solver, under Microsoft Excel; Microsoft Corp., Redmond, WA, USA) to estimate the parameters of the compartment model, solving the system of equations by numerical integration (4^{th} order Runge-Kutta; in Visual Basic for Applications). I used the non-dynamic models to corroborate that both procedures provided equivalent parameter estimates.

I used information theoretics (Burnham and Anderson 2002) to compare multiple hypotheses simultaneously, by ranking the models in terms of the support each had in the data. This support is quantified using Akaike's Information Criterion (AIC_c), a measure of the expected relative value of the Kullback-Leibler information discrepancy. This discrepancy reflects the information lost when a model is used to approximate truth (Burnham and Anderson 2002; Appendix 4.3). Differences in AIC_c between candidate models indicate whether the data support various hypotheses equally, or whether there is a clear best model (Burnham and Anderson 2002; Appendix 4.3). I selected the models in each set that met the SAS default convergence criterion, were within 6 AIC units of the top model (i.e. models with at least moderate support), had relevant coefficients (i.e. 95% confidence intervals did not overlap zero, signs of the coefficients made ecological sense) and explained at least 10% of the variability in the dependent variable.

RESULTS

Temporal dynamics of the detrital pools

All dead wood classes showed a peak in pool size between 7 and 23 years after fire, which decreased rapidly to a minimum (at 26-92 years) before increasing nonlinearly (except for medium branches, which stabilized) (Fig. 4.3). The statistical models best described these dynamics, explaining between 39 and 72% of the variability (Table 4.1). For the three smaller diameter classes this was a Gamma distribution combined with a power function (Table 4.1; Fig. 4.3a-c); for logs and total dead wood, it was a combination of a Cauchy distribution and a linear function (Table 4.1; Fig. 4.3d-e). Litter increased monotonically with time since fire; my data equally supported the

logistic and linear models, explaining 68 and 65% of the variability, respectively (Table 4.1, Fig. 4.4a). No single equation model described more than 10% of the variability in duff.

The compartment model reproduced the temporal dynamics of the dead wood pools (Fig. 4.3a-e), as well as the logistic accumulation pattern seen in litter (Fig. 4.4a) and some of the complex dynamics of duff accumulation (Fig. 4.3f). However, it was not selected for any detrital pool (AIC_c more than 6 units from the best model). In all cases, modeled live biomass followed a sigmoidal curve, and standing dead decreased monotonically for 10 to 60 years, increasing slowly toward a maximum thereafter (results not shown). The estimated rate constants for detrital fall were similar to those found in the literature (Table 4.2), while those for mortality and decomposition were respectively lower and higher than published values (Table 4.2).

Stand structure and environmental constraints

Topographic position partially explained the variability in dead wood classes (except branches) and litter (Table 4.1). Pool size was positively related to variables reflecting exposure (aspect, TI and HLI), and negatively related to elevation (Table 4.1). Soils variables explained 10 to 54% of the variability in total dead wood, medium branches, logs, litter and duff (Table 4.1). Dead wood pools were related to rock depth (negatively) and available water content (positively), as well as clay content (negatively) (Table 4.1). Total dead wood and logs were positively related to organic matter content, and the former was positively related to permeability (Table 4.1). Litter was positively related to available water content (Table 4.1). Rock depth and permeability explained

30% of the variability in duff. The direction of these correlations was opposite to those for the dead wood pools (Table 4.1).

Litter was the only detrital pool that was related to stand structure, alone and interacting with sun exposure. Linear functions of canopy cover and basal area explained over 70% of the variability (Table 4.1, Fig. 4.4b). Both explanatory variables were strongly correlated with time since fire (r^2 = 83 and 63%, respectively). At more exposed sites, the slope of the litter pool size-canopy cover was steeper (Table 4.1, Fig. 4.4b). These interactions decreased AIC_c by about one unit relative to the linear canopy cover model, and increased the explanatory power by 1% (Table 4.1).

Model selection summary

The statistical models described the temporal dynamics of dead wood pools better than the single equation models, supporting hypothesis (e). These ranked above (i.e. better reflect the processes involved) all the topographic and soils models (Table 4.1). A linear function of canopy cover best described variations in litter, and interactions with topographic variables added little (Table 4.1). Soil characteristics were the best predictors of duff, as indicated by the selected models (Table 4.1). The compartment model explained similar proportions of the variability as the best model for each detrital pool (Table 4.3, Figs. 4.3 and 4.4a). However, it was strongly penalized, in terms of AIC_c, for the high number of parameters that needed to be fit, relative to the sample size (11 parameters for duff, and 9 for the rest of the detrital pools; Table 4.3, Appendix 4.2).

DISCUSSION

Temporal dynamics of the detrital pools

My results strongly support hypothesis (e), which quantifies Harmon et al.'s (1986) conceptual model of dead wood dynamics: low initial amounts, followed by a distinct peak at 7 (twigs) to 23 (total dead wood) years after fire, as the material killed by the fire accumulated on the ground. This peak decomposed more quickly than expected based on results of other studies (Table 4.2), and the pools reached a minimum between 26 to 92 years after fire. Pool size for medium branches leveled off, rather than reaching a minimum. Accumulation of detritus from the regenerating forest may have stabilized before the residual material decomposed completely. The time it took pool sizes to reach peak and minimum values were similar to those found in mountain hemlock forests (Boone et al. 1988). Coarse woody debris (> 7.6 cm diameter) was still accruing after 159 years, a result that is consistent with studies of old-growth forests in this area (Robertson and Bowser 1999).

Both the statistical and compartment models reproduced these temporal trends. The statistical models describing hypothesis (e) were ranked well above the models that quantified hypotheses (a) through (d), showing that the data clearly supported the former hypothesis for all dead wood pools. The compartment model was generally ranked below at least other temporal model (hypotheses (a) through (d)), because of the large number of parameters it contained, relative to the sample size. However, the ability to interpret the rate constants estimated by this model is valuable, even if the model competed poorly with the statistical models. Moreover, the plausible values of the rate constants give me confidence that this model did not overfit the data. Furthermore, this model was based on

my understanding of the mechanisms that control detrital accumulation, and provided insights into pool turnover times and dynamics. For example, I found a single exponential function within the compartment model sufficient to describe the fall and decomposition of dead wood in this system, in contrast to Everett et al. (1999) and Bond-Lamberty et al.'s (2003) conclusion that multiple exponential models are needed to describe the dynamics of dead wood. This may be because of the overwhelming effect of a single fire event at my sites (i.e. most of the decomposing wood was added at the same moment in time, and therefore decomposed under the same conditions; Harmon et al. 1986). In addition, the estimated values of the rate constants in the compartment model (Table 4.2) quantify the processes that determine turnover of the different pools, which can be used independently of the model itself.

My *a priori* decision to quantify hypothesis (e) with two different approaches proved fruitful. The use of the statistical models unambiguously supported hypothesis (e) over the other proposed hypotheses on the temporal dynamics of dead wood. On the other hand, the compartment model provided a tool that can increase our understanding of detrital dynamics, and can be applied to other detritus pools (e.g. litter, duff) and other systems, or can be expanded to address more complex issues (e.g. modeling all detrital pools simultaneously; a spatially explicit variant).

Time since fire was a better predictor of large diameter dead wood dynamics than it was for smaller diameter classes. Finer material turns over faster than coarse wood, which can stay on the ground for over a century (McFee and Stone 1966), and is therefore more responsive to interannual variations in inputs. Disturbance has an extraordinarily large impact on inputs of coarse woody detritus (Harmon et al. 1986):

peak values were two orders of magnitude greater than minimum values. So, though large wood may be spatially more variable, fine wood varies more through time. Finally, time since fire explained a greater proportion of the variability in total dead wood dynamics than those of any of the diameter classes, even though I expected the accumulation and decomposition rates of the different size classes to be significantly different. The values of the rate constants of the compartment model indicated that, with the possible exception of twigs, the dynamics of woody debris were relatively independent of diameter, as seen in other studies (Bond-Lamberty et al. 2003, but see Harmon et al. 1986).

Litter did not show an initial peak of residual material because all the young sites I sampled were in high severity burns, where the foliage was consumed in the fire, leaving little material to then accumulate on the ground. The litter pool stabilized after approximately 120 years, as seen in other temperate coniferous forests (Boone et al. 1988). Variability in litter pool size was greater in older stands (Fig. 4.4). This is likely related to spatial variation in environmental conditions, as well as variation in fire severity or pre-fire stand structure, which reflect historical legacies of past conditions on ecosystem structure (Veblen 2003). Litter accumulation was strongly related to canopy cover dynamics, showing how stand development (which is a temporal phenomenon) controlled the size of this detrital pool. This suggests that litter fall was more important (or more variable across the age sequence) than decomposition in controlling these dynamics. The relation to canopy cover was stronger than to time since fire, suggesting that there was time-independent variability in canopy cover that affected litter pool size.

Temporal trends of duff were complex and hard to capture. Possibly, my point measures of duff, which is spatially very heterogeneous, were not as accurate or

representative of area-based values as measurements of the other detrital pools. These trends, however, seemed to mirror those of dead wood: as one increased, the other decreased (Fig. 4.3). Outputs from the dead wood pools (fragmentation and partial decomposition) provide inputs into the duff pool, which could explain the mirrored dynamics. Having to model this further step (which I did as a first order function; Appendix 4.2), with potentially different drivers, made it harder to accurately predict this pool's size. The exception to the mirrored dynamics between duff and dead wood is the low initial duff values (1-3 years since fire). These were likely determined by the severity of the preceding fire, which would have consumed a greater proportion of the finer duff than of the coarser dead wood.

Stand structure and environmental constraints

Time since disturbance was more important in controlling detrital pool sizes than were environmental factors. Similar conclusions were reached in studies in fire prone sub-boreal spruce forests (Clark et al. 1998) and secondary growth ponderosa pine/Douglas-fir forests (MacKenzie et al. 2004), but environmental variables better explained fuel loads in mixed conifer forests with varying species composition (Sánchez-Flores and Yool 2004). This difference could be because the soils data available to me were at a very coarse scale (USDA 1994), or because my study focused on ponderosa pine forests, limiting the range of topographic conditions studied (Appendix 4.1). High elevation sites (> 2500 m) tended to have less woody debris (except twigs) than predicted by the compartment model, while lower elevation sites had more than predicted. This suggests that elevation may account for some of the unexplained variability, though topographic variables alone were not strongly related to pool size (Table 4.1).

The direction of the relationships observed between detrital pool sizes (except duff) and topography consistently indicated that sites that were more exposed to radiation (i.e. south-facing) had greater debris loads. I would expect more exposed, warmer sites to have less detritus if temperature were controlling decomposition. This suggests that topographic controls were expressed through the effect of moisture on this process. There is evidence that moisture limits decomposition in dry forests (Klopatek et al. 1998) and fungal wood decay is negligible when wood water contents fall below 30% (Griffin 1977), as commonly occurs in logs in this area (Bradshaw et al. 2003). Dead wood pools were generally greater where the soil A horizon characteristics indicated that soils were less able to retain moisture: more permeable soils, and soils with lower clay content. This supports the hypothesis that surface moisture limited dead wood decomposition. However, the relative importance of inputs and outputs for dead wood pools was not as clear as for litter. Mean available soil water content, a variable that integrates the whole soil profile, was positively related to dead wood amounts. Deeper water sources unavailable for surface detrital decomposition can stimulate tree productivity, particularly given ponderosa pine's deep roots (Oliver and Ryker 1990). The observed relationship between available water content and pool size highlights the role of inputs (through tree productivity) on detrital dynamics. The relations between duff and the same environmental variables had opposite signs to those for dead wood. A low proportion of the variability in duff was explained, but it is noteworthy that this inversion was similar to that observed in the temporal trends.

Ecological insights and management implications

In the ponderosa pine forests of the Colorado Front Range, dead wood accumulated on the ground following predictable temporal patterns. Variations in stand structure or environmental conditions did not appear to constrain these dynamics. The temporal signal was strong enough to overcome the main disadvantage of the chronosequence approach: confounded spatial and temporal sources of variability. This approach, on the other hand, has a singular advantage. As I selected this chronosequence to reflect variations in time since fire, my results provide evidence that it is lack of fire, rather than other changes that occurred after Euro-American settlement (grazing, logging or climatic variability; Covington and Moore 1994, Veblen et al. 2000), that is driving the observed dynamics. The portion of the variability in pool sizes that was unexplained could be related to a variety of temporal and non-temporal factors that I was unable to examine in this study. Historical fire occurrence is associated with medium term climatic oscillations (e.g. El Niño Southern Oscillation), which likely drive accumulation of fine fuels during wet periods, followed by dry periods conducive to fire (Veblen et al. 2000). Potential sources of non-temporal variability include logging, mountain pine beetle outbreaks (such as occurred in the 1970s; Merrill R. Kaufmann, personal communication), and mistletoe infestation, but there was no extensive evidence of these at my sites.

The temporal scale of the maximum variation in woody debris (time between maximum and minimum values) varied between 17 and 67 years, depending on the diameter class and the model used. Overlapping the historical fire return intervals (1 to >100 years; Brown et al. 1999, Veblen et al. 2000) with the time frames of maximum

variation in dead wood suggests that fires may have burned under a large range of fuel conditions, supporting the characterization of the fire regime of these forests as mixed severity (Brown et al. 1999, Veblen et al. 2000). A necessary caveat is that this study was not designed to address whether the range of historical fire return intervals was due to variations in how long it takes fuels to accumulate to a minimum fire-bearing threshold, or to other factors such as weather (see Veblen et al. 2000). Given the extent of the overlap, however, it is possible that at least part of the variability is independent of detrital accumulation thresholds, and fires may have burned under a variety of fuel conditions, even where the fire regime has not been altered. The range of detrital pool sizes I observed was related to variations in fire behavior at some of my sites, which burned during the Hayman fire (2002) (Hall and Burke, *in revision*). The magnitude and timing of variations in detritus provide a baseline against which future long-term studies in dry forests may be compared, to determine whether climate change is affecting these pools, either directly or through changes in the disturbance regime.

Litter pool size was strongly related to canopy cover, highlighting the importance of litter fall, rather than decomposition, as controls over pool size. Cover in relatively sparse forests, such as these ponderosa pine systems (Peet 2000), can be estimated from remotely sensed data (Spanner et al. 1994). Spatially heterogeneous litter pools could then be modeled using remotely sensed canopy cover values. These data could be used to estimate carbon sequestered in litter, or as inputs to fire behavior models. Similar relationships between litter and canopy cover could be developed in other dry, fire prone forests, where the need to obtain spatially explicit estimates of litter distribution is critical. The duff pool was the hardest to model, and there is need for greater

understanding of the processes and variables that control its dynamics, as duff can comprise a large pool of carbon, which may be affected by fire or climate change.

I was able to satisfactorily model the dynamics of woody debris and litter using a simple compartment model. This model, and the plausible turnover rate constants I estimated, can be used to make projections of detritus, aboveground biomass and standing dead biomass accumulation. These model estimates would aid in quantifying carbon sequestration in ponderosa pine forests. The spatial distribution of these pools on a landscape can have important implications for fire behavior and fuel reduction strategies, as well as ecological implications for our understanding of the role of disturbance in controlling ecosystem structure. Model predictions of snag (standing dead) dynamics may be useful for addressing wildlife habitat concerns. The compartment model is intuitive, easy to implement, and there is a variety of sources for rate constant values, which make it ideal for providing insights into the biomass, snag and detritus dynamics in similar forests around the world.

REFERENCES

Agee, J.K. and M.H. Huff. 1987. Fuel succession in a western hemlock Douglas-fir forest. Canadian Journal of Forest Research 17:697-704.

Bonan, G. 2002. Ecological Climatology - Concepts and applications. Cambridge University Press, New York, New York, USA.

Bond-Lamberty, B., C. Wang, and S.T. Gower. 2003. Annual carbon flux from woody debris for a boreal black spruce fire chronosequence. Journal of Geophysical Research 108:8220.

Boone, R.D., P. Sollins, and K.Jr. Cromack. 1988. Stand and soil changes along a mountain hemlock death and regrowth sequence. Ecology 69:714-722.

Bormann, F.H. and G.E. Likens. 1979. Catastrophic disturbance and the steady state in Northern Hardwood forests. American Scientist 67:660-669.

Bradshaw, L., Bartlette, R., McGinely, J., and Zeller, K. 2003. Fire, weather, meteorology and climate. Pages 36-58 in R. T. Graham, editor. Hayman fire case study. Forest Service General Technical Report RMRS-GTR-114. US Department of Agriculture, Rocky Mountain Research Station, Fort Collins, Colorado, USA.

Brown, J.K. 1974. Handbook for inventorying downed woody material. Forest Service General Technichal Report GTR-INT-16. US Department of Agriculture, Intermountain Forest and Range Experimental Station, Ogden, Utah, USA.

Brown, J.K. 1978. Weight and density of crowns of Rocky Mountain conifers. Forest Service Research Paper RS-INT-197. US Department of Agriculture, Intermountain Forest and Range Experimental Station, Ogden, Utah, USA.

Brown, J.K., R.D. Oberheu, and C.M. Johnston. 1982. Handbook for inventorying surface fuels and biomass in the Interior West. Forest Service General Technical Report GTR-INT-129. US Department of Agriculture, Intermountain Forest and Range Experimental Station, Ogden, Utah, USA.

Brown, P.M., M.K. Kaufmann, and W.D. Shepperd. 1999. Long-term, landscape patterns of past fire events in a montane ponderosa pine forest of central Colorado. Landscape Ecology 14:513-532.

Burnham, K.P. and D.R. Anderson. 2002. Model selection and multimodel inference - A practical information-theoretic approach. Springer-Verlag, New York, New York, USA.

Chapin, F.S. III, P.A. Matson, and H.A. Mooney. 2002. Principles of Terrestrial Ecosystem Ecology. Springer-Verlag, New York, New York, USA.

Clark, D.F., D.D. Kneeshaw, P.J. Burton, and J.A. Antos. 1998. Coarse woody debris in sub-boreal spruce forests of west-central British Columbia. Canadian Journal of Forest Research 28:284-290.

Cottam, G. and J.T. Curtis. 1956. The use of distance measures in phytosociological sampling. Ecology 37:451-460.

Covington, W.W. and M.M. Moore. 1994. Southwestern ponderosa forest structure - Changes since Euro-American settlement. Journal of Forestry 92:39-47.

Dale, V.H., L.A. Joyce, S. McNulty, R.P. Neilson, M.P. Ayres, M.D. Flannigan, P.J. Hanson, L.C. Irland, A.E. Lugo, C.J. Peterson, D. Simberloff, F.J. Swanson, B.J. Stocks, and B.M. Wotton. 2001. Climate change and forest disturbances. BioScience 51:723-734.

Edminster, C. B., Beeson, R. T., and Metcalf, G. E. 1980. Volume tables and point sampling factors for ponderosa pine in the Front Range of Colorado. Forest Service Research Paper RM-218. US Department of Agriculture, Rocky Mountain Research Station, Fort Collins, Colorado, USA.

Everett, R., J. Lehmkuhl, R. Schellhaas, P. Ohlson, D. Keenum, H. Riesterer, and D. Spurbeck. 1999. Snag dynamics in a chronosequence of 26 wildfires on the east slope of the Cascade Range in Washington State, USA. International Journal of Wildland Fire 9:223-234.

Gholz, H.L., C.C. Grier, A.G. Campbell, and A.T. Brown. 1979. Equations for estimating biomass and leaf area of plants in the Pacific Northwest. Forest Research Laboratory Research Paper 41. School of Forestry, Oregon State University, Corvallis, Oregon, USA.

Griffin, D.M. 1977. Water potential and wood-decay fungi. Annual Review of Phytopathology 15:319-329.

Hall, S.A., and I.C. Burke. In revision. Considerations for developing fuel input layers for fire behavior models. Forest Ecology and Management.

Harmon, M.E., J.F. Franklin, F.J. Swanson, P. Sollins, S.V. Gregory, J.D. Latiin, N.H. Anderson, S.P. Cline, N.G. Aumen, J.R. Sedell, G.W. Lienkaemper, K.Jr. Cromack, and K.W. Cummins. 1986. Ecology of coarse woody debris in temperate ecosystems. Advances in Ecological Research 15:133-302.

Harrington, M. G. 1996. Fall rates of prescribed fire-killed ponderosa pine. Forest Service Research Paper INT-RP-489. US Department of Agriculture, Intermountain Research Station, Ogden, Utah, USA.

Hart, S.C., M.K. Firestone, and E.A. Paul. 1992. Decomposition and nutrient dynamics of ponderosa pine needles in a Mediterranean-type climate. Canadian Journal of Forest Research 22:306-314.

Hély, C., Y. Bergeron, and M.D. Flannigan. 2000. Coarse woody debris in the southestern Canandian boreal forest: composition and load variations in relation to stand replacement. Canadian Journal of Forest Research 30:674-687.

Huckaby, L.S., M.R. Kaufmann, J.M. Stoker, and P.J. Fornwalt. 2001. Landscape patterns of montane forest age structure relative to fire history at Cheesman Lake in the Colorado Front Range. Pages 19-27 in Vance, R. K., Covington, W. W., and Edminster, C. B., editors. Ponderosa pine ecosystems restoration and conservation:

steps towards stewardship. Forest Service Proceedings RMRS-P-22. US Department of Agriculture, Rocky Mountain Research Station, Ogden, Utah, USA.

Janisch, J.E. and M.E. Harmon. 2002. Successional changes in live and dead wood carbon stores: implications for net ecosystem productivity. Tree Physiology 22:77-89.

Klopatek, J.M., R.T. Conant, J.M. Francis, R.A. Malin, K.L. Murphy, and C.C. Klopatek. 1998. Implications of patterns of carbon pools and fluxes across a semiarid environmental gradient. Landscape and Urban Planning 39:309-317.

Lauenroth, W.K., H.E. Epstein, J.M. Paruelo, I.C. Burke, M.R. Aguiar, and O.E. Sala. 2004. Potential effects of climate change on the temperate zones of North and South America. Revista Chilena de Historia Natural 77:439-453.

MacKenzie, M.D., T.H. DeLuca, and A. Sala. 2004. Forest structure and organic horizon analysis along a fire chronosequence in the low elevation forests of western Montana. Forest Ecology and Management 203:331-343.

McCune, B. and D. Keon. 2002. Equations for potential annual direct incident radiation and heat load. Journal of Vegetation Science 13:603-606.

McFee, W.W. and E.L. Stone. 1966. The persistence of decaying wood in the humus layers of northern forests. Soil Science Society of America Proceedings 30:513-516.

Meentemeyer, V.. 1978. Macroclimate and lignin control of litter decomposition rates. Ecology 59:465-472.

Nalder, I.A. and R.W. Wein. 1999. Long-term forest floor carbon dynamics after fire in upland boreal forests of western Canada. Global Biogeochemical Cycles 13:951-968.

Oliver, W.W. and Ryker, R.A. 1990. Pinus ponderosa Dougl. ex Laws. Pages 413-424 in R. M. Burns and B. H. Honkala, editors. Silvics of North America - Volume 1: Conifers. Forest Service Agricultural Handbook 654. Washington, D.C., USA.

Overpeck, J.T., D. Rind, and R. Goldberg. 1990. Climate-induced changes in forest disturbance and vegetation. Nature 343:51-53.

Peet, R.K. 2000. Forests and meadows of the Rocky Mountains. Pages 75-121 in M. G. Barbour and W. D. Billings, editors. North American terrestrial vegetation. Cambridge University Press, Cambridge, U.K.

Perruchoud, D.O. and A. Fischlin. 1995. The response of the cabon cycle in undisturbed forest ecosystems to climate change: a review of plant-soil models. Journal of Biogeography 22:759-774.

Pregitzer, K.S. and E.S. Euskirchen. 2004. Carbon cycling and storage in world forests: biome patterns related to forest age. Global Change Biology 10:2052-2077.

Robertson, P.A. and Y.H. Bowser. 1999. Coarse woody debris in mature Pinus ponderosa stands in Colorado. Journal of the Torrey Botanical Society 126:255-267.

Rothermel, R.C. 1972. A mathematical model for predicting fire spread in wildland fuels. Forest Service Research Paper RS-INT-115. US Department of Agriculture, Intermountain Forest and Range Experimental Station, Ogden, Utah, USA.

Sánchez-Flores, E. and S.R. Yool. 2004. Site environment characterization of downed woody fuels in the Rincon Mountains, Arizona: a regression tree approach. International Journal of Wildland Fire 13:467-477.

Spanner, M., L. Johnson, J. Miller, R. McCreight, J. Fremantle, J. Runyon, and P. Gong. 1994. Remote sensing of seasonal leaf area index across the Oregon transect. Ecological Applications 4:258-271.

Spies, T.A., J.F. Franklin, and E.B. Thomas. 1988. Coarse woody debris in Douglas-fir forests of western Oregon and Washington. Ecology 69:1689-1702.

Sturtevant, B.R., J.A. Bissonette, J.N. Long, and D.W. Roberts. 1997. Coarse woody debris as a function of age, stand structure and disturbance in boreal Newfoundland. Ecological Applications 7:702-712.

Ter-Mikaelian, M.T. and M.D. Korzukhin. 1997. Biomass equations for sixty-five North American tree species. Forest Ecology and Management 97:1-24.

US Department of Agriculture. 1994. State Soil Geographic (STATSGO) Data Base. National Soil Survey Center Miscellaneous Publication Number 1492 (revised). Natural Resources Conservation Service, Fort Worth, Texas, USA.

Van Wagner, C.E. 1977. Conditions for the start and spread of crown fire. Canadian Journal of Forest Research 7:23-34.

Veblen, T.T. 2003. Historic range of variability of mountain forest ecosystems: concepts and applications. The Forestry Chronicle 79:223-226.

Veblen, T.T., T. Kitzberger, and J. Donnegan. 2000. Climatic and human influences on fire regimes in ponderosa pine forests in the Colorado Front Range. Ecological Applications 10:1178-1195.

Vogt, K.A., C.C. Grier, and D.J. Vogt. 1986. Production, turnover, and nutrient dynamics of above- and nelowground detritus of world forests. Advances in Ecological Research 15:303-377.

Wang, C., B. Bond-Lamberty, and S.T. Gower. 2003. Carbon distribution of a well- and poorly-drained black spruce fire chronosequence. Global Change Biology 9:1066-1079.

Whittaker, R. H. 1970. Communities and Ecosystems. The Macmillan Co., London, UK.

Winsor, C.P. 1932. The Gompertz curve as a growth curve. Proceedings of the National Academy of Sciences 18:1-8.

Yin, X.. 1999. The decay of forest woody debris: numerical modeling and implications based on some 300 data cases from North America. Oecologia 121:81-98.

Table 4.1. Selected model from each candidate set (temporal, structure, topography, soils, and interactions), predicting each detrital pool. Selection criteria are defined under *Model fitting, ranking and selection* in the **Methods** section.

Detrital pool	Model set	Model [1]	AIC_c	r^2	SE [2]
Dead twigs	temporal [3]	α = 3.84 (0.21), λ = 2.29 (0.26), b = 0.14 (0.068), c = 0.17 (0.11)	-104.2	39	0.16
	topographical	0.56 (0.15) – 0.01 (0.006) SLOPE + 0.01 (0.11) ASPECT	-96.8	15	0.19
Dead branches	temporal [3]	α = 5.48 (0.14), λ = 4.23 (0.36), b = 0.47 (0.22), c = 0.29 (0.10)	-15.4	56	0.68
Dead medium	temporal [3]	α = 6.24 (0.16), λ = 3.51 (0.32), b = 0.92 (0.25), c = 0.17 (0.067)	-25.7	60	0.57
branches [4]	topographical	4.36 (4.12) + 8.67 (4.15) TOPOGR. INDEX – 0.004 (0.002) ELEVATION	-7.2	18	0.80
	soils	3.82 (0.86) – 0.095 (0.044) CLAY	-7.1	10	0.82
	soils	-0.41 (1.23) – 0.015 (0.007) ROCK DEPTH + 0.51 (0.18) AVAILABLE WATER	-6.4	16	0.81
Logs [4]	temporal [5]	a = 22.07 (1.63), h = 17.24 (6.78), s = 2802 (905), b_0 = -19.42 (7.99), b_1 = 0.205 (0.068)	-2.3	65	0.81
	topographical	38.29 (16.0) + 25.91 (11.19) TOPOGR. INDEX – 0.023 (0.007) ELEVATION	16.5	19	1.18
	soils	-2.45 (0.98) – 0.097 (0.019) ROCK DEPTH + 2.26 (0.41) AVAILABLE WATER	-0.5	54	0.89
	soils	16.24 (3.22) – 0.56 (0.12) CLAY	3.4	42	0.98
	soils	-0.68 (0.55) + 5.90 (1.26) ORGANIC MATTER	3.8	42	0.98
Total dead	temporal [5]	a = 22.87 (1.52), h = 17.22 (5.84), s = 3776 (1158), b_0 = -24.44 (10.34), b_1 = 0.29 (0.083)	-26.1	72	0.56
wood [4]	soils	-4.86 (3.38) – 0.11 (0.031) ROCK DEPTH + 3.17 (0.66) AVAILABLE WATER	-3.1	29	0.86
	soils	21.30 (4.49) – 0.63 (0.20) CLAY	-1.7	19	0.90
	soils	5.64 (2.32) + 0.38 (0.16) PERMEABILITY	-1.0	17	0.91
	soils	2.95 (2.34) + 5.94 (2.00) ORGANIC MATTER	0.3	13	0.93

Table 4.1. *continued*

Detrital pool	Model set	Model [1]	AIC_c	r^2	SE [2]
Litter [4]	temporal [6]	DP_{SS} = 5.41 (1.85), f = 16.79 (6.63), a = 0.040 (0.013)	-6.8	68	0.81
	temporal	0.25 (0.09) + 0.03 (0.007) TIME SINCE FIRE	-6.6	65	0.83
	structure	0.28 (0.061) + 0.086 (0.015) CANOPY COVER	-19.2	77	0.68
	structure	0.39 (0.078) + 0.19 (0.040) BASAL AREA	-13.3	72	0.75
	topographical	4.03 (2.41) + 5.20 (1.77) HEAT LOAD INDEX – 0.003 (0.001) ELEVATION	20.8	22	1.26
	topographical	2.91 (2.90) + 7.39 (2.62) TOPOGR. INDEX – 0.004 (0.001) ELEVATION	23.1	16	1.31
	soils	-1.98 (0.44) + 0.45 (0.097) AVAILABLE WATER	13.6	33	1.15
	interactions	0.28 (0.060) + 0.094 (0.016) TOPOGR. INDEX x CANOPY COVER	-20.3	78	0.67
Duff	soils	19.73 (2.04) – 0.31 (0.086) PERMEABILITY	119.6	30	6.37
	soils	8.03 (1.99) – 0.094 (0.027) ROCK DEPTH	119.8	30	6.39

[1] Model and/or fit parameters, with standard error of parameters between parentheses.

[2] Standard error of estimates. Values in Mg/ha for non-transformed variables, and in natural log space for log-transformed variables.

[3] Combination of a Gamma distribution (parameters α, λ) and a power function (base b and exponent c) (Fig. 4.2A).

[4] Log-transformed variables.

[5] Combination of a Cauchy distribution (parameters a, h, scaling factor s) and a linear function (slope b_1 and intercept b_0) (Fig. 4.2A).

[6] Logistic function with maximum DP_{SS}, exponential rate a and multiplier f (Fig. 4.2A).

Table 4.2. Rate constants for single exponential terms in the compartment model and in examples from the published literature.

Flux	Rate constants and relative growth rate of the compartment model (yr^{-1})							References
	Twigs	*Branches*	*Medium branches*	*Logs*	*Total dead wood*	*Litter*	*Duff*	
mortality	0.0014	0.00036	0.010	0.0028	0.0029	0.059	0.079	this study
m	0.012 – 0.073				-	-	-	Harmon et al. 1986, Harrington 1996
fall	0.026	0.055	0.059	0.066	0.052	0.57	0.21	this study
f	-	0.151		0.069 – 0.19		NA [1]	-	Harrington 1996, Everett et al. 1999
decomposition	0.26	0.057	0.047	0.065	0.053	0.041	1.3	this study
k	0.004 – 0.017					0.07 – 0.19	-	Harmon et al. 1986, Hart et al. 1992, Yin 1999
fragmentation	-	-	-	-	-	-	0.27	this study
NPP [2] r_{max}	1.29	0.93	0.75	0.45	0.64	0.38	0.11	this study
NPP [2] *c*	0.08	0.06	0.06	0.03	0.04	0.06	0.08	this study

[1] Published values of litter fall are expressed in Mg $ha^{-1}yr^{-1}$, not as a rate constant [my mean values (0.015 Mg ha^{-1} yr^{-1}) are an order of magnitude lower than published values (0.5 Mg ha^{-1} yr^{-1}; Vogt et al. 1986)].

[2] NPP: net primary productivity; r_{max}: maximum relative growth rate; *c*: temporal decay rate of the maximum relative growth rate.

Table 4.3. Comparing the compartment model to the best selected model for each detrital pool.

Detrital pool	Selected best mathematical model [1]			Compartment model			Δ AIC_c [4]
	Model type	Parameters [2]	r^2	Parameters [2]	r^2	Penalization [3]	
Dead twigs	temporal (statistical)	5	39	9	39	14.1	14.5
Dead branches	temporal (statistical)	5	56	9	58	14.2	13.5
Dead medium branches	temporal (statistical)	5	60	9	63	14.5	13.7
Dead logs	temporal (statistical)	6	65	9	62	11.4	18.4
Total dead wood	temporal (statistical)	6	72	9	80	11.1	11.0
Litter	interaction (TI x COVER)	3	78	9	69	19.7	29.3
Duff	soils (PERMEABILITY)	3	30	11	35	29.0	27.0

[1] Model with minimum AIC_c listed in Table 4.1.

[2] Number of estimated parameters (including an estimate of variance).

[3] Difference in AIC_c units due solely to the difference in parameters fit by the selected best and the compartment models (i.e. difference between the AIC_c of the compartment model and the value of AIC_c it would have if it had the same unexplained variance but equal number of parameters as the selected mathematical model).

[4] Difference in AIC_c between the best mathematical model and the compartment model (Appendix 4.2).

Figure 4.1. Sites that composed the 160 year chronosequence of time since fire, and location of the study area within the western states (inset). Site characteristics are shown in Appendix 4.1.

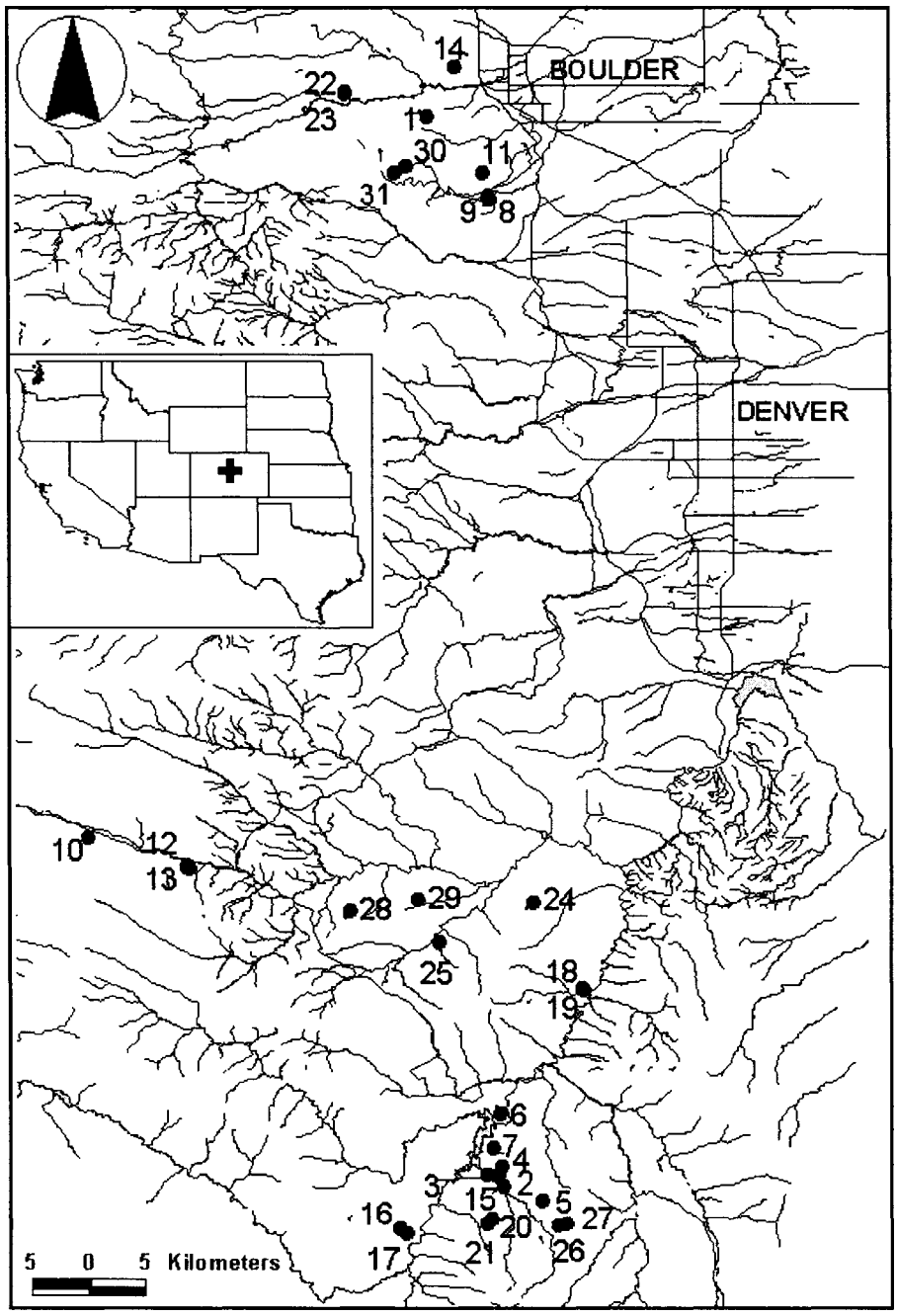

Figure 4.2. Conceptual graphs and mathematical equations for the hypothesized relationships between detrital pool size (*DP*) and ***(left panel)*** time since fire (*TSF*); ***(right panel)*** stand structure variables (*S*). Detrital pools were litter, duff, dead twigs, branches, medium branches, logs and total dead wood (Mg/ha). Stand structure variables were basal area (m^2/ha), live tree density (trees/ha), canopy cover (%), and aboveground biomass (total, branch or foliage, depending on the detrital pool being modeled; Mg/ha). DP_{SS}, DP_{res}, a, b, b_0, b_1, b_2, c, f, h, k, s, α and λ are parameters which were fit using proc NLIN in SAS 9.1 (SAS Institute Inc., Cary, North Carolina, USA); $\pi = 3.14159$ and e is the base of the natural log.

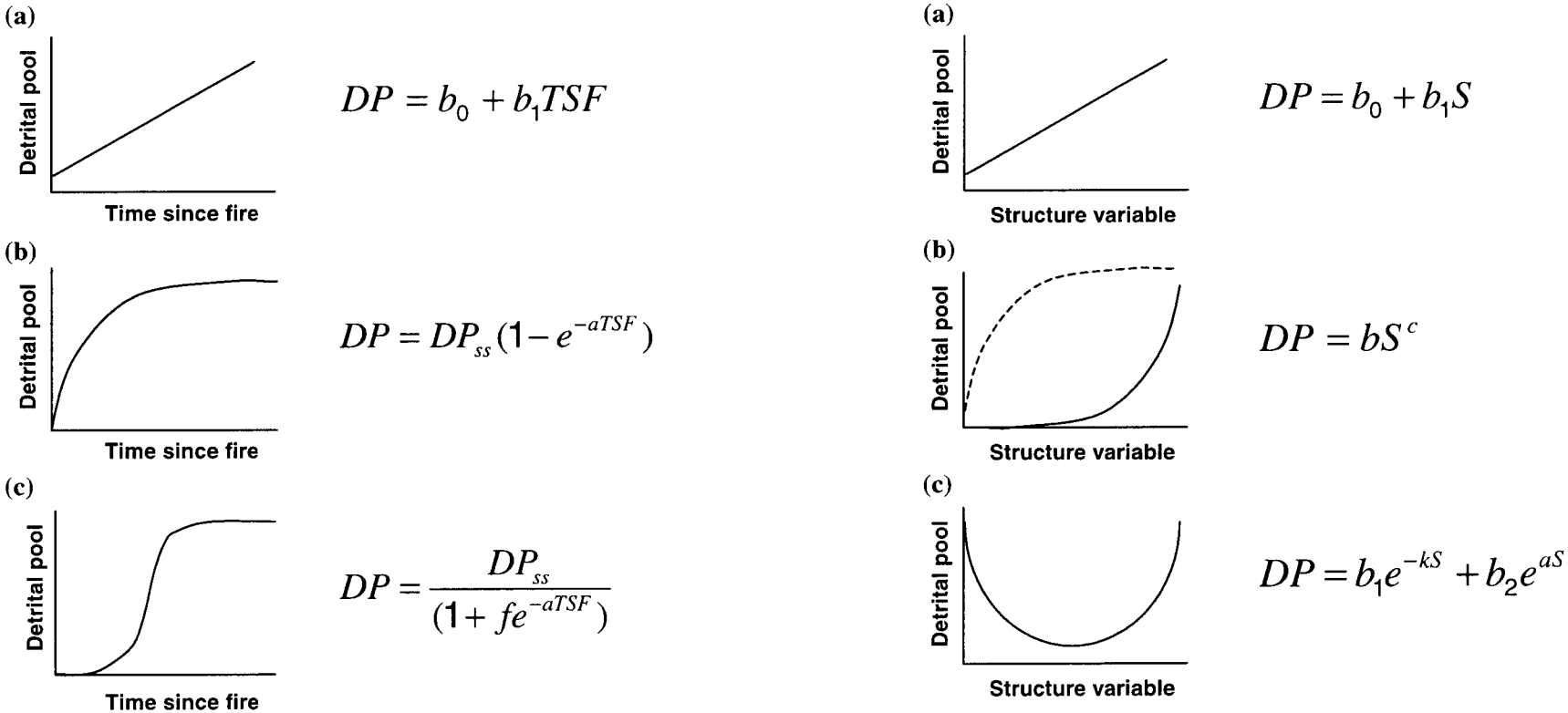

Figure 4.2. *continued*

(d)

$$DP = DP_{res}(1 - e^{-kTSF}) + \frac{DP_{ss}}{(1 + fe^{-aTSF})}$$

(e)

Example 1: Gamma distribution + power function:

$$DP = \left(\frac{TSF}{\lambda}\right)^{\alpha-1} \frac{e^{\left(-\frac{TSF}{\lambda}\right)}}{\lambda} + bTSF^{c}$$

Example 2: Cauchy distribution + linear function:

$$DP = \left(\frac{h}{\pi}(h^2 + (TSF - a)^2)\right)m + b_0 + b_1 TSF$$

Figure 4.3. Temporal dynamics of detrital pools: (**a**) twigs; (**b**) branches; (**c**) medium branches; (**d**) logs; (**e**) total dead wood; (**f**) duff. Black diamonds represent the data, with bars showing standard errors. Black lines represent predicted values from the statistical age models (Table 4.1, Fig. 4.2A) (no statistical model was selected for duff); gray lines represent values predicted by the compartment models (Table 4.2, Appendix 4.2).

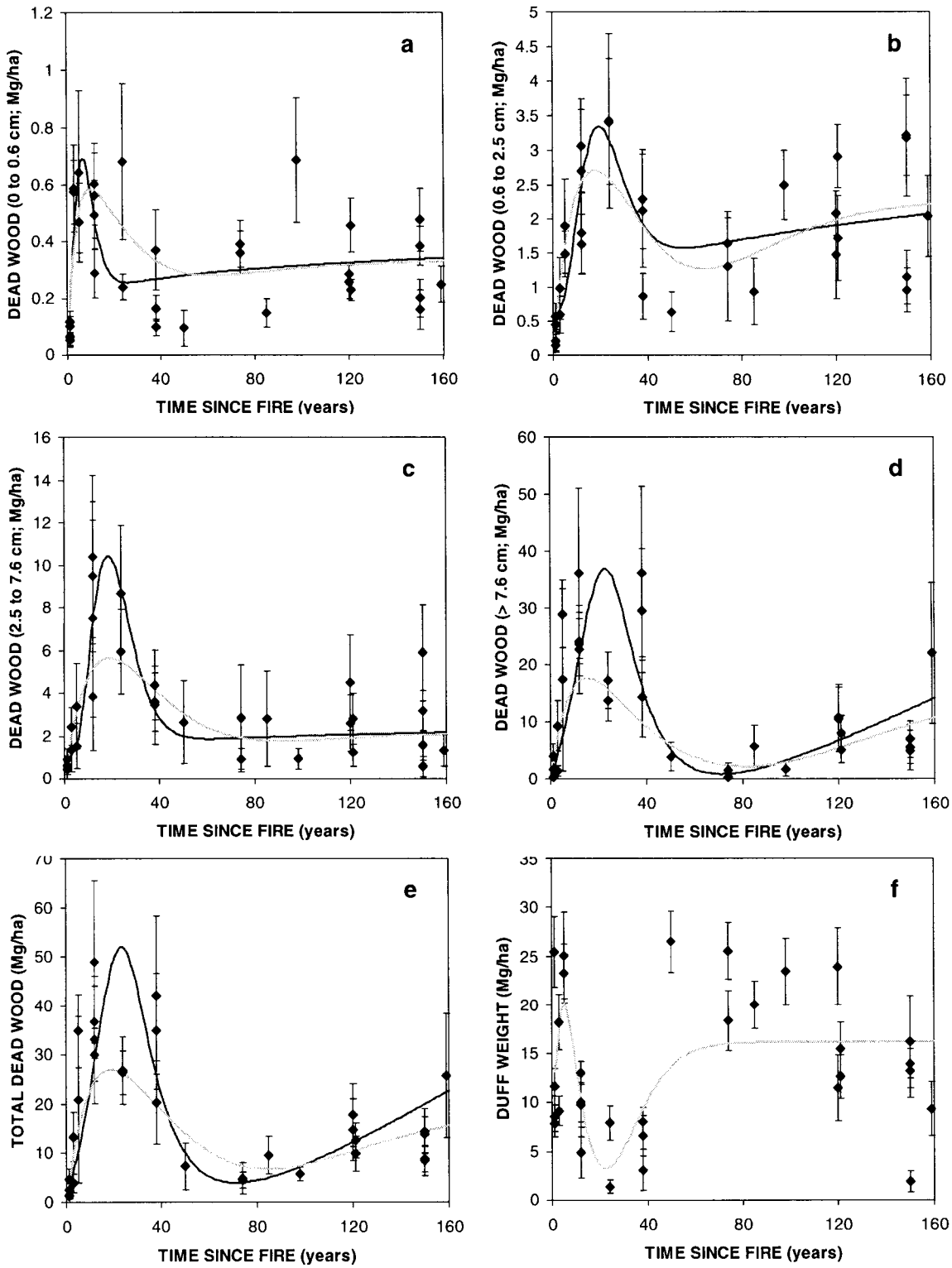

Figure 4.4. Dynamics of litter accumulation. (**a**) Temporal dynamics of the litter pool, showing predictions from the linear (dark gray line) and logistic (black line) models (Table 4.2, Fig. 4.2A), as well as the compartment model (light gray line; Table 4.2, Appendix 4.2). (**b**) Litter as a function of canopy cover. The dotted line represents the linear cover model predictions (Table 4.2, Fig. 4.2B). The three solid lines represent the predictions of the interaction model, where each line was based on a different value of the Topographical Index (surrogate for sites' exposure): low TI = 0.77 (light gray), medium TI = 0.86 (dark gray) and high TI = 0.95 (black line). Black diamonds represent the data, with bars showing the standard errors.

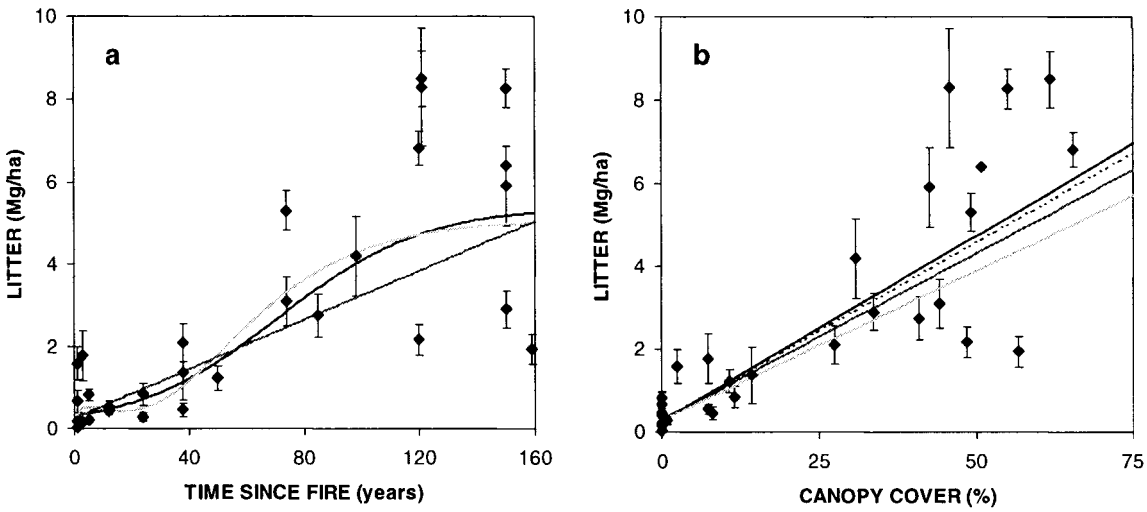

Appendix 4.1 – STAND STRUCTURE, TOPOGRAPHICAL AND SOILS CHARACTERISTICS OF THE SITES THAT COMPOSED THE 160 YEAR CHRONOSEQUENCE OF TIME SINCE FIRE.

Table A.4.1. Time since fire, environmental and stand structure characteristics of the study sites. Site numbers as in Fig. 4.1.

Site [1]	Time since fire (years)	Slope (°)	Aspect (°)	Elevation (m)	Aboveground biomass (live; Mg/ha)	Tree density (live; trees/ha)	Basal area (live; m^2/ha)	Soil classification
1	159	25	281	2225	182.9	629.2	32.8	Typic Haploborolls
2	150	17	176	2227	313.7	1617.1	59.3	Typic Ustorthents
3	150	29	27	2167	87.0	127.8	14.9	Typic Ustorthents
4	150	14	100	2295	96.7	213.7	16.3	Typic Ustorthents
5	150	12	172	2415	90.3	181.0	15.4	Typic Ustorthents
6	121	15	71	2200	126.5	277.2	23.5	Typic Ustorthents
7	121	12	292	2220	183.5	793.3	34.7	Typic Ustorthents
8	120	23	59	1929	47.5	257.0	11.1	Typic Eutroboralfs
9	120	22	245	1899	166.0	1286.4	39.1	Typic Eutroboralfs
10	98	14	141	2673	87.6	120.0	16.6	Typic Cryoboralfs
11	85	15	139	1948	56.4	119.6	10.6	Typic Eutroboralfs
12	74	9	55	2530	180.0	360.9	33.3	Typic Cryoboralfs
13	74	16	162	2521	103.0	197.8	20.2	Typic Cryoboralfs
14	50	23	42	1886	24.5	41.3	5.0	Typic Eutroboralfs
15	38	15	249	2191	64.1	206.7	11.3	Typic Ustorthents
16	38	21	65	2439	1.6	35.9	0.4	Typic Ustorthents
17	38	16	201	2340	16.7	74.2	2.9	Typic Ustorthents

Table A.4.1. *continued*

Site [1]	Time since fire (years)	Slope (°)	Aspect (°)	Elevation (m)	Aboveground biomass (live; Mg/ha)	Tree density (live; trees/ha)	Basal area (live; m^2/ha)	Soil classification
18	24	16	58	2040	0.0	0.0	0.0	Typic Ustorthents
19	24	19	78	2020	9.3	30.6	2.0	Typic Ustorthents
20	12	19	111	2505	0.1	0.0	0.0	Typic Ustorthents
21	12	9	82	2493	1.2	0.0	0.0	Typic Ustorthents
22	12	22	143	2111	0.0	0.0	0.0	Typic Haploborolls
23	12	28	34	2091	0.0	0.0	0.0	Typic Haploborolls
24	5	11	131	2343	0.7	0.0	0.0	Entic Haploborolls
25	5	12	310	2276	0.0	0.0	0.0	Entic Haploborolls
26	3	10	296	2527	0.9	0.0	0.0	Typic Ustorthents
27	3	8	237	2566	0.0	0.0	0.0	Typic Ustorthents
28	1	19	43	2548	0.0	0.0	0.0	Typic Cryoboralfs
29	1	9	165	2378	0.2	0.0	0.0	Entic Haploborolls
30	1	19	153	2220	0.0	0.0	0.0	Typic Haploborolls
31	1	21	101	2234	0.0	0.0	0.0	Typic Haploborolls

Appendix 4.2 – DIAGRAM AND EQUATIONS CHARACTERIZING THE CONTINUOUS TIME COMPARTMENT MODEL I DEVELOPED TO DESCRIBE THE TEMPORAL DYNAMICS IN THE ACCUMULATION OF EACH DETRITAL POOL (*DET*).

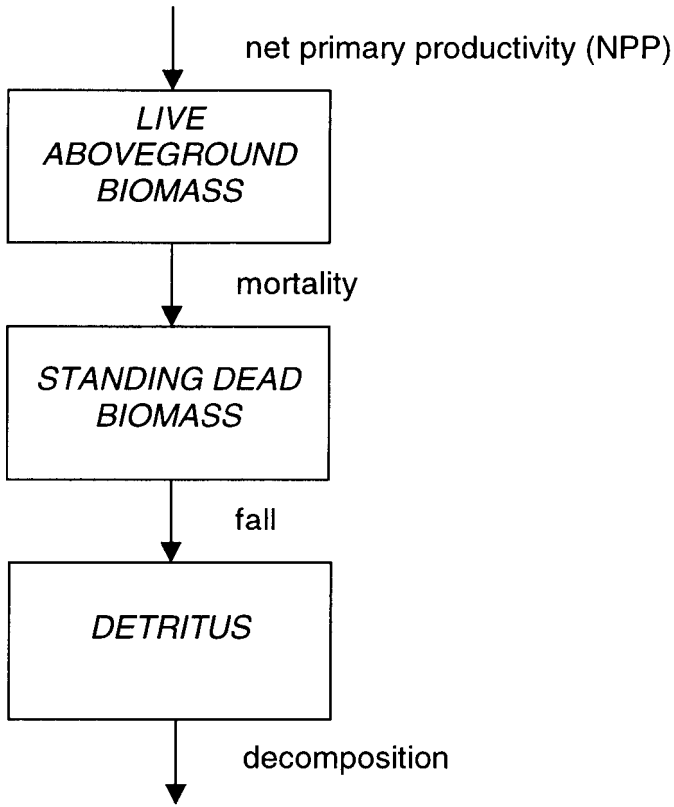

Fluxes

$$NPP = r_{max} e^{-ct} AB = r_{max} AB\left(1 - \frac{c}{r_{max}} \ln \frac{AB}{AB_0}\right)$$

$$mortality = mAB$$

$$fall = fSD$$

$$decomposition = kDet$$

Differential equations

$$\frac{dAB}{dt} = r_{max} AB\left(1 - \frac{c}{r_{max}} \ln \frac{AB}{AB_0}\right) - mAB$$

$$\frac{dSD}{dt} = mAB - fSD$$

$$\frac{dDet}{dt} = fSD - kDet$$

Detrital pools (Mg/ha) are litter, dead twigs (0-0.6 cm diameter), branches (0.6-2.5 cm), medium branches (2.5-7.6 cm) and logs (>7.6 cm), total dead wood. Live aboveground biomass (AB; Mg/ha) and standing dead biomass (SD; Mg/ha) components correspond to the tissue types found in the analogous detrital pool. AB_0 (initial aboveground biomass; Mg/ha), r_{max}, c, m, f and k (rate constants; yr^{-1}) are parameters that were fit separately for each detrital pool. I used a nonlinear steepest gradient search [applied with the Solver Add-In in Microsoft Excel (Microsoft Corp., Redmond, WA, USA)] to estimate the parameters that minimized the residual sums of squares, solving the system of differential equations by numerical integration (using a 4^{th} order Runge-Kutta method applied through Visual Basic for Applications). Parameters that varied to obtain the best fit were the initial pool sizes (3), plus the 5 rate constants. The estimated variance is also counted as a parameter (Burnham and Anderson 2002). A similar compartment model was developed for duff, adding a new pool called *DUFF*, and replacing the above "decomposition" flux with a "fragmentation" flux between the *DETRITUS* pool and the *DUFF* pool, and including the "decomposition" flux as an output from the *DUFF* pool. The "fragmentation" flux was quantified as a first order function of the source pool, in the same way as all the other fluxes between two modeled pools. This model had 6 rate constants, estimates for the initial size of four pools, plus the variance.

Appendix 4.3 – PHILOSOPHY AND CALCULATIONS USED TO DETERMINE THE RELATIVE SUPPORT THE DATA PROVIDED EACH HYPOTHESIS, BY RANKING CANDIDATE MODELS USING AN INFORMATION THEORETIC APPROACH (*sensu* Burnham and Anderson 2002).

To determine how well supported each hypothesis was, I ranked the candidate models in each set (temporal, structure, topography, soils), as well as in the final set that included interactions, using an information theoretic approach based on Akaike's Information Criterion (AIC). This methodology is used to simultaneously contrast a number of hypotheses to data assumed to represent the true nature of the process of interest. Each hypothesis must be mathematically stated and developed *a priori*. An AIC value is calculated for each model. AIC is a measure of the expected relative value of the Kullback-Leibler information discrepancy, which reflects the information lost when a model is used as an approximation to the truth. The smaller the AIC value, the closer a particular model is to the (unknown) truth. These values are relative, as they do not provide information on how far each model is from the truth (since the truth is unknown). The main advantage of AIC is that it informs me on how much more or less support one model has than the others in the set. The distance between models, in AIC units, provides information on whether the models ranked below the best one are close competitors or not. That is, can the data used really discriminate between two hypotheses? Or do they support two or more hypotheses equally? A rule of thumb is that models within 1 to 2 AIC units of the best model have substantial support; models 3 to 7 units from the best model have less support, and models more than 10 units away from the best model have essentially no support.

AIC is based on the maximum likelihood estimates of the parameters, assuming the data represent the truth. When the assumptions of least squares model fitting techniques are satisfied, there is a direct relationship between the maximum likelihood and the residual sums of squares (RSS) obtained through least squares fitting. Given the structure of my field data (all detrital components were approximately normally or log-normally distributed), I used least squares techniques to fit the models (log-transforming the data where necessary), and estimated the maximum likelihood of each model given the field data as:

$$\log(\ell(\hat{\theta})) = -\frac{n}{2}\log(\hat{\sigma}^2)$$

where $\ell(\hat{\theta})$ is the maximum likelihood of the model given the data and $\hat{\sigma}^2$ is RSS divided by the sample size (n; n = 30 for medium branches and logs, n = 31 for all other variables). I fitted the candidate models to the data of each detrital pool independently, using the procedure for nonlinear estimation in SAS 9.1 (NLIN; SAS Institute Inc., Cary, North Carolina, USA) for all non-dynamics models (see Appendix 4.2 for the procedure used for the compartment model). I calculated the AIC for each model, as well as the value corrected for the bias introduced by small sample sizes (AIC_c):

$$AIC_c = -2\log(\ell(\hat{\theta})) + 2K + \frac{2K(K+1)}{(n-K-1)}$$

where K is the number of estimated parameters (including an estimate of the variance). I ranked the models based on AIC_c. I selected models in each set that met the default convergence criterion, and were within 6 AIC_c units of the top model (i.e. models with at least moderate support), had relevant coefficients (i.e. 95% confidence intervals did not overlap zero, signs of the coefficients made ecological sense) and explained at least 10% of the variability in the dependent variable.

Burnham, K.P. and D.R. Anderson. 2002. Model selection and multimodel inference - A practical information-theoretic approach. Springer-Verlag, New York, New York, USA.

CHAPTER 5: CONCLUSIONS

The three studies of my dissertation potentially deepen present understanding of fire behavior and its controls, and facilitate the estimation of carbon stocks in different aboveground components of ponderosa pine forests of the Colorado Front Range.

In **Chapter 2**, I successfully used lidar data to estimate stand height, total aboveground biomass, basal area and foliage biomass. I was unable to generate robust explanatory models for tree density, canopy base height and canopy bulk density. My results suggest that lidar does have potential for estimating these variables, and larger datasets may be able to better capture existing relationships. They also highlight the need to broaden the focus of lidar studies to include low density forests, particularly where the vertical structure can strongly affect processes such as fire. So far, this technology has been used mainly in high biomass forests (Lefsky et al. 1999, Drake et al. 2002, Naesset 2002). These results can be used to generate carbon stock estimates for ponderosa pine forests. However, further work is needed before inputs maps of canopy structure for fire behavior models can be obtained. Therefore, the only insight into the fuel and fire debates provided by this study is a minor step: the selection of a subset of lidar metrics that were related to the variables of interest, which should be used in subsequent studies. This study has been published in Forest Ecology and Management (Hall et al. 2005).

In **Chapter 3**, I identified the variables that simulated fire behavior was sensitive to, as reflected in the predicted burn patterns using a simple spreadsheet model. Model

outputs corresponded well with observed fire severities at sites burnt in the Hayman fire, strengthening my conclusions. The model predicted that it was generally harder for a fire to reach the canopy than it was for it to spread through the canopy. This led me to the conclusion that active crown fire hazard was particularly sensitive to the description of the surface fuels, and to canopy base height. Characterizing the shape of tree crowns in the field would allow researchers to obtain more realistic estimates of canopy base height. Care must be taken to correctly identify the best descriptors of the surface fuels. These results, as well as other studies (Stephens 1998), highlight the importance of taking a landscape level perspective when analyzing crown fire hazard, because fire behavior can be hysteretic (Scott and Reinhardt 2001).

This study provides support for the role of fuels on fire behavior. Though I did not explicitly test the relative importance of fuels and weather in determining crown fire hazard, I did run the model under mean and extreme moisture conditions, thereby providing useful results in the context of this debate. Burn patterns under the range of fuel conditions I looked at included both surface and active crown fires. This information, combined with the hypothesized changes to historical fuel and stand conditions, can enlighten the debate on whether present fires, such as the Hayman fire, are outside the historical range of variability. This Chapter did not address questions of carbon sequestration. However, the insights my results provide to the fire behavior debates, as outlined above, can then be used to suggest the consequences fires in these forests will have for the regional carbon budgets. This paper has been submitted to Forest Ecology and Management, and is presently in revision.

In **Chapter 4**, I found that a simple compartment model was able to reproduce the temporal dynamics of different detrital pools after fire. Litter increased nonlinearly and leveled off around 120 years after fire. All the dead wood pools increased steeply soon after fire, as killed aboveground biomass accumulated on the ground, and then decreased, due to decomposition of this residual material. After that, most pools reached a minimum and then increased slowly again, as a new stand got reestablished. Duff was the hardest pool to model, either because it is spatially more heterogeneous and harder to represent accurately, or because more processes need to be modeled to describe its dynamics. Soil and topographical variables in general added little as constraints over the temporal dynamics of detrital pools, though in some cases were related to pool size. Stand structural variables were only important as predictors of litter pool size. These results quantify the magnitude and timing of changes in the different detrital pools. The range of variation in pool sizes will affect the role of fuels, relative to weather, in controlling fire behavior. Contrasting the timing of these variations with existing knowledge of the historical and present timing of fires (e.g. Brown et al. 1999, Veblen et al. 2000) will help scientists decipher whether recent fires in these forests were more severe than historically.

The overall goal of my dissertation was to provide ecological and methodological insights into fire ecology debates and carbon sequestration issues. My conclusions provide some new pieces of a complex puzzle, particularly with respect to our capacity to obtain spatially explicit estimates of vertical structure, the importance of surface fuels as controls over active crown fire hazard, and the magnitude and variability in detrital pools, which comprise the surface fuels. Some important questions still remain. How much

carbon is released during wildfires, and how does that vary across fire severities? How does the timing of changes in detrital pools relate to historical variability in fire behavior? Under what range of weather conditions do fuels control fire behavior? Consequently, when and where are fuel treatments likely to be effective? Addressing these gaps will generate new questions and highlight failings in our understanding, driving the continuous cycle of scientific research.

REFERENCES

Brown, P.M., Kaufmann, M.K., Shepperd, W.D., 1999. Long-term, landscape patterns of past fire events in a montane ponderosa pine forest of central Colorado. Landscape Ecology 14, 513-532.

Drake, J.B., Dubayah, R.O., Clark, D.B., Knox, R.G., Blair, J.B., Hofton, M.A., Chazdon, R.L., Weishampel, J.F., Prince, S.D., 2002. Estimation of tropical forest characteristics using large-footprint lidar. Remote Sensing of Environment 79, 305-319.

Hall, S.A., I.C. Burke, D.O. Box, M.R. Kaufmann, and J.M. Stoker. 2005. Estimating stand structure using discrete-return lidar: an example from low density, fire prone ponderosa pine forests. Forest Ecology and Management 208:189-209.

Lefsky, M.A., Cohen, W.B., Acker, S.A., Parker, G.G., Spies, T.A., Harding, D., 1999. Lidar remote sensing of the canopy structure and biophysical properties of Douglas-fir western hemlock forests. Remote Sensing of Environment 70, 339-361.

Naesset, E., 2002. Predicting forest stand characteristics with airborne scanning laser using a practical two-stage procedure and field data. Remote Sensing of Environment 80, 88-99.

Scott, J.H., Reinhardt, E.D., 2001. Assessing crown fire potential by linking models of surface and crown fire behavior. U.S. Forest Service, Rocky Mountain Research Station Research Paper RMRS-RP-29.

Stephens, S.L., 1998. Evaluation of the effects of silvicultural and fuels treatments on potential fire behaviour in Sierra Nevada mixed-conifer forests. Forest Ecology and Management 105, 21-35.

Veblen, T.T., Kitzberger, T., Donnegan, J., 2000. Climatic and human influences on fire regimes in ponderosa pine forests in the Colorado Front Range. Ecological Applications 10, 1178-1195.